Functional dissection of the two domains of Tim50, the main receptor of the TIM23 complex

Dissertation

zur Erlangung des Doktorgrades der Naturwissenschaften

der Fakultät für Biologie

der Ludwig-Maximilians-Universität München

vorgelegt von

Marcel Gilbert Genge

aus

Berlin, Deutschland

München

2023

Diese Dissertation wurde angefertigt

unter der Leitung von **PD Dr. Dejana Mokranjac**

im Bereich der Zellbiologie, der Fakultät für Biologie

an der Ludwig-Maximilians-Universität München

Erstgutachter/in: PD Dr. Dejana Mokranjac

Zweitgutachter/in: Prof. Dr. Christof Osman

Tag der Abgabe: 18.10.2023

Tag der mündlichen Prüfung: 22.03.2024

Eidesstattliche Erklärung:

Ich versichere hiermit an Eides statt, dass meine Dissertation selbständig und ohne unerlaubte Hilfsmittel angefertigt worden ist.

Die vorliegende Dissertation wurde weder ganz, noch teilweise bei einer anderen Prüfungskommission vorgelegt.

Ich habe noch zu keinem früheren Zeitpunkt versucht, eine Dissertation einzureichen oder an einer Doktorprüfung teilzunehmen.

München, den 23.03.2024 _____

Marcel Gilbert Genge

What I strive for is that

wherever I go, whatever I do and whoever I meet,

I want to leave a positive impact.

Table of Contents

1. INTRODUCTION

Eukaryotic cells contain different cell organelles, each of which provides a specific milieu for a variety of cellular processes to take place under vastly different conditions. Mitochondria have a prominent place among the organelles. They are a central hub where many cellular processes converge and decisions between life and death of the cell are made - on one hand, mitochondria are involved in the production of ATP and several other essential metabolites and, on the other, they initiate programmed cell death (apoptosis) (Spinelli and Haigis, 2018; Pfanner et al., 2019; Alberts, 2022). The importance of mitochondria is best reflected in numerous human diseases that are associated with defective mitochondria, like neurodegenerative and cardiovascular diseases, as well as cancer. Furthermore, multiple diseases have been directly linked to mutations in mitochondrial proteins (Nunnari and Suomalainen, 2012; Suomalainen and Battersby, 2018). Research on mitochondria and understanding, on the molecular level, of the processes that take place in the organelle are therefore important both for basic science and for medicine.

1.1 Protein translocation into mitochondria

Mitochondria are double membrane-bounded organelles with the mitochondrial outer membrane (OM) and inner membrane (IM) enclosing the intermembrane space (IMS) and the innermost matrix. The resulting four subcompartments accommodate a variety of specific mitochondrial proteins and provide different conditions for the structural and functional specialization within mitochondria (Harner et al., 2012). Targeting of proteins into the correct mitochondrial subcompartment is crucial to ensure that these proteins will reach their correct place of function. Evolutionary, mitochondria carry their own genome, the mitochondrial DNA (mtDNA), with a complete apparatus for its expression. However, out of ca. 1000 – 1500 mitochondrial proteins only 8 in yeast *Saccharomyces cerevisiae*, and 13 in humans are expressed from the mtDNA, while all the others are encoded on the nuclear genome. Therefore, to produce new mitochondria from the pre-existing ones, the process called biogenesis of mitochondria, cells have to fulfil essential tasks that include expressing mitochondrial proteins from the nuclear DNA, translating them on cytosolic ribosomes as precursor proteins with specific targeting signals and finally importing them from the cytosol into mitochondria with the help of highly specific protein translocases present in all four subcompartments of mitochondria (Neupert, 2015; Wiedemann and Pfanner, 2017; Grevel et al., 2019; Hansen and Herrmann, 2019; Araiso et al., 2022; Busch et al., 2023).

The targeting signals of mitochondrial proteins are highly diverse, mirroring the complexity of the organelle, however, mitochondrial protein translocation follows the basic principle of protein translocation that is used across different organelles. Specific receptors, usually present on the surface of the organelle and exposed to the cytosol, recognize the targeting signals of proteins. After this initial recognition, proteins are translocated across or inserted into the membrane of the organelle through some kind of import channel or pore usually requiring an energy input (Schatz and Dobberstein, 1996; Blobel, 2000). Protein translocation into mitochondria poses specific challenges as this organelle contains two membranes that have to be crossed and therefore requires a variety of protein translocases in the four subcompartments of mitochondria to import proteins in a coordinated manner.

1.2 Overview of mitochondrial protein translocases

The translocase of the outer membrane (TOM) complex is the main entry gate for essentially all mitochondrial precursor proteins (Baker et al., 1990; Kiebler et al., 1990). It coordinates with downstream protein translocases the import of precursor proteins, depending on their mitochondrial targeting signal and hence the subcompartment they need to reach as their final place of function. Here, the various import pathways into mitochondria are briefly described (Figure 1.1).

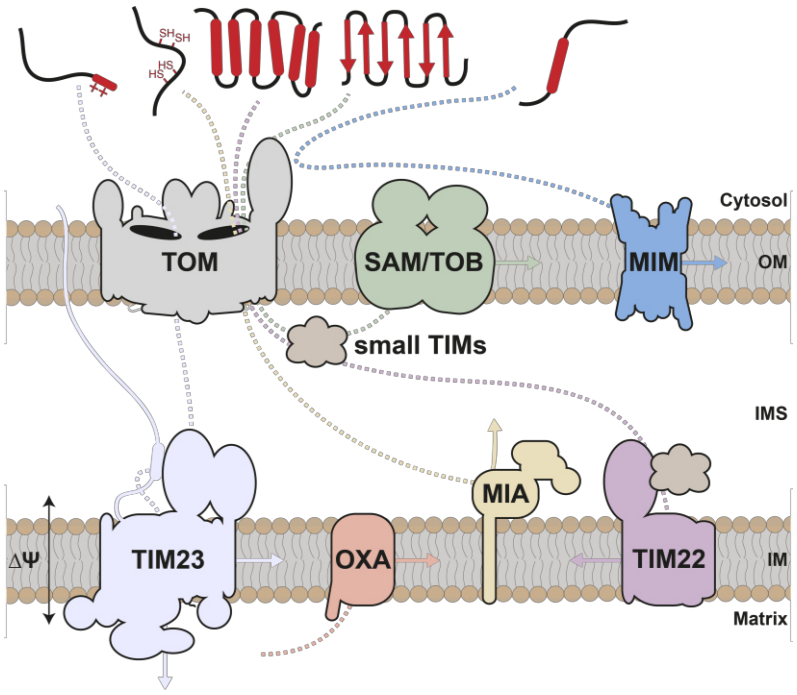

Figure 1.1 Overview of protein translocation pathways into mitochondria. See text for details. OM, outer membrane; IMS, intermembrane space; IM, inner membrane; ΔΨ, membrane potential.

Biogenesis of mitochondrial OM proteins can be divided into two pathways, depending on structural characteristics of the mitochondrial targeting signal used. On one hand, β-barrel membrane proteins initially use the TOM complex to translocate across the OM. Subsequently, these proteins are guided through the IMS by chaperones, the small TIM proteins, and finally are inserted into the OM by the sorting and assembly machinery (SAM) complex (also known as the topogenesis of mitochondrial OM β-barrel proteins (TOB) complex) (Paschen et al., 2003; Wiedemann et al., 2003). On the other hand, single- and multi-spanning α-helical transmembrane (TM) proteins use a special membrane insertion machinery, the mitochondrial import (MIM) complex, for their insertion into the OM (Becker et al., 2008; J. Popov-Celeketić et al., 2008). Even though the general entry gate formed by the TOM complex is typically not used by these proteins, components of the TOM or SAM complex may be involved to guide insertion of these proteins into the OM through a combination of protein- and lipid-assisted mechanisms. Mitochondrial proteins with specific, conserved cysteine motifs that are targeted to the IMS are imported by the mitochondrial intermembrane space assembly (MIA) pathway, also called disulfide relay system (Chacinska et al., 2004; Mesecke et al., 2005). After passing the TOM complex in the reduced form, substrates of this pathway undergo oxidative folding with the help of an oxidoreductase receptor. The folding keeps them in the IMS and prevents their release back into the cytosol. Multi-spanning IM proteins with internal targeting signals translocate through the TOM complex and require the small TIM proteins to be guided through the IMS, analogously to the β-barrel membrane proteins targeted to the OM. To be inserted into the IM, they use the translocase of the inner membrane 22 (TIM22) complex in a process driven by the membrane potential (ΔΨ) across the IM (Sirrenberg et al., 1996; Koehler et al., 1998). In contrast, hydrophobic IM proteins that are encoded in the mtDNA and synthesized on mitochondrial ribosomes, as well as some polytopic IM proteins that are imported into the matrix first, use the oxidase assembly (OXA) complex for their insertion into the IM (Herrmann et al., 1997; Hell et al., 2001). The vast majority of nuclear encoded mitochondrial proteins, about 70 % of them, however, carry N-terminal, 15-55 amino acid residues long, cleavable extensions called presequences, that by default target precursor proteins into the matrix. Presequences are not conserved on the level of their primary sequence but share the common feature that they all have, which is the ability to form an amphipathic helix with one hydrophobic and one positively charged side (Vögtle et al., 2009; Mossmann et al., 2012). Translocation of presequence-containing precursor proteins along the so-called “presequence pathway” is mediated by the TOM and the translocase of the inner membrane 23 (TIM23) complexes and requires the membrane potential across the IM and ATP hydrolysis in the matrix as energy sources (Neupert, 2015;

Schulz et al., 2015; Demishtein-Zohary and Azem, 2017; Craig, 2018; Hansen and Herrmann, 2019; Mokranjac, 2020; Busch et al., 2023).

Most of the knowledge of the complex mitochondrial protein translocases stems from the work carried out in Fungi, primarily with using baker´s yeast *Saccharomyces cerevisiae* as a model system. However, the various import pathways and even the majority of the involved components are universally conserved all the way to humans with only very few differences among eukaryotes (Dolezal et al., 2006; Demishtein-Zohary and Azem, 2017; Fukasawa et al., 2017; Kang et al., 2018). One example of a difference is the MIM complex that is fungi-specific, however, analogous proteins in mammals (MTCH2) or trypanosomas (pATOM36) carry out the same functions and, at least for the latter, are interchangeable with the protein in yeast (Vitali et al., 2018; Guna et al., 2022). Therefore, knowledge obtained with mitochondria in *Saccharomyces cerevisiae* as a model system can be essentially directly extrapolated to understand the basic molecular processes in human cells and potentially set the groundworks for understanding mitochondrial diseases.

The focus of my thesis is on the coordinated protein translocation along the presequence pathway and therefore both TOM and TIM23 complexes are described in more detail in the following sections.

1.3 The TOM complex

The TOM complex is the major protein translocase of the OM and the main entry gate for essentially all nuclear-encoded mitochondrial precursor proteins. It mediates the initial stages of protein translocation and coordinates protein import into mitochondria with downstream protein translocases (Gupta and Becker, 2021; Araiso et al., 2022). The TOM complex consists of seven subunits: the β-barrel protein Tom40 and six α-helical TM proteins Tom20, Tom22, Tom70, Tom5, Tom6 and Tom7 (Figure 1.2 A). The core protein Tom40 forms the translocation pore in the OM. Tom20, Tom22 and Tom70 are the receptors and are mainly responsible for precursor recognition and tethering of cytosolic chaperones (Yamano et al., 2008; Backes et al., 2021). The remaining three subunits, Tom5, Tom6 and Tom7, are the so-called small TOM proteins. Their functions are still relatively poorly understood but they are implicated in the assembly and stability of the TOM complex (Dekker et al., 1998). Tom5 and Tom7, additionally have been suggested to be involved in presequence-binding on the cytosolic and the IMS sides of the TOM complex, respectively (Esaki et al., 2004).

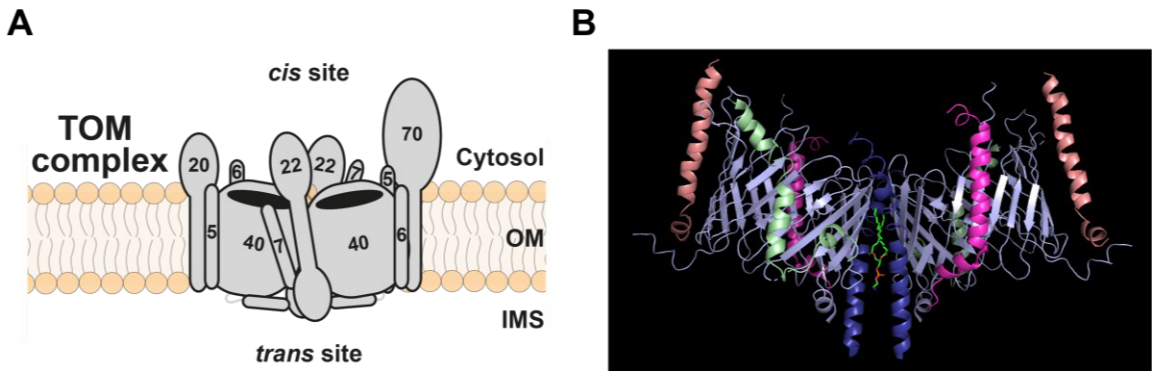

Figure 1.2 Schematic representation and structure of the TOM complex. (A) The TOM complex consists of seven subunits: receptors, Tom20, Tom22 and Tom70, and the translocation pore, Tom40, associated with the small TOM proteins, Tom5, Tom6 and Tom7. The TOM complex contains precursor binding sites in the cytosol (*cis*) and in the IMS (*trans*). See text for details. OM, outer membrane; IMS, intermembrane space. (B) Cryo-EM structure of the TOM complex as a dimer from yeast (PDB: 6JNF), generated with Pymol. Tom40 (lightblue), Tom22 (darkblue), Tom7 (palegreen), Tom6 (lightmagenta), Tom5 (salmon). Tom20 and Tom70 were not present in the solved structure.

Tom70 is inserted in the OM with a TM segment and exposes its receptor domain to the cytosol. Initially, it was suggested that Tom70 functions as a receptor for precursor proteins with internal targeting signals (Brix et al., 1999; Backes et al., 2018). More recent work, however, has shown that Tom70´s function may be more general and that it is involved in tethering of cytosolic chaperones like Hsp70 and Hsp90, and their bound substrates, to the mitochondrial surface (Backes et al., 2021). Hsp70 and Hsp90 chaperones bind newly synthesized mitochondrial precursor proteins in the cytosol, delivering them in an unfolded and import-competent state to the mitochondrial surface, while preventing misfolding and aggregation (Becker et al., 2019; Bykov et al., 2020). Tom20 is the main receptor of the TOM complex for presequence-containing precursor proteins and, like Tom70, contains a TM segment and exposes a C-terminal receptor domain to the cytosol. The high-resolution structures of the soluble receptor domain of Tom20 bound to presequence peptides showed that it recognizes the hydrophobic side of the amphipathic helix (Abe et al., 2000; Saitoh et al., 2007). The data has been presented that Tom20 may also be involved in the recognition of presequence-less precursor proteins (Brix et al., 1999; Yamano et al., 2008). The third receptor of the TOM complex is Tom22 which exposes its N-terminal receptor domain to the cytosol and, together with Tom20, recognizes presequence-containing precursor proteins (Yamano et al., 2008). The two receptors, Tom20 and Tom22, specifically recognize and bind the hydrophobic and positively charged sides, respectively, of the amphipathic helix formed by the presequence of precursor proteins (Brix et al., 1999; Yamano et al., 2008). The TM segment of Tom22 is crucial for the structural stability of the

entire TOM complex (van Wilpe et al., 1999). In contrast to the two other receptors of the TOM complex, Tom22 carries an additional domain exposed to the IMS that can also bind presequences (Moczko et al., 1997; Kanamori et al., 1999; Shiota et al., 2011).

Precursor proteins that are recognized by the cytosol-exposed receptors at the so-called *cis* site of the TOM complex, are subsequently transferred to the central protein import pore, formed by the β-barrel protein Tom40 and embedded in the OM. Tom40 forms an aqueous channel with chaperone-like properties which interacts with unfolded or partially folded segments of precursor proteins through multiple precursor binding sites inside the β-barrel pore. These multiple precursor binding sites together with the rather negatively charged pore interior towards the IMS mediate a dynamic movement of precursor proteins through the import channel (Esaki et al., 2003; Shiota et al., 2015; Araiso et al., 2019; Tucker and Park, 2019). However, the TOM complex alone is not sufficient to completely translocate proteins across the outer membrane. Rather, subsequent recognition of the translocating precursor proteins at the IMS side of the TOM complex by precursor-binding components of the TOM complex and by the downstream translocases is required to complete translocation across the OM (Mayer et al., 1995; Kanamori et al., 1999). Depending on the presence or absence of presequences, precursor proteins use distinct import routes through the Tom40 channel to translocate across the OM (Araiso et al., 2019). Presequence-less precursor proteins exit the TOM complex at the edges of the Tom40 dimer, close to Tom5 and the N-terminal segment of Tom40 that both seem to be involved in recruiting downstream protein translocases. Presequence-containing precursor proteins, however, exit the TOM complex in the center of the Tom40 dimer. Here the IMS exposed segments of Tom22, Tom7 and Tom40 protrude together, forming the so-called *trans* site of the TOM complex that specifically recognize and bind presequences (Kanamori et al., 1999; Esaki et al., 2004; Shiota et al., 2011; Araiso et al., 2019; Tucker and Park, 2019).

Pronounced understanding of the molecular architecture of the TOM complex through previous biochemical studies finally culminated when the first high-resolution cryo-EM structures of the entire protein translocase from yeast were solved (Figure 1.2 B) (Araiso et al., 2019; Tucker and Park, 2019). The structures revealed that the TOM core complex is formed by two Tom40 pores tethered together by the TM segments of two Tom22 molecules. Each pore has the three small TOM proteins bound to its outside walls. Additionally to the TOM core dimer, trimeric and higher-order oligomers of the TOM complex were also observed by cryo-EM, representing potential adaptations to different metabolic conditions or to the variety of precursor proteins using different import pathways

(Künkele et al., 1998; Model et al., 2002; Araiso et al., 2019; Tucker and Park, 2019). The loosely bound receptors Tom20 and Tom70 were lost either during the purification or during subsequent freezing of the complex and were thus not part of the final structure, even though the cryo-EM structure of the human TOM complex including Tom20 was solved shortly after through stabilizing it by prior cross-linking (Wang et al., 2020). The *trans* site of the TOM complex, formed by the IMS-exposed segments of Tom40, Tom22 and Tom7, was unfortunately not completely resolved in the final cryo-EM structure, but it is clear that all three proteins converge on one side of the TOM complex (Araiso et al., 2019; Tucker and Park, 2019). The *trans* site is also crucial for the coordination of the TOM complex with the TIM23 complex (Tamura et al., 2009; Shiota et al., 2011; Waegemann et al., 2015; Araiso et al., 2019; Günsel et al., 2020; Genge and Mokranjac, 2021).

1.4 The TIM23 complex

The TIM23 complex in the IM is the most complicated mitochondrial protein import machinery and consists of 11 highly evolutionary conserved subunits: the eight essential subunits Tim50, Tim23, Tim17, Tim44, Tim14 (Pam18), Tim16 (Pam16), mtHsp70 (Ssc1 in yeast), Mge1, and the remaining three, Tim21, Pam17 and Mgr2, that are non-essential for cell viability. The various subunits of the TIM23 complex can be functionally divided into the IMS-exposed receptor unit, the IM-embedded core of the complex and the matrix-exposed import motor (Figure 1.3 A and B).

Presequence-containing precursor proteins exiting the TOM complex at its *trans* site, are already at this stage recognized by the IMS exposed receptors of the TIM23 complex (Yamamoto et al., 2002; Mokranjac et al., 2003a; Chacinska et al., 2005; Mokranjac et al., 2009; Tamura et al., 2009; La Cruz et al., 2010; Marom et al., 2011; Lytovchenko et al., 2013). Tim50 is the main receptor of this complex and, together with the intrinsically disordered IMS-exposed segment of Tim23, binds presequences in the IMS (Mokranjac et al., 2009; Tamura et al., 2009; Marom et al., 2011). Additionally, cross-links between both Tim50 and the IMS segment of Tim23 with Tom22 and Tom40, respectively, have been reported lately (Tamura et al., 2009; Shiota et al., 2011; Waegemann et al., 2015; Araiso et al., 2019; Günsel et al., 2020; Gomkale et al., 2021), underlining not only their functions as receptors for recognition of presequences but also in the coordination and transfer of precursor proteins from the TOM to the TIM23 complex. In a membrane potential-dependent step, presequences are then transferred to the core of the TIM23 complex formed by the IM-embedded Tim17 and Tim23 (Truscott et al., 2001; Martinez-Caballero et al., 2007; van der Laan et al., 2007; Alder et al., 2008a; Malhotra et al., 2013; Demishtein-Zohary et al., 2015; Ramesh et al., 2016;

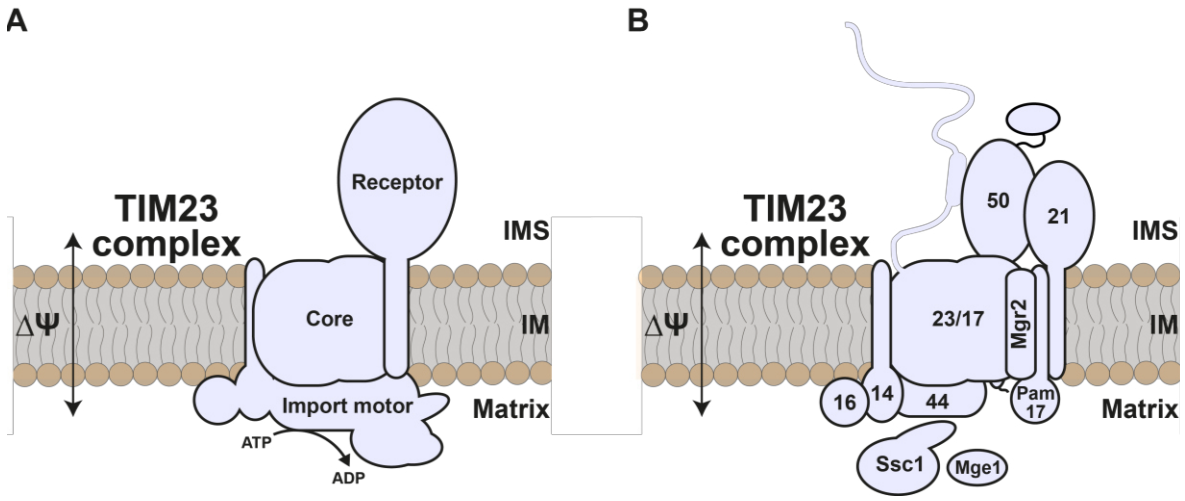

Figure 1.3 Schematic representation of the TIM23 complex. (A) The TIM23 complex can be functionally divided into the IMS-exposed receptor unit, the IM-embedded translocation core and the matrix exposed import motor. (B) The TIM23 complex consists of 11 subunits: Tim50 together with the IMS-exposed segment of Tim23 forms the receptor unit, the translocation core is formed by the IM-embedded segments of Tim23 and Tim17, the import motor consists of mtHsp70, Mge1, Tim14, Tim16 and Tim44 and the three non-essential subunits Tim21, Pam17 and Mgr2 modulate the activity of the complex. See text for details. IMS, intermembrane space; IM, inner membrane; ΔΨ, membrane potential.

Demishtein-Zohary et al., 2017; Fielden et al., 2023; Im Sim et al., 2023). Together with Tim22 from the TIM22 complex, Tim17 and Tim23 belong to the same family of mitochondrial IM proteins with four predicted α-helical TM segments that were suggested to form voltage-activated hydrophilic translocation channels (Truscott et al., 2001; Kovermann et al., 2002; Martinez-Caballero et al., 2007). Recent structural work rather indicates that these proteins form lipid-exposed cavities which represent translocation paths for precursor proteins (Zhang et al., 2021; Im Sim et al., 2023). In case of the TIM23 complex, Tim17 and Tim23 are arranged back-to-back and the available data suggests that the cavity of Tim17 is used for protein translocation with Tim23 having a more structural role (Fielden et al., 2023; Im Sim et al., 2023). The negatively charged patch on the IMS side of the Tim17 cavity and the membrane potential, negative on the matrix side, drive the initial translocation of the positively charged presequences across the IM (Martin et al., 1991; Im Sim et al., 2023; Fielden et al., 2003). Finally, presequences that reach the matrix are proteolytically removed by the mitochondrial processing peptidase (MPP) generating mature polypeptide chains that can fold and assemble into protein complexes (Mossmann et al., 2012). In some cases, additional processing enzymes like the intermediate cleaving peptidase (Icp55) or the octapeptidyl aminopeptidase (Oct1) further process mitochondrial proteins for stabilization and maturation purposes (Vögtle et al., 2009; Vögtle et al., 2011).

For complete translocation of the mitochondrial precursor proteins across the IM, the import motor of the TIM23 complex and an energy input in form of ATP hydrolysis are required. The import motor consists of the peripheral membrane protein Tim44, the ATP-consuming mitochondrial heat shock protein 70 (mtHsp70 or Ssc1 in *S. cerevisiae*) and its co-chaperones Tim14 (Pam18), Tim16 (Pam16) and Mge1. Tim44 is located at the exit of the translocation core of the TIM23 complex on the matrix side where it binds to translocating precursor proteins and recruits the other components of the import motor to the translocation core (Marom et al., 2011; Banerjee et al., 2015; Ting et al., 2017). The major player of the import motor is mtHsp70, a member of the conserved protein family of Hsp70 chaperones that contain a nucleotide-binding domain, which binds and hydrolyses ATP, and a substrate-binding domain, which binds to hydrophobic segments exposed in unfolded proteins (Rosenzweig et al., 2019). Even though the major function of mtHsp70 is protein folding in the mitochondrial matrix, during protein import it drives translocation across the IM through multiple cycles of precursor binding and ATP hydrolysis, regulated by the J-protein complex and the nucleotide exchange factor (NEF) (Craig, 2018; Mokranjac, 2020). The J-protein Tim14, stimulates ATP hydrolysis by mtHsp70, leading to the tight binding of the chaperone to the incoming precursor proteins (D'Silva et al., 2003; Mokranjac et al., 2003b). The J-like protein Tim16 recruits Tim14 to the TIM23 complex and regulates the activity of Tim14 (D'Silva et al., 2005; Mokranjac et al., 2006). Once ATP is hydrolysed, the NEF Mge1, mediates the release of ADP and therefore allows a new ATP molecule to bind to mtHsp70 (Miao et al., 1997). This releases the bound precursor protein from mtHsp70 and resets the ATP hydrolysis cycle. The understanding of the unidirectional import of precursor proteins with the help of the ATP consuming import motor on a molecular level is still missing. Two possible mechanisms were initially suggested. In the “Brownian ratchet” model, mtHsp70 traps precursor proteins in the matrix, preventing their backsliding. According to the second model, mtHsp70 actively pulls the precursor proteins into the matrix (Voisine et al., 1999; Neupert and Brunner, 2002). More recently, an entropic pulling model, which combines parts of both models, was proposed (Los Rios et al., 2006).

Additionally to importing precursor proteins into the matrix, the TIM23 complex can also laterally insert proteins into the IM. When downstream of the presequence precursor proteins carry a hydrophobic sorting signal (also called “stop-transfer” signal), translocation across the IM is stalled and the TIM23 complex inserts the hydrophobic segment of the precursor protein into the IM. The molecular mechanisms of lateral insertion are still not understood. However, previous studies have suggested Mgr2 to act as a lateral gatekeeper of the TIM23 complex and Tim14 and Tim21 to be

involved in lateral insertion as well (Chacinska et al., 2005; D. Popov-Celeketić et al., 2008; Popov-Čeleketić et al., 2011; Ieva et al., 2014; Schendzielorz et al., 2018). The complexity of this protein translocase is further mirrored by its ability to distinguish between *bona fide* TM segments and insert some of them laterally while translocating the others completely across the membrane for subsequent insertion into the IM from the matrix side through the OXA complex (Baumann et al., 2002). Some laterally sorted precursor proteins are further proteolytically processed by the inner membrane protease (IMP), releasing soluble proteins into the IMS (Nunnari et al., 1993). Additionally to matrix-, IM- and IMS-targeted precursor proteins, the TIM23 complex has also been shown to be involved in the unusual import of some OM proteins (Wenz et al., 2014; Sinzel et al., 2016).

The two non-essential subunits of the TIM23 complex, Pam17 and Tim21, seem to modulate the import of presequence-containing precursor proteins. Pam17 was suggested to, antagonistically to Tim21, influence conformational changes of the TIM23 complex (Chacinska et al., 2005; D. Popov-Celeketić et al., 2008) and to be involved, together with Tim50, in the membrane potential dependent import steps of the mature parts of the polypeptide chain (Schendzielorz et al., 2017). The exact molecular mechanisms of these functions remain unclear. Tim21, on the one hand, was shown to link the TIM23 complex to the respiratory chain (van der Laan et al., 2006), which may improve membrane potential-dependent protein translocation across the IM and the assembly of respiratory chain intermediates. On the other hand, Tim21 was also suggested to be involved in TOM-TIM23 cooperation as it efficiently binds to Tom22 *in vitro* (Chacinska et al., 2005; Mokranjac et al., 2005), as well as to modulate the interaction between Tim50 and the IMS segment of Tim23 and their recognition of presequences (Lytovchenko et al., 2013). However, these findings have not been recapitulated in intact mitochondria yet and therefore their biological significance *in vivo* remains unclear.

Even though the major components of the TIM23 complex have most likely all been identified until now, their multiple and dynamic interactions during translocation of presequence-containing precursor proteins remain unclear. To unravel the molecular mechanisms of action of this highly complex import machinery and to understand the different import steps of precursor proteins along the presequence pathway and especially precursor transfer between TOM and TIM23 complexes, high resolution structural analyses, ideally with precursor proteins in transit, coupled with functional biochemical studies will likely be required.

1.5 Coordination between TOM and TIM23 complexes

The TOM and TIM23 complexes coordinate import of presequence-containing precursor proteins into mitochondria. When mitochondria are solubilized and membrane proteins are extracted from the lipid bilayer, the TOM complex does not stably interact with the TIM23 complex or any other of the downstream protein translocases. Interestingly, in isolated mitochondrial OM vesicles or purified TOM components reconstituted into lipid vesicles it was shown that precursor proteins are recognized and their translocation across the OM is initiated. However, the reconstituted TOM complex was not able, on its own, to completely translocate precursor proteins across the membrane (Mayer et al., 1995; Künkele et al., 1998; Ahting et al., 2001; Model et al., 2002). In contrast, the TIM23 complex can transport precursor proteins, in a membrane potential and ATP-dependent manner, across the IM in mitoplasts, which are mitochondria with artificially removed OM (Hwang et al., 1989). When precursor proteins are imported into isolated mitochondria, with an intact OM and IM, presequences can be proteolytically cleaved in the matrix while a large portion of the precursor protein is still outside of mitochondria in the cytosol (Kanamori et al., 1999). If precursor proteins are artificially arrested at this stage of protein import, the two protein translocases are stabilized in a TOM-TIM23 supercomplex intermediate (Chacinska et al., 2003; D. Popov-Celeketić et al., 2008). These experiments indicate that the TOM and TIM23 complexes do not translocate proteins independently of each other but rather mediate import of presequence-containing precursor proteins across two mitochondrial membranes in a tightly coordinated manner (Callegari et al., 2020; Genge and Mokranjac, 2021). The subunits implicated in TOM-TIM23 coordination expose their segments into the IMS and include Tom22, Tom40 and Tom7, from the TOM complex side, and Tim50, Tim23 and Tim21, from the TIM23 side (Figure 1.4).

Initially, all three subunits, Tom22, Tom40 and Tom7, forming the *trans* site of the TOM complex, were shown to be cross-linked to precursor proteins that were artificially arrested in the TOM complex (Kanamori et al., 1999; Esaki et al., 2004). Additionally, genetic deletions of Tom7 and the IMS segment of Tom22 led to the accumulation of precursor proteins in the cytosol (Esaki et al., 2004), further supporting the notion that precursor binding on the IMS side of the TOM complex is required for translocation across the OM. Even in the absence of protein translocation, experiments performed in intact mitochondria and with isolated recombinant proteins showed that the TIM23 complex interacts with the *trans* site of the TOM complex. Both Tim23 and Tim50 were cross-linked to the IMS-exposed segments of Tom22 and Tom40, using chemical and/or site-specific UV cross-

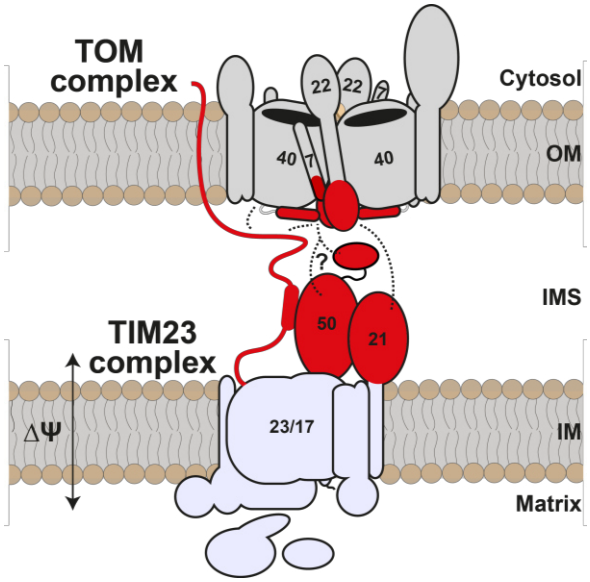

Figure 1.4 Cooperation between TOM and TIM23 complexes during precursor translocation across two mitochondrial membranes. TOM and TIM23 subunits implicated in their cooperation are highlighted in red. Dashed lines represent identified interaction points. OM, outer membrane; IMS, intermembrane space; IM, inner membrane.

linking (Tamura et al., 2009; Shiota et al., 2011; Waegemann et al., 2015; Araiso et al., 2019; Günsel et al., 2020; Gomkale et al., 2021). *In vitro* experiments recapitulated these findings when recombinantly expressed and purified IMS segments of Tim23 and Tim21 were shown to bind to the IMS segment of Tom22 (Chacinska et al., 2005; Mokranjac et al., 2005; Albrecht et al., 2006; Bajaj et al., 2014). Even though a direct interaction between any of these TIM23 subunits with Tom7 has not been reported yet, the recently solved cryo-EM structure of the TOM complex revealed that Tom7 is present in close proximity to the C-terminal, IMS-exposed segments of Tom22 and Tom40 at the *trans* site of the TOM complex (Araiso et al., 2019; Tucker and Park, 2019). Therefore, it is very likely that Tom7 may interact with or is at least in close vicinity of one of the three TIM23 subunits that expose their segments into the IMS. The observed negative genetic interactions of Tom7 with the N-terminal segment of Tim23 or the IMS segment of Tom22 also support this notion (Waegemann et al., 2015). The intrinsically disordered N-terminal segment of yeast Tim23 has an unusual feature to expose its first 20 N-terminal residues on the mitochondrial surface and is thus accessible to externally added proteases in intact mitochondria (Donzeau et al., 2000). This unique feature is dependent on the interaction between Tim50 and Tim23 (Yamamoto et al., 2002; Gevorkyan-Airapetov et al., 2009; Tamura et al., 2009), the presence of the translocating precursor proteins in the TIM23 complex (D. Popov-Celeketić et al., 2008), the membrane potential along the IM (Günsel et al., 2020) and the dynamics of the TOM complex (Waegemann et al., 2015). Even though this segment of Tim23 is not

essential for cell viability (Chacinska et al., 2003; Waegemann et al., 2015) and the mechanism of how it reaches the cytosol is not clear, it is tempting to speculate that by crossing the two mitochondrial membranes, Tim23 may bring the two protein translocases closer together and by that further helps in coordinating the transfer of precursor proteins between TOM and TIM23 complexes. The molecular mechanisms of precursor transfer between the two complexes in the OM and IM, coordinated by various interactions between the TOM and TIM23 subunits is still poorly understood. Tim50, as the main receptor of the TIM23 complex, seems to have a major role in precursor transfer between TOM and TIM23 complexes and the following section describes, in more detail, what is currently known about Tim50.

1.6 The main receptor of the TIM23 complex, Tim50

Tim50 was identified as the main receptor of the TIM23 complex, required for recognition and transfer of presequence-containing precursor proteins between TOM and TIM23 complexes. Tim50 consists of an N-terminal positively charged presequence, that is proteolytically cleaved during import, a short matrix-exposed segment followed by a TM segment and a large IMS-exposed segment (Figure 1.5). The matrix-exposed and TM segments of Tim50 can be deleted under standard growth conditions without any obvious impairment of growth (Mokranjac et al., 2009), however, they were recently shown to have regulatory roles during translocation of precursor proteins and recruitment of the import motor under specific growth conditions that require a particularly high mitochondrial activity (Caumont-Sarcos et al., 2020). The IMS segment of Tim50, however, is sufficient to replace the function of the full-length protein, demonstrating that it carries the essential functions of Tim50 (Mokranjac et al., 2009).

Tim50 is recruited to the TIM23 complex through its interaction with Tim23, which has been extensively analysed *in vitro*, *in vivo* and *in organello* (Geissler et al., 2002; Yamamoto et al., 2002; Mokranjac et al., 2003a; Alder et al., 2008b; Gevorkyan-Airapetov et al., 2009; Tamura et al., 2009; Qian et al., 2011; Schulz et al., 2011; Lytovchenko et al., 2013; Malhotra et al., 2017; Dayan et al., 2019; Günsel et al., 2020). Next to the IMS segment, it was suggested that the TM segment of Tim50 is involved in the interaction of Tim50 with Tim23 as well and that this interaction is regulated by the lipid composition in the IM (Malhotra et al., 2017). Additionally, Tim50 was efficiently cross-linked to Tim21 *in organello* (Lytovchenko et al., 2013), however, the biological relevance of this interaction is still not clear. As briefly mentioned before, Tim50 is also involved in TOM-TIM23 cooperation as the C-terminal, IMS-exposed segments of both Tom22 and Tom40 were shown to be cross-linked to Tim50

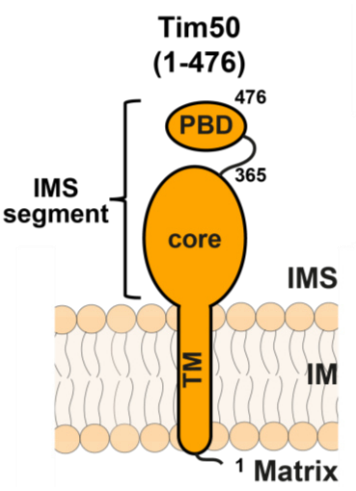

Figure 1.5 Tim50, the main receptor of the TIM23 complex. Schematic representation of the domain structure of Tim50. The IMS segment of Tim50 consists of two domains – the core domain and the presequence-binding domain (PBD). 1 and 476 indicate the first and the last amino acid residue of Tim50 precursor and 365 the last residue of the core domain. TM, transmembrane segment; IMS, intermembrane space; IM, inner membrane.

using chemical and site-specific UV cross-linking in intact mitochondria (Tamura et al., 2009; Shiota et al., 2011; Waegemann et al., 2015; Araiso et al., 2019).

As the main receptor, Tim50 is the first subunit of the TIM23 complex that recognizes incoming presequences, since it can be cross-linked to precursor proteins arrested at the *trans* site of the TOM complex in intact mitochondria (Yamamoto et al., 2002; Mokranjac et al., 2003a; Mokranjac et al., 2009). Mutations that destabilize the Tim50-Tim23 interaction led to impaired precursor binding to Tim50 and overall import defects showing that the receptor function of Tim50 depends on its interaction with Tim23 (Mokranjac et al., 2009; Tamura et al., 2009). Presequences can also bind directly to Tim23, but they do so with considerably lower binding affinity than to Tim50 (Bauer et al., 1996; La Cruz et al., 2010; Marom et al., 2011; Lytovchenko et al., 2013). Binding of precursor proteins by Tim50 and/or Tim23 was also recapitulated in *in vitro* binding studies with recombinantly expressed and purified proteins and presequence peptides (Marom et al., 2011). Both the interactions of Tim50 with Tom22 and with Tim21 are modulated by precursor proteins, which further highlights their involvement during precursor transfer from TOM to TIM23 complexes. While precursor proteins increased chemical cross-linking between Tim50 and Tom22 (Waegemann et al., 2015) and decreased a site-specific cross-link between the two proteins (Shiota et al., 2011), interaction between Tim50 and Tim21 was dissociated in the presence of presequence peptides (Lytovchenko et al., 2013).

A few years back, the actual presequence-binding site was surprisingly mapped to the C-terminal part of the IMS segment of Tim50 through *in vitro* experiments with recombinantly expressed and purified Tim50 and presequence peptides (Schulz et al., 2011). This led to the proposal that the IMS segment of Tim50 consists of two domains – the highly conserved core domain (aa 133-365) and the presequence-binding domain (PBD) (aa 366-476) (Figure 1.5 A). Even though the core domain is ubiquitously present among eukaryotes, the PBD of Tim50 was so far only identified in Fungi (Rahman et al., 2014; Callegari et al., 2020) and intriguingly, its deletion is lethal for yeast cells (Schulz et al., 2011). The crystal structure of the core domain of Tim50, however, revealed a negatively charged groove that was proposed to be a presequence-binding site as well (Qian et al., 2011). Subsequent biochemical experiments with recombinantly expressed and purified Tim50 variants showed that both the core and PBD of Tim50, can bind presequences on their own (Lytovchenko et al., 2013). NMR studies further suggested that the core and PBD of Tim50 interact with each other and that this is modulated by the presence of presequences (Rahman et al., 2014). Additionally to the observation of binding presequences, the PBD has been proposed to be involved in the interaction of Tim50 with Tim23 and Tom22. While all the so far identified mutations that impair the interaction of Tim50 with Tim23 have been mapped to two distinct regions on the core domain of Tim50 (Tamura et al., 2009; Qian et al., 2011; Dayan et al., 2019), a NMR study with recombinantly expressed and purified proteins suggested that an efficient complex formation of Tim50 with the IMS segment of Tim23 required the presence of the PBD (Bajaj et al., 2014). A recent publication also observed a specific cross-link between Tim23 and the PBD of Tim50 through MS (Gomkale et al., 2021). Chemical cross-links between Tom22 and Tim50 were abolished when the PBD was lacking (Waegemann et al., 2015), indicating that the PBD may be involved, directly or indirectly, in TOM-TIM23 cooperation as well.

Understanding of the multiple and dynamic interactions of the TOM and TIM23 subunits that coordinate the transfer of precursor proteins between two mitochondrial membranes, and in particular of presequence recognition in the IMS, is still very limited. Which domain of Tim50 is involved in which of the identified interactions of Tim50 and how do they change during translocation of proteins into mitochondria? Do the two domains of Tim50 also bind presequences individually *in vivo* or do they rather form a presequence-binding site together? Or are the core and PBD of Tim50 maybe involved in the recognition of presequences during different stages of protein translocation? If the PBD of Tim50 is indeed only fungi-specific, how do higher eukaryotes deal with the lack of this domain? These are just some of the open questions that remain unanswered so far, which this study tries to address.

1.7 Tim50 in human diseases

Tim50 is encoded by an essential gene in yeast and its homologues are present throughout the eukaryotic kingdom, including humans (Geissler et al., 2002; Yamamoto et al., 2002; Mokranjac et al., 2003a). The importance of understanding the molecular mechanisms of Tim50 function has recently gained unexpected support from several clinical findings. Namely, two recent studies demonstrated that severe intellectual disability and epilepsy as well as rapidly progressive encephalopathy in the affected individuals are caused by mutations in Tim50 (Shahrour et al., 2017; Reyes et al., 2018). Furthermore, it was shown that overexpression of human Tim50 (hTim50) is directly associated with the increased proliferation and migration rates of tumour cells in patients with breast cancer and non-small cell lung cancer (Gao et al., 2016; Zhang et al., 2019). Suppression of hTim50 expression inhibited proliferation of cancer cells and induced apoptosis, suggesting that this may be a potential approach to control the progression of breast cancer. Another publication demonstrated that Tim50 in humans is a negative regulator of pathological cardiac hypertrophy, primarily by reducing oxidative stress (Tang et al., 2017). Therefore, studying the functions of Tim50 may provide novel insights into the molecular mechanisms of biogenesis of mitochondria, and considering the involvement of Tim50 in various human pathologies, they may also help in understanding the underlying molecular mechanisms of these diseases.

1.8 Aim of study

The aim of this thesis was to gain novel insights into the molecular mechanisms of TOM-TIM23 cooperation during protein import into mitochondria using *Saccharomyces cerevisiae* as a model system. In particular, the contributions of the two domains of Tim50 in the IMS to the function of this protein were to be investigated. Therefore, the individual functions and interaction partners, as well as the dynamic interplay between the core and PBD of Tim50 were to be dissected both *in vivo* and *in vitro*.

2. MATERIALS AND METHODS

2.1 Molecular Biology

2.1.1 Isolation of plasmid DNA from *E. coli*

2.1.1.1 Small-scale crude plasmid isolation (Miniprep)

For small-scale plasmid DNA isolation (Mini prep), *Escherichia coli* (*E. coli*) (MH1) colonies were inoculated into 2 mL of LB+Amp and grown ON at 37 °C with vigorous shaking at 160 rpm. Next day, cells were harvested in a 2 mL Eppendorf tube at 16,000 x g, 1 min, RT, supernatant was discarded and the cell pellet was resuspended in 400 µL of "E1 - cell resuspension" buffer (50 mM Tris-HCl, 10 mM EDTA, pH 8). Cells were lysed by adding 400 µL of "E2 - cell lysis" buffer (0.2 M NaOH, 1 % (w/v) SDS) and gently inverting the tube 10 times. After 2 min incubation at RT, the cell lysate was neutralized by adding 400 µL of "E3 – neutralization" buffer (3.1 M KAc in 99 % acetic acid) and gently inverting the tube 10 times again. The lysate was clarified by centrifugation at 16.000 x g, 10 min, RT. Plasmid DNA was precipitated by adding 850 µL of the supernatant to 600 µL of isopropanol, inverting the tube 10 times and incubating it for 2 min at RT. Subsequently, the tube was centrifuged at 16,000 x g, 20 min, RT. Supernatant was discarded and the pellet was washed by adding 200 µL of ice-cold 70 % ethanol and centrifugation at 16,000 x g, 5 min, RT. Ethanol was removed and the pellet was air-dried for a couple of minutes at RT. Finally, DNA was resuspended in 20 µL sterile dH_2O containing 0.1 mg/mL RNase and the tube was shaken for 15 min at RT. Plasmid DNA was stored at -20 °C until use.

2.1.1.2 Large-scale plasmid isolation (Midiprep)

For large-scale plasmid DNA isolation (Midiprep) out of *E. coli* (MH1) cells the "PureYield Plasmid Midiprep kit" from Promega was used. Either a single colony from an LB+Amp plate or 200 µL of a remaining cell suspension for Miniprep was used to inoculate 45 mL of LB+Amp medium. Following the manufacturer`s instructions, the culture was grown ON at 37 °C with vigorous shaking at 160 rpm. Next day, cells were transferred into a centrifuge tube and pelleted by centrifugation at 10,000 x g, 10 min, RT. The supernatant was discarded and the pellet was resuspended in 6 mL of "Cell Resuspension Solution" and lysed through addition of 6 mL of "Cell Lysis Solution". After mixing by gently inverting the tube 3-5 times, cells were incubated for 3 min at RT with the lid open. Subsequently, 10 mL of "Neutralization Solution" was added and the mixture was inverted 3-5 times and incubated for another 2 min at RT. To remove precipitated proteins and genomic DNA, the

solution was centrifuged at 27,000 x g, 10 min, RT. The supernatant was poured into a blue PureYield Clearing Column placed on top of a white PureYield Binding Column on a vacuum manifold. Vacuum was applied to pass the supernatant through both columns. After removing the clearing column, the binding column was subsequently washed with 5 mL of "Endotoxin Removal Wash" solution followed by 20 mL of "Column Wash" solution. After the washing steps, the membrane was dried by applying vacuum for 30 sec to remove residual ethanol. To elute plasmid DNA, the binding column was placed on top of a 1.5 mL Eppendorf tube and 600 µL of sterile dH_2O were added onto the membrane of the binding column. After 1 min incubation at RT, vacuum was applied to elute the plasmid DNA into the Eppendorf tube. Plasmid DNA was stored at -20 °C until use.

2.1.2 Isolation of genomic DNA from *S. cerevisiae*

Yeast genomic DNA was isolated using the "Wizard Genomic DNA Extraction Kit" (Promega) according to the manufacturer´s instructions. Briefly, yeast culture was grown ON in 3 mL YPD medium at 30 °C and vigorous shaking at 160 rpm. Next day, 1.5 mL of yeast culture was harvested in a 2 mL Eppendorf tube by centrifugation at 3,000 x g, 5 min, RT and the cell pellet was resuspended in 293 µL of 50 mM EDTA, pH 8.0. To the resuspended cells, 7.5 µL zymolase (10 mg/mL) was added and the samples were incubated for 1 h at 30 °C. After incubation, cells were reisolated by centrifugation at 16,000 x g, 2 min, RT and subsequently resuspended in 300 µL of "Nuclei Lysis Solution". To the resuspended cells, 100 µL of "Protein Precipitation Solution" was added and the samples were incubated for 5 min on ice. After centrifugation at 16,000 x g, 3 min, RT, the supernatant was transferred into a 1.5 mL Eppendorf tube containing 300 µL of isopropanol. The samples were centrifuged at 16,000 x g, 2 min, RT, the supernatant was removed and the precipitated DNA was washed using 1 mL of ice-cold 70 % ethanol. Finally, the DNA was reisolated by centrifugation at 16,000 x g, 2 min, RT, the supernatant was removed, and residual ethanol was evaporated for around 10 min at RT. To rehydrate the DNA, 50 µL of "DNA Rehydration Solution" containing 100 µg/µL RNase was added and the DNA was incubated first for 15 min at 37 °C, followed by 1 h at 65 °C. Isolated yeast genomic DNA was stored at -20 °C until use.

2.1.3 Amplification of DNA fragments

2.1.3.1 Polymerase chain reaction (PCR)

DNA fragments were amplified by Polymerase chain reaction (PCR). For the amplification of DNA fragments used in restriction enzyme cloning (REC) (2.1.8.1), a purified plasmid was used as a

template. A PCR reaction was usually set in a 50 µL PCR mix with the following reagents in given quantities: 1 µL dNTPs (10 mM each), 2.8 µL forward and reverse primers (20 mM) respectively, 10 µL of Phusion HF (5x) buffer, 0.5 µL Phusion HF polymerase, 20 ng purified plasmid and sterile dH_2O to a final volume of 50 µL. The following PCR cycle protocol was used for amplification (Table 2.1). Elongation time was determined depending on the length of the DNA Fragment to be amplified (30 sec per 1 kb). PCR reactions were analysed by agarose gel electrophoresis (2.1.4.1). In case of unspecific amplification products, gel extraction (2.1.4.2) was used to purify the desired PCR product for further applications.

Table 2.1 PCR cycle protocol for restriction enzyme cloning.

PCR step	Temperature	Time
Initial denaturation	95 °C	3 min
PCR cycles (30 cycles)		
Denaturation	95 °C	30 sec
Annealing	50 °C	30 sec
Extension	72 °C	30 sec/kb
Final extension	72 °C	10 min
Hold	8 °C	∞

To introduce point mutations by site-directed mutagenesis (SDM) (2.1.8.2), a gradient PCR was performed. Primers used to amplify the whole plasmid during a gradient PCR, were first phosphorylated for 1 h at 37 °C using T4 polynucleotide kinase (PNK) with the following reagents in given quantities: 2 µL of ATP (10 mM), 7 µL of primer (100 µM), 2 µL of PNK (10x) buffer, 1 µL of T4 PNK and sterile dH_2O to a final volume of 20 µL. The reaction was stopped by heating to 95 °C for 5 min and adding 50 µL dH_2O, generating phosphorylated primers with a concentration of 10 µM. The master mix for the gradient PCR was usually set with 61.8 µL dH_2O, 2 µL dNTPs (10 mM each), 5.6 µL phosphorylated forward and reverse primers (10 µM) respectively, 20 ng purified plasmid as template, 20 µL Phusion HF (5x) buffer and 1 µL Phusion HF polymerase. The master mix was split into 8 PCR tubes á 10 µL and the PCR reaction was performed using following gradient PCR cycle protocol (Table 2.2). PCR reactions were analysed by loading 1 µL on an agarose gel (2.1.4.1). Clean PCR products were directly used for ligation (2.1.5.2).

Table 2.2 Gradient PCR cycle protocol for site-directed mutagenesis.

PCR step	Temperature	Time
Initial denaturation	95 °C	5 min
PCR cycles (25 cycles)		
Denaturation	95 °C	30 sec
Annealing	50-70°C	30 sec
Extension	72 °C	30 sec/kb
Final extension	72 °C	10 min
Hold	8 °C	∞

2.1.3.2 Colony PCR

One approach to pre-select and identify the correct clones after transformation, was colony PCR. *E. coli* colonies were picked from LB+Amp plates and resuspended in 10 µL of sterile dH_2O in a 1.5 mL Eppendorf tube. A colony PCR reaction was usually set in multiple 10 µL PCR mixes with the following reagents in given quantities: 0.08 µL dNTPs (10 mM each), 2 µL OneTaq Quick-Load Reaction (5x) buffer, 0.25 µL forward and reverse primers (20 mM) respectively, 0.1 µL OneTaq polymerase, 1 µL of the *E. coli* cell suspension and sterile dH_2O to a final volume of 10 µL. The remaining *E. coli* cell suspension was kept to subsequently inoculate for Midiprep, in case of a positive result. The colony PCR reaction was performed using following colony PCR cycle protocol (Table 2.3). For yeast colony PCRs, a small tip of yeast cells was transferred into a PCR tube and microwaved for 1 min at full power, before the PCR mix was added to the cells.

Table 2.3 Colony PCR cycle protocol.

PCR step	Temperature	Time
Initial denaturation	95 °C	3 min
PCR cycles (35-40 cycles)		
Denaturation	95 °C	30 sec
Annealing	50°C	30 sec
Extension	72 °C	1 min/kb
Final extension	72 °C	10 min
Hold	8 °C	∞

2.1.4 Detection and analysis of DNA

2.1.4.1 Agarose gel electrophoresis

For the analysis of DNA fragments from PCR reactions or restriction enzyme digestions, agarose gel electrophoresis was performed. An 0.8 % agarose solution was prepared by weighing in 4 g of agarose, mixing it with 500 mL of TAE buffer (40 mM Tris-acetate, 20 mM Na-acetate, 1 mM EDTA, pH 7.5) and boiling in a microwave until a clear solution was obtained. The liquid agarose was stored in a 65 °C incubator to avoid solidification. The agarose solution was poured into a cast and one drop of ethidium bromide (ca. 250 µg/mL) was added. After mixing the agarose solution with the ethidium bromide, a comb was inserted and the cast was left under the fume hood until the agarose gel was solidified completely. DNA samples were mixed with a DNA Gel Loading Dye (6x) and then loaded into the wells of the agarose gel. The agarose gel was run at constant voltage of 100 V for 20-25 min. DNA fragments were made visible by exposing the agarose gel to UV light at 360 nm using a Vilber Fusion FX6 Edge system.

2.1.4.2 DNA extraction from the gel

DNA extraction from an agarose gel was performed using the "mi-Gel Extraction Kit" from Metabion. After agarose gel electrophoresis (2.1.4.1) was performed, the DNA fragments were visualized by exposing the agarose gel to UV light at 360 nm and the DNA band of interest was cut out of the gel by using a sharp scalpel. The gel slice was transferred into a 2 mL Eppendorf tube and gel extraction was performed according to the manufacturer`s instructions. Briefly, 0.7 mL of "GEX buffer" was added to the gel slice and the tube was shaken at 60 °C and 1600 rpm for at least 10 min until the gel was fully dissolved. Subsequently, a maximum of 0.7 mL of the gel solution was loaded on a "GP column" placed on a collection tube and centrifuged at 10,000 x g for 30 sec. Flow-through was discarded and the procedure was repeated until the complete gel solution was passed through the column. The column was then washed with 0.5 mL of "WN buffer" by centrifuging at 10,000 x g for 30 sec. After discarding the flow-through, this step was repeated with 0.5 mL of "WS buffer". Finally, residual buffer and ethanol was removed by centrifuging at 16,000 x g for 1 min. DNA was eluted from the column into a sterile 1.5 mL Eppendorf tube by adding 30 µL of sterile dH_2O and incubating it for 1 min followed by centrifugation at 16,000 x g for 1 min. DNA was analysed by agarose gel electrophoresis (2.1.4.1) and stored at -20 °C until further use.

2.1.4.3 Column purification of DNA fragments

PCR fragments without unspecific DNA bands were directly purified after PCR using the "mi-PCR Purification Kit" by Metabion. Following the manufacturer's instructions for the "purification by centrifugation", 10-100 µL of the PCR reaction was pipetted into a 1.5 mL Eppendorf tube and diluted with 500 µL of "PX buffer". For PCR fragments smaller than 500 or larger than 5,000 base pairs, 0.25x the total sample volume of isopropanol was added, to increase the DNA recovery rate. The mixture was loaded onto a "GP column" placed on top of a collection tube and centrifuged at 10,000 x g for 30 sec. Subsequent steps were identical to the ones in the protocol for "DNA extraction from the gel" (2.1.4.2).

2.1.4.4 Quantification of DNA

Concentration of purified DNA plasmids was determined with a NanoDrop spectrophotometer by measuring the absorbance at 260 nm of 1.5 µL of DNA sample. Sterile dH_2O was used as a blank.

2.1.5 Enzymatic manipulation of DNA

2.1.5.1 Restriction digestion

Restriction digestion was used on preparative scale to generate overhangs with sticky ends for the subsequent ligation of DNA fragments and on analytical scale to identify correct clones of transformed DNA after colony PCR as well as to pre-check the DNA plasmids after Mini- or Midiprep plasmid isolation. Reaction buffers and temperature for digestion were chosen for each restriction enzyme according to the instructions of the manufacturer New England Biolabs (NEB). On a preparative scale, a 60 µL reaction was pipetted typically with the following reagents in given quantities: 10–40 µL of vector or purified PCR product, 2 µL CutSmart (10x) buffer, 1,5 µL of each restriction enzyme from NEB respectively, and sterile dH_2O to a final volume of 60 µL. The reaction was incubated for 1,5 h typically at 37 °C. The digested DNA products were analysed by agarose gel electrophoresis (2.1.4.1) and either purified through gel extraction (2.1.4.2) or column purification (2.1.4.3). On an analytical scale, a 20 µL reaction was pipetted typically with the following reagents in given quantities: 500-1,000 ng of DNA, 2 µL of CutSmart (10x) buffer and 0,5 µL of each restriction enzyme from NEB respectively. The reactions were incubated for 45 min at 37 °C and analysed by agarose gel electrophoresis (2.1.4.1).

2.1.5.2 Ligation

Digested DNA fragments with compatible sticky ends, as well as PCR products from site-directed mutagenesis cloning were set for ligation to obtain the final plasmid of interest. For restriction enzyme cloning, a 10 µL reaction was set, using following reagents in given quantities: 100 ng of digested vector, 10 fold molar excess of digested insert, 1 µL of T4 DNA Ligase (10x) buffer, 0,5 µL of T4 DNA Ligase and sterile dH_2O to reach the total volume of 10 µL. For SDM cloning, 0,5–8 µL of PCR product (depending on the PCR efficiency) was used, instead of digested vector and insert. The reaction was incubated for 2 h at 25 °C (and ON at 16 °C after transformation). Finally, 1 µL of the ligation mix was directly transformed into electrocompetent *E. coli* (MH1) cells (2.1.7).

2.1.6 Preparation of electrocompetent *E. coli* (MH1 and BL21(DE3)) cells

Electrocompetent bacterial MH1 or BL21(DE3) *E. coli* cells (Table 2.4) were inoculated in 50 mL of LB medium and grown ON at 37°C with vigorous shaking at 160 rpm. Next day, 2 mL of the ON culture was diluted into 1 L of fresh LB medium and further grown at 37 °C until OD_{600} of 0.5-0.6 was reached. After cooling on ice for 30 min, the culture was centrifuged at 4,400 x g, 5 min, 4 °C. The cell pellet was resuspended sequentially in 400, 200 and 50 mL of 10 % glycerol and centrifuged each time at 4,400 x g, 5 min, 4 °C, respectively. In the last step, cells were resuspended in 1 mL of 10 % glycerol and portioned in 45 µL aliquots. Electrocompetent *E. coli* cells were stored at –80 °C until use.

Table 2.4 *E. coli* strains used in this thesis.

***E. coli* strain**	**Method**	**Reference**
MH1	Cloning (REC/SDM) (2.1.8)	(Casadaban and Cohen, 1980)
BL21(DE3)	Recombinant protein expression (2.4.2.1)	From Novagen

2.1.7 Transformation of *E. coli* cells by electroporation

For the transformation of *E. coli* cells by electroporation, an aliquot of electrocompetent MH1 or BL21(DE3) cells was taken out of the -80 °C freezer and immediately put on ice. Once the cells were thawed, 1 µL of a purified plasmid or the ligation mix was pipetted into 45 µL of electrocompetent *E. coli* cells. The cell suspension was stirred using a sterile pipette tip and subsequently pipetted into an ice-cold electroporation cuvette. Electroporation of the cells was performed using an Electroporator (Eppendorf) set to a high voltage pulse of 2500 V. Transformed cells were resuspended in 1 mL of liquid LB medium, transferred into a 1.5 mL Eppendorf tube and shaken for 30 min at 37 °C and

160 rpm for recovery. Finally, cells were either directly diluted into liquid LB+Amp medium or plated on LB+Amp plates and grown ON at 37 °C.

2.1.8 Cloning strategies

2.1.8.1 Restriction enzyme cloning (REC)

Restriction enzyme cloning (REC) was used to integrate an PCR amplified insert into a vector to generate a new DNA plasmid (Table 2.5). DNA fragments were usually PCR amplified (2.1.3.1) with primers carrying suitable restriction sites and a corresponding template, summarised in Table 2.6. After amplification, PCR products were run on an agarose gel (2.1.4.1) and the DNA fragment of the correct size was cut out and extracted from the gel (2.1.4.2). Typically, another small analytical agarose gel was run to analyse PCR efficiency. Then, both the PCR amplified insert and the vector were digested with the same restriction enzymes (2.1.5.1). In some cases, the insert was directly cut out from another plasmid for subcloning. Digested insert and vector were run on an agarose gel and extracted out of the gel once more. Subsequently, another analytical agarose gel was run to estimate the ratio between digested insert and vector to be used during ligation (2.1.5.2). After ligation, *E. coli* cells were transformed (2.1.7) and plated on LB+Amp plates for ON growth at 37 °C. Correct colonies were identified by Miniprep (2.1.1.1) followed by restriction digestion (2.1.5.1) or colony PCR (2.1.3.2). Usually, two colonies carrying the correct plasmids were inoculated for Midiprep (2.1.1.2), re-tested via restriction digestion and finally, sent for sequencing for sequence confirmation.

2.1.8.2 Site-directed mutagenesis (SDM)

Site-directed mutagenesis (SDM) was used to generate point mutations into or truncate the coding sequence of an existing DNA plasmid. Primers were designed to PCR amplify (2.1.3.1) the complete DNA sequence of a template (Table 2.6), usually introducing a silent mutation, which either added or removed a restriction site for the identification of the correct clones. Primers were phosphorylated before PCR amplification to allow direct ligation of the PCR products. After PCR amplification (2.1.3.1) and agarose gel electrophoresis (2.1.4.1) of the PCR reactions, the PCR products were either directly set for ligation (2.1.5.2) or if multiple unspecific PCR bands were obtained, PCR products were first purified through gel extraction (2.1.4.2) or column purification (2.1.4.3). After ligation, *E coli* cells were transformed (2.1.7) and plated on LB+Amp plates for ON growth at 37 °C. Correct colonies carrying the final plasmid of interest were identified and confirmed as described for restriction enzyme cloning (2.1.8.1).

2.1.9 Overview of used plasmids and primer pairs

Table 2.5 List of plasmids used in this thesis. The plasmids are numbered from 1 to 49 and the corresponding primer pairs are listed in Table 2.6.

No.	Plasmid	Reference
1	pETDuet-1-6xHis-TEV-Tim50IMS(164-476)	This thesis
2	pETDuet-1-6xHis-TEV-Tim50core(164-361)	This thesis
3	pETDuet-1-6xHis-TEV-Tim50PBD(366-476)	This thesis
4	pRS314-prom-Tim50(1-476)-flank	(Mokranjac et al., 2009)
5	pRS314-prom-Tim50(1-365)-flank	This thesis
6	pRS315-prom-b_2(1-167)-Tim50(131-476)-flank	(Mokranjac et al., 2009)
7	pRS315-prom-b_2(1-167)-Tim50(366-476)-flank	This thesis
8	pRS315-prom-Tim50(Δ131-365)-flank	This thesis
9	pRS317-GPD-Tim50(1-476)	This thesis
10	pRS317-GPD-Tim50(1-365)	This thesis
11	pRS315-prom-Tim50(Δ164-365)	This thesis
12	pRS317-GPD-Tim50(Δ164-365)	This thesis
13	pRS314-prom-Tim50(Δ164-365)+15flex-flank	This thesis
14	pRS317-GPD-b_2(1-167)-Tim50(366-476)-flank	This thesis
15	pRS315-prom-b_2(1-167)-Tim50(132-365)-flank	This thesis
16	pRS314-prom-b_2(1-167)-Tim50(132-365)-flank	This thesis
17	pRS314-prom-Tim50(1-370)-flank	This thesis
18	pRS314-prom-Tim50(1-380)-flank	This thesis
19	pRS314-prom-Tim50(1-390)-flank	This thesis
20	pRS314-prom-Tim50(1-394)-flank	This thesis
21	pRS315-prom-b_2(1-167)IMPmut(E80G)-Tim50(366-476)-flank	This thesis
22	pGEM4-AAC	(Banerjee et al., 2015)
23	pGEM4-b_2(1-167)Δ19DHFR	(Banerjee et al., 2015)
24	pGEM4-b_2(1-167)DHFR	(Banerjee et al., 2015)
25	pGEM4-DLD1	(Banerjee et al., 2015)
26	pGEM4-F1α	Mokranjac group
27	pGEM4-F1β	(Banerjee et al., 2015)
28	pGEM4-Oxa1	(Banerjee et al., 2015)
29	pGEM4-Su9(1-69)DHFR	(Banerjee et al., 2015)
30	pRS314-prom-Tim50(1-476)_A257C-flank	This thesis
31	pRS314-prom-Tim50(1-476)_A257C_I413C-flank	This thesis
32	pRS314-prom-Tim50(Δ366-394)+15flex1-flank	This thesis
33	pRS314-prom-Tim50(Δ366-394)+15rig1-flank	This thesis
34	pRS314-prom-Tim50(Δ366-389)+15flex1-flank	This thesis
35	pRS314-prom-Tim50(Δ366-389)+15rig1-flank	This thesis
36	pRS314-prom-Tim50(Δ366-389)+15flex2-flank	This thesis
37	pRS314-prom-Tim50(Δ366-389)+15rig2-flank	This thesis
38	pRS314-prom-Tim50(Δ371-389)+15flex1-flank	This thesis
39	pRS314-prom-Tim50(Δ371-389)+15rig1-flank	This thesis
40	pRS314-prom-Tim50(Δ371-389)+15flex2-flank	This thesis
41	pRS314-prom-Tim50(Δ371-389)+15rig2-flank	This thesis
42	pRS314-prom-Tim50(Δ371-389)+15rig3-flank	This thesis
43	pRS314-prom-Tom22(1-152)-His_6-flank	(Waegemann et al., 2015)

44	pRS315-prom-Tim50(1-476)-flank	Mokranjac group
45	pRS315-prom-Tim50(Δ371-389)+15flex1-flank	This thesis
46	pRS315-prom-Tim50(Δ371-389)+15rig1-flank	This thesis
47	pETDuet-1-6xHis-TEV-Tim50IMS(133-476)	Mokranjac group
48	pETDuet-1-6xHis-TEV-Tim50core(133-370)	This thesis
49	pVT-102U-Tim50(1-476)	(Mokranjac et al., 2009)

Table 2.6: List of primers used in this thesis. Primers are listed as pairs of forward (fw) and reverse (rv) primers with their corresponding name and sequence from 5' to 3' end. Templates, cloning method (REC or SDM), restriction enzymes and the final generated plasmid are stated for each pair of primers. REC, restriction enzyme cloning (2.1.8.1); SDM, site-directed mutagenesis (2.1.8.2).

Mutation	Forward (fw)/ reverse (rv) primer	Name	Sequence (5' → 3')	Template	Method	Restr. enzyme	Final plasmid
Tim50(164-476) in pET-Duet1	fw	BamTEVTim50IMS164F	CCGGATCCTGAAAATCTATATTTTCAAGGTTTCAACTCAATGTTCACCTACTTC	47	REC	BamHI	1
	rv	Tim50Hind	CCCAAGCTTTTATTTGGATTCAGCAATCTTC			HindIII	
Tim50core(164-361) in pET-Duet1	fw	BamTEVTim50IMS164F	(same as for plasmid No. 1)	47	REC	BamHI	2
	rv	HindTim50IMS361R	CCAAGCTTTTATTTTTTCACACGATGATC			HindIII	
Tim50PBD(366-476) in pET-Duet1	fw	Fw366for50PBD	TTTTACGGAGATCATAAATCTGGTG	47	SDM	-	3
	rv	TEVRevfor50PBD	ACCTTGAAAATATAGATTTTCAGG				
Tim50(1-365) in pRS314	fw	FwAfter50_476flank	TTTTCATGTAAACCCTCTTCTCATG	4	SDM	-	5
	rv	Tim50_365StopHind	GGGAAGCTTTTATTTATCCTTCAATTTTTTCACAC				
b_2(1-167)-Tim50(366-476) in pRS315	fw	Fw366for50PBD	(same as for plasmid No. 3)	6	SDM	-	7
	rv	Revb2_50pRS	GGATCCTTGAAGGGGACCCAATTTTTTC				
Tim50(Δ131-365) in pRS315	fw	Fw366for50PBD	(same as for plasmid No. 3)	44	SDM	-	8
	rv	Rev_50_TM_130	GTAGATTGCAGTACCTGTCAACGCAGACAACG				
Tim50(1-476) in pRS317-GPD	fw	EcoTim50	CCCGAATTCATGCTGTCCATTTTAAGAAATTC	4	REC	EcoRI	9
	rv	Tim50Hind	(same as for plasmid No. 1)			HindIII	
Tim50(1-365) in pRS317-GPD	fw	EcoTim50	(same as for plasmid No. 9)	4	REC	EcoRI	10
	rv	Tim50_365StopHind	(same as for plasmid No. 5)			HindIII	
Tim50(Δ164-365) in pRS315	fw	Fw366for50PBD	(same as for plasmid No. 3)	44	SDM	-	11
	rv	Rev_50_TM_163	CCTGGCCTTGAATCTTTTATACATAAGTG				
Tim50(Δ164-365) in pRS317-GPD	fw	EcoTim50	(same as for plasmid No. 9)	11	REC	EcoRI	12
	rv	Tim50Hind	(same as for plasmid No. 1)			HindIII	

Tim50(Δ164-365)+15flex-flank in pRS314	fw	Fw_8flex_366_50	GGTGGTAGTGGTGGCGGAGGATCCTTTTACGGAGATCATAAATCTGGTGGC	4	SDM	-	13
	rv	Rv_50_TM_163+7flex	ACCTCCAGACCCTCCGCCGCCCCTGGCCTTGAATCTTTTATACATAAGTG				
b_2(1-167)-Tim50(366-476) in pRS317-GPD	fw	EcoCytb2	CCCGAATTCATGCTAAAATACAAACCTTTAC	7	REC	EcoRI	14
	rv	Tim50Hind	(same as for plasmid No. 1)			HindIII	
b_2(1-167)-Tim50(132-365) in pRS315	fw	FwAfter50_476flank	(same as for plasmid No. 5)	6	SDM	-	15
	rv	Tim50_365StopHind	(same as for plasmid No. 5)				
b_2(1-167)-Tim50(132-365) in pRS314	Subclone from pRS315			15	REC	SacI	16
						Xho	
Tim50(1-370) in pRS314	fw	FwAfter50_476flank	(same as for plasmid No. 5)	4	SDM	-	17
	rv	Rv_Tim50_370_stopp	TTAATGATCTCCGTAAAATTTATCCTTC				
Tim50(1-380) in pRS314	fw	FwAfter50_476flank	(same as for plasmid No. 5)	4	SDM	-	18
	rv	Rv_Tim50_380_stopp	TTATGCCGTCATTGCCCAGTTGCCACCAG				
Tim50(1-390) in pRS314	fw	FwAfter50_476flank	(same as for plasmid No. 5)	4	SDM	-	19
	rv	Rv_Tim50_390_stopp	TTAGCTGCCGCCCAGGGAATTTCCGAGACC				
Tim50(1-394)-in pRS314	fw	FwAfter50_476flank	(same as for plasmid No. 5)	4	SDM	-	20
	rv	Rv_Tim50_394_Stopp	TTACGGGAACTTGGTGCTGCCGCCCAGGGAATTTC				
b_2(1-167) IMPmut(E80G)-Tim50(366-476) in pRS315	fw	Fw_b2_E80G	GGGCCGAAGCTTGATATGAATAAACAAAAG	7	SDM	HindIII added	21
	rv	Rv_b2_E80G	GTTGTCTATTTGGCCATTATGCCAGTTTAG				
Tim50(1-476)_A257C in pRS314	fw	Fw_Tim50A257C	GCTGAAAAATTGGATCCAATCCATTGCTTC	4	SDM	BamHI added	30
	rv	Rv_Tim50A257C	GATTTTGTCAGAGTACATCATATAGTTGGATG				
Tim50(1-476)_A257C_I413C in pRS314	fw	Fw_Tim50I413C	AGGATCCAGCAGGAGCAAATGGGCGGGCAAAC	30	SDM	BamHI added	31
	rv	Rv_Tim50I413C	AATTTTTTCCTTTTCTTCCTCACACATCTTC				
Tim50(Δ366-394)+15flex1 in pRS314	fw	Fw_396for50PBD	CTCGATTTGATTCATGAAGAAGG	4	SDM	BamHI added	32
	rv	Rev_Tim50_365+15_f-L	GGATCCTCCGCCACCACTACCACCACCTCCAGACCCTCCGCCGCCTTTATCCTTCAATTTTTTCACACGATGATC				
Tim50(Δ366-394)+15rig1 in pRS314	fw	Fw_396for50PBD	(same as for plasmid No. 32)	4	SDM	PstI added	33
	rv	Rev_Tim50_365+15_r-L	CTTAGCTGCGGCTTCTTTGGCTGCGGCCTCCTTTGCTGCAGCTTCTTTATCCTTCAATTTTTTCACACGATGATC				
Tim50(Δ366-389)+15flex1-flank in pRS314	fw	Fw_50_15flex+5AS	AGCACCAAGTTCCCGCTCGATTTGATTCATGAAGAAGGAC	32	SDM	-	34
	rv	Rv_50_15flex	GGATCCTCCGCCACCACTACCACCACCTCCAG				
	fw	Fw_50_15flex+5AS	(same as for plasmid No. 34)	33	SDM	-	35

Tim50(Δ366-389)+15rig1-flank in pRS314	rv	Rv_50_15rig	CTTAGCTGCGGCTTCTTTGGCTGCGGCCTC				
Tim50(Δ366-389)+15flex2 in pRS314	fw	Fw_8ASflex2_Tim50	GGTTCAGGAGAATTTGGGAGCGCGACCAAGTTCCCGCTCGATTTGATTC	4	SDM	NaeI added	36
	rv	Rev_Tim507ASflex2	GGCAGCGGAGCCGGCAGAACCTTTATCCTTCAATTTTTTCACACG				
Tim50(Δ366-389)+15rig2 in pRS314	fw	Fw_8ASrig2_Tim50	GCCCCTGGCCCCTCCCCTGCTCCCAGCACCAAGTTCCCGCTCGATTTG	4	SDM	NaeI added	37
	rv	Rev_Tim507ASrig2	TGGTGCCGGCGATGGACCTGGTTTATCCTTCAATTTTTTCACACG				
Tim50(Δ371-389)+15flex1 in pRS314	fw	Fw_Tim50_inflex	GGCGGCGGAGGGTCTGGAGGTGGTGGTAGTGG	34	SDM	HindIII added	38
	rv	Rv_Tim50_365+5AS	ATGATCTCCGTAAAATTTATCCTTAAGCTTTTTCACACGATGATC				
Tim50(Δ371-389)+15rig1 in pRS314	fw	Fw_Tim50_inrig	GAAGCTGCAGCAAAGGAGGCCGCAGCCAAAG	35	SDM	HindIII added	39
	rv	Rv_Tim50_365+5AS	(same as for plasmid No. 38)				
Tim50(Δ371-389)+15flex2 in pRS314	fw	Fw_Tim50_15flex2	GGTTCTGCCGGCTCCGCTGCCGGTTCAGGAG	36	SDM	HindIII added	40
	rv	Rv_Tim50_365+5AS	(same as for plasmid No. 38)				
Tim50(Δ371-389)+15rig2 in pRS314	fw	Fw_Tim50_15rig2	CCAGGTCCATCGCCGGCACCAGCCCCTGGC	37	SDM	HindIII added	41
	rv	Rv_Tim50_365+5AS	(same as for plasmid No. 38)				
Tim50(Δ371-389)+15rig3 in pRS314	fw	Fw_Tim50_15rig3	GAAGAAGCTCAAGAAGCTTTGAGAAGCACCAAGTTCCCGCTCGATTTG	4	SDM	HindIII added	42
	rv	Rv_Tim50_15rig3	TTCAAATTTTTTAGCAGCATCATGATCTCCGTAAAATTTATCCTTC				
Tim50(Δ371-389)+15flex1 in pRS315	fw	Subclone from pRS314		38	REC	SacI	45
	rv					Xho	
Tim50(Δ371-389)+15rig1 in pRS315	fw	Subclone from pRS314		39	REC	SacI	46
	rv					Xho	
Tim50core(133-370) in pET-Duet1	fw	Fw476for50dPBD	AAGCTTGCGGCCGCATAATGCTTAAG	47	SDM	-	48
	rv	Rv_Tim50_370_stopp	TTAATGATCTCCGTAAAATTTATCCTTC				

2.2 Yeast Genetics

2.2.1 *S. cerevisiae* strains

Wild-type haploid yeast strain YPH499 was used for all genetic manipulations (Sikorski and Hieter, 1989). A Tim50 shuffling strain (2.2.3) in YPH499 background was used to generate Tim50 mutant strains (Mokranjac et al., 2009). Tim50 variants were cloned into centromeric yeast plasmids pRS314 (TRP marker) or pRS315 (LEU marker) under the control of the endogenous TIM50 promoter

and 3'-untranslated regions (3'UTR). For overexpression, Tim50 variants were cloned into pRS317 (LYS marker) under the control of an overexpression GPD promoter. Tim50 variants targeted into the IMS were cloned as fusion proteins, starting with residues 1-167 of yeast cytochrome b_2 followed by the indicated Tim50 coding sequence (Mokranjac et al., 2009). Essentially all Tim50 variants were transformed into the Tim50 shuffling strain, followed by 5-FOA selection (2.2.3). Tim50(1-476), Tim50(Δ371-389)+15flex1 and Tim50(Δ371-389)+15rig1 were additionally transformed into a Tim50 shuffling strain in the background of C-terminally His-tagged Tom22 (YPH499 *Δtom22*::KAN + pRS314-prom-Tom22(1-152)-His6-flank, *Δtim50*::HIS3 + pVT-102U-Tim50(1-476)) and subsequently selected on 5-FOA. A complete list of all the yeast strains used and generated in this thesis is listed below (Table 2.7).

Table 2.7 Yeast strains used in this thesis. Parental yeast strain and plasmids used to generate the indicated yeast strain are stated below.

No.	Yeast strain	Parent strain	Used plasmid(s)	Reference
Y1	YPH499	-	-	(Sikorski and Hieter, 1989)
Y2	YPH499 *Δtim50::HIS3* + pVT-102U-Tim50(1-476)	-	-	(Mokranjac et al., 2009)
Y3	YPH499 *Δtim50::HIS3* + pRS314-prom-Tim50(1-476)-flank	Y3	4	This thesis
Y4	YPH499 *Δtim50::HIS3* + pRS314-prom-Tim50(1-365)-flank	Y3	5	This thesis
Y5	YPH499 *Δtim50::HIS3* + pRS315-prom-b_2(1-167)-Tim50(366-476)-flank	Y3	7	This thesis
Y6	YPH499 *Δtim50::HIS3* + pRS315-prom-Tim50(Δ131-365)-flank	Y3	8	This thesis
Y7	YPH499 + pRS317-GPD-Tim50(1-476)	Y1	9	This thesis
Y8	YPH499 + pRS317-GPD-Tim50(1-365)	Y1	10	This thesis
Y9	YPH499 + pRS317-GPD-Tim50(Δ164-365)	Y1	12	This thesis
Y10	YPH499 *Δtim50::HIS3* + pRS314-prom-Tim50(Δ164-365)+15flex-flank	Y3	13	This thesis
Y11	YPH499 *Δtim50::HIS3* + pRS314-prom-Tim50(1-365)-flank + pRS315-prom-b_2(1-167)-Tim50(366-476)-flank	Y3	5 + 7	This thesis
Y12	YPH499 *Δtim50::HIS3* + pRS314-prom-Tim50(1-365)-flank + pRS315-GPD-b_2(1-167)-Tim50(366-476)-flank	Y3	5 + 14	This thesis
Y13	YPH499 *Δtim50::HIS3* + pRS314-prom-b_2(1-167)-Tim50(132-365)-flank	Y3	16	This thesis
Y14	YPH499 *Δtim50::HIS3* + pRS314-prom-b_2(1-167)-Tim50(132-365)-flank + pRS315-prom-b_2(1-167)-Tim50(366-476)-flank	Y3	16 + 7	This thesis
Y15	YPH499 *Δtim50::HIS3* + pRS314-prom-b_2(1-167)-Tim50(132-365)-flank + pRS315-prom-Tim50(Δ164-365)	Y3	16 + 11	This thesis
Y16	YPH499 *Δtim50::HIS3* + pRS314-prom-Tim50(1-365)-flank + pRS315-prom-Tim50(Δ164-365)	Y3	5 + 11	This thesis
Y17	YPH499 *Δtim50::HIS3* + pRS314-prom-Tim50(1-370)-flank	Y3	17	This thesis
Y18	YPH499 *Δtim50::HIS3* + pRS314-prom-Tim50(1-380)-flank	Y3	18	This thesis
Y19	YPH499 *Δtim50::HIS3* + pRS314-prom-Tim50(1-390)-flank	Y3	19	This thesis

Y20	YPH499 *Δtim50::HIS3* + pRS314-prom-Tim50(1-394)-flank	Y3	20	This thesis
Y21	YPH499 *Δtim50::HIS3* + pRS314-prom-Tim50(1-370)-flank + pRS315-prom-b_2(1-167)-Tim50(366-476)-flank	Y3	17 + 7	This thesis
Y22	YPH499 *Δtim50::HIS3* + pRS314-prom-Tim50(1-380)-flank + pRS315-prom-b_2(1-167)-Tim50(366-476)-flank	Y3	18 + 7	This thesis
Y23	YPH499 *Δtim50::HIS3* + pRS314-prom-Tim50(1-390)-flank + pRS315-prom-b_2(1-167)-Tim50(366-476)-flank	Y3	19 + 7	This thesis
Y24	YPH499 *Δtim50::HIS3* + pRS314-prom-Tim50(1-394)-flank + pRS315-prom-b_2(1-167)-Tim50(366-476)-flank	Y3	20 + 7	This thesis
Y25	YPH499 *Δtim50::HIS3* + pRS314-prom-Tim50(1-370)-flank + pRS315-prom-b_2(1-167)IMPmut(E80G)-Tim50(366-476)-flank	Y3	17 + 21	This thesis
Y26	YPH499 *Δtim50::HIS3* + pRS314-prom-Tim50(1-476)_A257C_I413C-flank	Y3	31	This thesis
Y27	YPH499 *Δtim50::HIS3* + pRS314-prom-Tim50(Δ371-389)+15flex1-flank	Y3	38	This thesis
Y28	YPH499 *Δtim50::HIS3* + pRS314-prom-Tim50(Δ371-389)+15flex2-flank	Y3	40	This thesis
Y29	YPH499 *Δtim50::HIS3* + pRS314-prom-Tim50(Δ371-389)+15rig1-flank	Y3	39	This thesis
Y30	YPH499 *Δtim50::HIS3* + pRS314-prom-Tim50(Δ371-389)+15rig2-flank	Y3	41	This thesis
Y31	YPH499 *Δtim50::HIS3* + pRS314-prom-Tim50(Δ371-389)+15rig3-flank	Y3	42	This thesis
Y32	YPH499 *Δtom22::KAN* + pRS314-prom-Tom22(1-152)-flank	-	-	(Waegemann et al., 2015)
Y33	YPH499 *Δtom22::KAN* + pRS314-prom-Tom22(1-152)-His_6-flank	-	-	(Waegemann et al., 2015)
Y34	YPH499 *Δtom22::KAN* + pRS314-prom-Tom22(1-152)-His_6-flank, *Δtim50::HIS3* + pVT-102U-Tim50(1-476)	Y33	43 + 49	This thesis
Y35	YPH499 *Δtom22::KAN* + pRS314-prom-Tom22(1-152)-His_6-flank, *Δtim50::HIS3* + pRS315-prom-Tim50(1-476)-flank	Y34	43 + 44	This thesis
Y36	YPH499 *Δtom22::KAN* + pRS314-prom-Tom22(1-152)-His_6-flank, *Δtim50::HIS3* + pRS315-prom-Tim50(Δ371-389)+15flex1-flank	Y34	43 + 45	This thesis
Y37	YPH499 *Δtom22::KAN* + pRS314-prom-Tom22(1-152)-His_6-flank, *Δtim50::HIS3* + pRS315-prom-Tim50(Δ371-389)+15rig1-flank	Y34	43 + 46	This thesis

2.2.2 Transformation of *S. cerevisiae* cells (Li-Ac transformation)

Yeast cells were picked from a freshly streaked YPD plate, inoculated into 50 mL liquid YPD medium and grown ON at 30 °C with vigorous shaking at 160 rpm. Next morning, the ON culture of yeast cells was typically diluted to an OD_{600} of ~0.1 in 50 mL of liquid YPD medium and further grown for at least two cell divisions. When OD_{600} reached between 0.5–0.6, yeast cells were harvested at 3,000 x g, 5 min, RT and resuspended in 50 mL of sterile dH_2O. After washing, centrifugation was repeated and the supernatant discarded. Cells were resuspended in 1 mL of 100 mM lithium acetate (LiAc), transferred into a 1.5 mL Eppendorf tube and pelleted again through centrifugation at

16,000 x g for 15 sec. Supernatant was removed and the cell pellet was resuspended in 400 µL of 100 mM LiAc to a final volume of approximately 500 µL. Then, 50 µL of cell suspension per transformation were pipetted into fresh 1.5 mL Eppendorf tubes and centrifuged at 3,000 x g, 5 min, RT. Meanwhile, salmon sperm DNA (ss-DNA) was boiled for 5 min and then immediately cooled on ice. After centrifugation and removing the LiAc, following reagents were successively layered on top of the cell pellet: 240 µL PEG-3350 (50 % w/v), 36 µL LiAc (1 M), 5 µL ss-DNA (10 mg/mL), 60 µL dH_2O and 5 µL of plasmid DNA (when two plasmids were transformed 2.5 µL each was used). The tubes were vortexed vigorously for 1 min until most of the pellet was resuspended. After that, cells were incubated for 30 min at 30 °C under constant shaking (1200 rpm), followed by 25 min at 42 °C. Transformed cells were pelleted at 7,000 rpm for 20 sec and the supernatant was removed. Finally, the cells were resuspended in 150 µL of sterile dH_2O, plated on SD plates with respective selection markers and incubated at 30 °C until transformants appeared. In some cases, when plasmids with an antibiotic resistance marker were transformed, yeast cells were resuspended in 1 mL YPD media instead and grown ON at 30 °C and vigorous shaking at 160 rpm before being plated the next day.

2.2.3 Plasmid shuffling by 5-FOA selection

The ability of the various Tim50 variants to rescue the function of the wild-type protein *in vivo* was analysed by plasmid shuffling followed by 5-FOA selection in yeast. The Tim50 shuffling strain used in this thesis is based on the haploid yeast strain YPH499, in which the essential TIM50 gene is chromosomally deleted and made viable by the presence of a *URA3* plasmid (pVT-102U) encoding a wild-type copy of Tim50.

For analysis, the Tim50 shuffling strain was transformed with one or two plasmids simultaneously and the transformants were streaked on SD plates lacking the respective markers at 30 °C. Tim50 variants were either co-transformed or, when transformed individually, empty plasmids were transformed in addition, to have the auxotrophic markers equal among all the strains. The full-length copy of TIM50 on a plasmid was used as positive and the empty plasmids as negative controls, respectively. Transformants, appearing on SD plates after 2-3 days, were streaked for single colonies first, and then amplified on fresh SD plates. Finally, cells were plated on SD medium containing 5-fluoroorotic acid (5-FOA) at 30 °C, unless otherwise indicated. 5-FOA is converted to the cytotoxic 5-fluorouracil by the orotidine-5'-monophosphate decarboxylase, which is encoded by the *URA3* gene present in the pVT-102U plasmid. Therefore, only yeast cells that lost the wild-type copy of Tim50 on

the *URA3* plasmid and contain a functional copy of Tim50 on the transformed plasmid were able to grow on this medium.

2.3 Cell Biology

2.3.1 Bacterial culture

E. coli cells (MH1/BL21(DE3)) were usually cultured at 37 °C with vigorous shaking at 160 rpm in lysogeny broth (LB) medium (Table 2.8). The medium was sterilized by autoclaving and stored on RT. Ampicillin (Amp) was added freshly to the medium before inoculating with *E. coli* cells. For LB+Amp plates, 20 g/L bacto-agar was added to the medium before autoclaving and ampicillin was supplemented after the medium cooled down to about 50 °C before pouring the plates.

Table 2.8 Media for *E. coli* growth.

Medium	Components for 1 Liter
LB	5 g/L yeast extract, 10 g/L bacto-tryptone, 10 g/L NaCl, dH_2O to 1 L total volume
LB+Amp	LB medium supplemented with 100 µg/mL of ampicillin

2.3.2 Yeast culture

Yeast cells were usually grown in YPD medium at 24°C with vigorous shaking at 160 rpm, unless otherwise indicated. In some cases, for instance when generating growth curves (2.3.3.2) yeast cells were cultivated in SLac medium + 0.1 % glucose at 30 °C. Non-selective YP medium was prepared as in Table 2.9, sterilized by autoclaving and stored at RT. To prepare YPD medium, 2 % (w/v) glucose from an autoclaved 40 % glucose stock solution was added. YPLac medium was made by adding 2 % of a 90 % lactic acid stock solution before pH adjustment. Selective media (Table 2.9) was used to generate a selective pressure on yeast cells to retain the transformed plasmids. To prepare SD medium, a 5xS stock solution was diluted in sterile dH_2O and supplemented with 2 % glucose. SLac medium was made by adding 2 % of a 90 % lactic acid stock solution before pH adjustment.

Table 2.9 Non-selective and selective media for cultivating *S. cerevisiae* cells.

Non-selective medium	Components for 1 Liter
YP	10 g/L yeast exctract, 20 g/L bacto-peptone, dH_2O to 1 L, pH 5.0 (adjusted with HCl)
YPD	YP medium supplemented with 2 % (w/v) of 40 % glucose (D) stock
YPLac	YP medium supplemented with 2 % (w/v) of 90 % lactic acid (Lac) stock
Lactate + 0.1 % Glc	3 g yeast extract, 1 g KH_2PO_4, 1 g NH_4Cl, 0.5 g $CaCl_2x2H_2O$, 0.5 g NaCl, 1.1 g $MgSO_4x6H_2O$, 0.3 mL 1% $FeCl_3$, 22 mL of 90 % lactic acid, dH_2O to 1 L, pH 5.5 (adjusted with KOH), supplemented with 0.1 % glucose
Selective medium	**Components for 1 Liter**
S	1.7 g yeast nitrogen base, 5 g $(NH_4)_2SO_4$, dH_2O to 1 L
SD	S medium supplemented with 2 % (w/v) of 40 % glucose (D) stock
SLac	S medium supplemented with 2 % (w/v) of 90 % lactate acid (Lac) stock

Selection markers were added to the media from sterile stocks in given quantities (Table 2.10). Except for Tryptophan, which was filter sterilized, all markers were autoclaved before use. For selective and non-selective plates, 20 g/L Bacto-agar was added to the medium before autoclaving. To prepare 5-FOA plates, selective medium was supplemented with 1 mg/mL of 5-FOA and filter sterilized before mixing with autoclaved agar.

Table 2.10 Stock solutions of selection markers for selective media.

Selection marker	Stock solution
Adenine (*ADE2*)	2 mg/mL (100x)
Histidine (*HIS1*)	10 mg/mL (500x)
Leucine (*LEU2*)	10 mg/mL (333x)
Lysine (*LYS2*)	10 mg/mL (333x)
Tryptophan (*TRP1*)	2 mg/mL (500x)
Uracil (*URA3*)	10 mg/mL (100x)

2.3.3 Assays with yeast cells

2.3.3.1 Serial dilution spot assay

Growth of yeast cells was analysed by serial dilution spot assay. For this, yeast cells were grown in liquid YPD medium ON at 24°C, unless otherwise indicated. ON cultures were diluted into fresh medium to OD_{600} ~0.1 and, when they reached logarithmic growth phase (OD_{600} 0.5-0.6), 1 mL of cells were transferred into a sterile 1.5 mL Eppendorf tube and pelleted at 16,000 x g, 2 min, RT. Cells were resuspended in sterile dH_2O to obtain 1 OD_{600} of cells and subsequently, five times of a ten-fold serial dilution were made, respectively. Finally, 2 µL of cell suspension were spotted on YPD and YPLac plates, as fermentable and non-fermentable carbon source, respectively. The plates were incubated at indicated temperatures.

2.3.3.2 Growth curves

Growth curves were used to analyse the growth of yeast cells under oxidizing conditions in selective media. Yeast cells were grown ON in SLac medium (+ 0.1 % Glc) supplemented with indicated concentrations of 4,4'-dipyridyl disulfide (4-DPS) at 30 °C. Next day, cells were diluted to OD_{600} ~0.1 into fresh medium and further grown until they reached logarithmic growth phase (OD_{600} 0.5-0.6). Then, 0.015 OD_{600} of cells per well were collected and diluted in fresh medium, so that in each well 5 µL of yeast culture in 150 µL of medium had a starting OD_{600} of 0.1. Absorbance at 600 nm was determined over a time frame of 24-48 h at 30 °C under constant shaking in a multi-plate reader (SPECTROstar Nano, BMG Labtech).

2.3.3.3 Total cell extracts

Yeast cells were grown ON in YPD medium at 24 °C, unless otherwise indicated. Next morning, ON cultures were diluted in fresh medium to an OD_{600} ~0.1 and further grown until they reached OD_{600} ~ 0.5. Three OD_{600} of cells were harvested in 15 mL Falcon tubes by centrifugation at 3,000 x g, 5 min, RT. Supernatant was discarded, cell pellet resuspended in 150 µL dH_20 and transferred into a 1.5 mL Eppendorf tube. Cells were pelleted at 16,000 x g, 30 sec and resuspended in 100 µL dH_20. To the cell suspension, 100 µL of 0,2 M NaOH were added, the mixture was shortly vortexed and kept for 5 min at RT. After incubation, the samples were centrifuged at 16,000 x g, 2 min, RT and the supernatant removed. Finally, the pellets were resuspended in 200 µL of 2x Laemmli buffer (+ ß-Me) (2.4.1.2). After heating at 95 °C for 3 min, cells were centrifuged at 16,000 x g for 30 sec and 10-20 µL of the supernatant were loaded on a SDS-PA gel (2.4.1.2).

2.3.3.4 Large-scale mitochondria isolation from *S. cerevisiae*

Yeast cells were grown usually in YPD medium at 24°C for 2-3 days, while diluting into fresh medium and increasing the total volume of culture. In some cases, where indicated, yeast cells were grown in lactate medium at 30 °C instead. When cells reached OD_{600} ~ 0.8, they were harvested by centrifugation at 4,400 x g, 5 min, RT, washed with dH_2O and repeating the centrifugation step. The resulting pellet was resuspended in DTT buffer (100 mM Tris-SO_4, 10 mM DTT, pH not adjusted) to a final concentration of 2 mL of buffer per gram of cells and incubated for 10 min at 24 °C with vigorous shaking at 160 rpm. Then, cells were centrifuged at 4,400 x g, 5 min, RT and washed with 100 mL of 1.2 M sorbitol. Cells were resuspended in sorbitol buffer (6.6 mL of 1.2 M sorbitol, 20 mM KH_2PO_4-KOH, pH 7.4, per gram of cells) supplemented with 3 mg of zymolyase per gram of cells and incubated for 45 min–1 h under vigorous shaking (160 rpm) to digest the cell wall. Spheroplasts were harvested by centrifugation at 3,000 x g, 5 min, 4 °C and resuspended with 6.6 mL of homogenization buffer (0.6 M sorbitol, 10 mM Tris-HCl, 1 mM EDTA, 0.2 % (w/v) BSA, 1 mM phenylmethylsulfonyl fluoride (PMSF), pH 7.4.) per gram of cells. From now on, further steps were performed on ice. After resuspension, spheroplasts were homogenised using 10–12 strokes of a dounce-homogenizer. Cell debris was removed by centrifuging twice at 1,900 x g, 5 min, 4 °C and subsequently, the supernatant was collected into a fresh centrifugation tube. Mitochondria were pelleted out of the supernatant by centrifugation at 17,400 x g, 12 min, 4 °C. Finally, pelleted mitochondria were resuspended in SH buffer (20 mM HEPES-KOH, 0.6 M sorbitol, pH 7.2) and concentration was determined by Bradford assay (2.4.1.5). Mitochondria were diluted with SH buffer to a final concentration of 10 mg/mL, aliquoted in 1.5 mL Eppendorf tubes, flash frozen in liquid nitrogen and stored at -80 °C.

2.4 Protein Biochemistry

2.4.1 Protein detection and analysis

2.4.1.1 TCA protein precipitation

Trichloroacetic acid (TCA) precipitation was used to denature proteins out of solution. For this, 20 µL of 12 % TCA was added to a 50 µL protein solution, mixed thoroughly and incubated for 20 min at -20 °C. Precipitated proteins were collected by centrifugation at 36,500 x g, 20 min, 4 °C. After washing the pellet with 200 µL of ice-cold acetone, the centrifugation step was repeated for 10 min. The precipitated protein pellet was resuspended in 20 µL 2x Laemmli buffer (+ β-Me), boiled at 95 °C for 5 min and loaded on an SDS-PA gel (2.4.1.2).

2.4.1.2 SDS-PAGE

Proteins were separated based on their different molecular weights using sodium dodecylsulphate polyacrylamide gel electrophoresis (SDS-PAGE). SDS-PA gels were made of a separating gel at the bottom and a stacking gel on top (Table 2.11). Each gel was sequentially poured into a gel cast out of two glass plates, clamped together, and left for polymerisation until solidified, respectively. Before the stacking gel was left for polymerising, an 18- or 21-pocket comb was inserted.

Table 2.11 Composition of a SDS-PA gel.

Gel	Composition
Separating gel	8-12 % (w/v) acrylamide, 0.16-0.33 % (w/v) bis-acrylamide, 377 mM TRIS-Cl (pH 8.8), 0.1 % (w/v) SDS, 0.05 % (w/v) APS, 0.05 % (v/v) TEMED
Stacking gel	5 % (w/v) acrylamide, 0.1 % (w/v) bis-acrylamide, 60 mM TRIS-Cl (pH 6.8), 0.1 % (w/v) SDS, 0.07 % (w/v) APS, 0.35 % (v/v) TEMED

To run the SDS-PAGE, the in the glass cast polymerised SDS-PA gel was assembled into a gel chamber filled with SDS running buffer. The samples were resuspended in 2x Laemmli buffer (-/+ β-Me) and cooked at 95 °C for 3-5 min. Buffer compositions are listed below (Table 2.12).

Table 2.12 Buffer compositions for running an SDS-PA gel.

Buffer	Composition
SDS running buffer	50 mM Tris-Cl, 384 mM glycine, 0.1 % (w/v) SDS, pH 8.3 without adjustment
2x Laemmli buffer	120 mM Tris-Cl (pH 6.8), 20 % (v/v) glycerol, 4 % (w/v) SDS, 0.02 % (w/v) bromophenol blue
2x Laemmli buffer (+ β-Me)	2x Laemmli buffer supplemented with 3 % (v/v) β-Mercaptoethanol

Samples were loaded into the wells of the SDS-PA gel and electrophoresis was started at 35 mA constant current for ca. 1 h 40 min (for big gels) and at 25 mA for ca. 50 min (for small gels). Separation was stopped when the blue bromophenol running front reached the end of the separating gel and proteins were analysed by coomassie brilliant blue (CBB) staining (2.4.1.6) or Western blotting (2.4.1.4).

2.4.1.3 Transfer of proteins onto nitrocellulose membranes

Proteins separated by SDS-PAGE (2.4.1.2) were subsequently transferred on a nitrocellulose membrane (142,5 cm^2, 0.2 µm pore size) by a semi-dry botting method. A blotting sandwich was assembled containing the SDS-PA gel on top of the nitrocellulose membrane in between two sheets of blotting paper, all components soaked thoroughly in transfer buffer (20 mM Tris, 150 mM glycine, 20 % (v/v) methanol and 0.02 % SDS). Transfer was performed at a constant current of 250 mA for 1 h (or 1 h 15 min for cross-linking experiments) using a blotting chamber with two graphite electrode panels. After transfer, the nitrocellulose membrane was briefly washed with dH_2O and stained with Ponceau S (0.2 % (w/v) Ponceau S in 3 % (w/v) TCA) and left to dry ON.

2.4.1.4 Western blotting

The whole nitrocellulose membrane or cut membrane stripes were destained with dH_2O and TBS buffer (50 mM Tris-Cl, 150 mM NaCl, pH 7.5) and subsequently blocked under shaking with 5 % (w/v) milk powder in TBS buffer for 30 min. After blocking, membranes were incubated for 2 h (or 3 h for cross-linking experiments) under constant shaking with primary antibodies, diluted 250-1,000 fold in 5 % milk in TBS buffer. Membranes were then washed with TBS buffer, TBS buffer with 0,05 % (v/v) Triton X-100 and again TBS buffer for 10 minutes each. After washing, membranes were incubated for 1 h (or 2 h for cross-linking experiments) with secondary antibodies labelled with horse radish peroxidase (HRP) (diluted 1:10,000 for anti-Rabbit and 1:5,000 for anti-Mouse in 5 % milk in TBS buffer) under constant shaking. The three washing steps were repeated, and proteins visualized via chemiluminescence using X-ray films for signal detection. The chemiluminescent reaction was initiated by mixing equal volumes of ECL1 (100 mM Tris-Cl, pH 8.5, 440 µg/mL luminol, 65 µg/mL p-coumaric acid) and ECL2 (100 mM Tris-Cl, pH 8.5, 0.6 % hydrogen peroxide) and pipetting the mixture onto the membranes. Primary antibodies, raised against several components of the TOM and TIM23 complexes as well as against further mitochondrial proteins, used in this thesis, were taken from the library of the Mokranjac group.

2.4.1.5 Determination of protein concentration

For estimation of the protein concentration, the Bradford assay was performed. A protein standard curve was prepared, by serially diluting a 1.4 mg/mL bovine IgG (Bio-Rad) stock solution to 24, 12, 6, 3 and 0 µg of proteins per tube. Protein samples of unknown concentration were simultaneously diluted in dH_2O. Then, 1 mL of 1:5 diluted Bradford reagent (Bio-Rad) was added to the protein standards and samples of unknown concentration, mixed by inverting the tubes, followed

by a 10 min incubation at RT. To determine the protein concentration, absorbance was measured at 595 nm and the unknown concentrations were determined on the basis of the standard curve.

2.4.1.6 Coomassie Brilliant Blue (CBB) staining

To analyse the expression and purification of recombinant proteins, the SDS-PA gel (2.4.1.2) was usually incubated in a CBB staining solution (0.1 % (w/v) CBB R-250, 40 % methanol, 10 % glacial acetic acid) to visualize the protein signals. After 15-30 min incubation at RT under constant shaking, the CBB stained SDS-PA gel was briefly washed with dH_2O and then incubated in a destaining solution (40 % methanol, 10 % glacial acetic acid) until protein bands were clearly visible.

2.4.2 Isolation of recombinant proteins

2.4.2.1 Expression of recombinant proteins in *E. coli* cells

His_6-tagged Tim50 variants in pET-Duet1 vectors were transformed in *E. coli* BL21(DE3) cells for their recombinant protein expression. Bacteria were grown ON in LB+Amp medium at 37 °C under vigorous shaking at 160 rpm. Next day, 40 mL of ON culture were diluted into 2 L fresh medium and grown at 37 °C until an OD_{600} of 0.2-0.3 was reached. After that, the temperature was lowered to 18 °C and the growth continued till OD_{600} of 0.6, at which stage the protein expression was induced by adding 0.5 mM isopropyl β-D-1-thiogalactopyranoside (IPTG). After ON expression, bacteria were harvested by centrifugation at 4,500 x g, 10 min, 4 °C, resuspended in dH_2O and transferred into 50 mL Falcon tubes. After another centrifugation step at 3,000 x g, 20 min, 4 °C, the bacterial cell pellets were stored at -20 °C until further use.

2.4.2.2 Purification of His-tagged Tim50 variants

All recombinant His_6-tagged Tim50 variants were purified as follows, using buffers listed in Table 2.13.

Table 2.13 Buffers used for purification of recombinant His_6-tagged Tim50 variants.

Buffer	Composition
Resuspension buffer	50 mM Tris, 150 mM NaCl, 20 mM imidazole, 1 mM PMSF, pH 7.0
Ni-NTA elution buffer	50 mM Tris, 150 mM NaCl, 300 mM imidazole, pH 7.0
SEC buffer	50 mM tris, 150 mM NaCl, pH 7.0

Frozen *E. coli* cell pellets with expressed proteins of interest were thawed and resuspended in 50 mL resuspension buffer. Subsequently the cells were disrupted three times using a microfluidizer and the cell lysate was centrifuged at 27,000 x g, 20 min and 4 °C to remove cell debris. In the meantime, 1 mL of Ni-NTA-agarose beads were washed with 30 mL dH_2O and equilibrated with 20x the column volume (CV) of resuspension buffer. The supernatant of the centrifuged cell lysate was loaded on the Ni-NTA column, using a peristaltic pump. After loading, the Ni-NTA column was washed with 30x the CV of resuspension buffer. Bound proteins were eluted with 15 mL of Ni-NTA elution buffer and collected in 1 mL fractions in 1.5 mL Eppendorf tubes. The Ni-NTA elution fractions with the highest protein concentration were pooled and further purified by size exclusion chromatography (SEC) on a Superdex 75 10/300 (GE Healthcare) using an Äkta Pure system. After equilibrating the SEC column with 10x CV of SEC buffer, 1 mL of pooled Ni-NTA elution fractions were injected on the column and SEC elution fractions were collected in 1 mL aliquots in 1.5 mL Eppendorf tubes. Purification process was analysed by taking samples after each step and running a small SDS-PA gel (2.4.1.2), followed by CBB staining (2.4.1.6). Protein concentration was determined by Bradford assay (2.4.1.5) and subsequently, purified Proteins were aliquoted, flash frozen in liquid nitrogen and stored in -80 °C until use.

2.4.3 Assays with recombinant proteins

2.4.3.1 Pull-down with recombinant proteins immobilized to CNBr Sepharose beads

2.4.3.1.1 Immobilization of recombinant proteins to CNBr Sepharose beads

Lyophilized CNBr Sepharose 4B (GE-Healthcare) beads were swollen in 1 mM HCl and subsequently washed with 200 mL of 1 mM HCl. Then, 0.8 mL of washed beads were packed in a Poly-Prep Chromatography column (BioRad). In the meantime, the buffer, in which the recombinantly expressed and purified proteins were stored, was exchanged to the coupling buffer (0.1 M $NaHCO_3$, 0.5 M NaCl, pH 8.3) using a PD10 column (GE Healthcare). 3.5-8.0 mg of protein (same molar amount of all Tim50 variants) were added per 800 µL of CNBr Sepharose beads and incubated for 1 h at RT on a rotating platform to allow proteins to bind to the CNBr Sepharose. Non-bound material was removed by gravity flow in the flow-through and subsequently the beads were washed with 20x the beads volume of coupling buffer. To block the remaining active sites of the beads 6 mL of 1 M ethanolamine was added and the column incubated for 2 h at RT on a rotating platform. The column was washed again with the same volume of coupling buffer and the beads were stored in 6 mL of 0.05 % NaN_3 in coupling buffer at 4 °C until use.

2.4.3.1.2 Pull-down of interacting proteins

Isolated mitochondria from YPH499 wild-type cells were solubilized at 1 mg/mL in solubilization buffer (20 mM HEPES, 100 mM KOAc, 10 mM $Mg(OAc)_2$, 10 % glycerol, pH 7.4, supplemented with 2 mM PMSF and 0.5 % Triton X-100) for 30 min at 4 °C. Subsequently, insoluble material was removed by ultracentrifugation at 124,500 x g, 20 min, 2 °C. In the meantime, 100 µL of CNBr Sepharose beads with immobilized protein each were equilibrated 3x with solubilization buffer supplemented with 0.5 % Triton X-100. After ultracentrifugation, 900 µL of the mitochondrial lysate were added to the equilibrated CNBr Sepharose beads with immobilized protein and incubated for 30 min at 4°C on a rotating platform. Beads were centrifuged at 18,000 x g, 2 min, 4 °C and unbound material was removed. For washing, 500 µL solubilization buffer with 0.1 % Triton X-100 was added, beads were incubated for 5 min at 4°C on a rotating platform and subsequently, centrifuged at 18,000 x g, 2 min, 4°C. This washing step was repeated three times until bound proteins were eluted by adding 2x Laemmli (+ β-Me) and heating the beads at 95 °C for 3 min. Beads were settled by short centrifugation and elution samples as well as the mitochondrial lysate as total fraction (2 %) were loaded on a SDS-PA gel (2.4.1.2) and analysed by Western blotting (2.4.1.4).

2.4.4 Assays with isolated mitochondria

Common buffers used in various experiments with isolated mitochondria are listed in Table 2.14.

Table 2.14 Common buffers used in this thesis for experiments with isolated mitochondria.

Buffer	Composition
SH buffer	20 mM HEPES-KOH, 0.6 M sorbitol, pH 7.2
SHK buffer	20 mM HEPES-KOH, 0.6 M sorbitol, 80 mM KCl, pH 7.2
SI buffer	50 mM HEPES-KOH, 0.6 M sorbitol, 80 mM KCl, 10 mM $MgAc_2$, 2 mM KH_2PO_4, 2.5 mM $MnCl_2$, 2.5 mM EDTA, pH 7.2

2.4.4.1 Carbonate extraction

Isolated mitochondria were diluted at 1 mg/mL in 0.1 M of ice-cold NA_2CO_3, pH 11.4 and incubated for 30 min at 4 °C on a rotating platform. After ultracentrifugation at 124,500 x g, 30 min, 4 °C, the supernatant was collected and further processed by TCA precipitation (2.4.1.1). The pellet was resuspended in 2x Laemmli (+ β-Me), cooked at 95 °C for 5 min and loaded, together with the TCA precipitated samples, on a SDS-PA gel (2.4.1.2), followed by Western blotting (2.4.1.4).

2.4.4.2 Co-immunoprecipitation

Before starting the co-immunoprecipitation experiment, 100 µL of Protein A-Sepharose CL-4B (PAS) beads were washed once with dH_2O and three times with TBS by centrifuging at 18,000 x g, 2 min, RT each time. Then, indicated affinity purified antibodies against TIM23 subunits as well as pre-immune (PI) serum, serving as a negative control, were coupled to the beads by incubating them for at least 1 h at 4 °C on a rotating platform. Beads were subsequently washed twice in TBS and equilibrated in 20 mM TRIS/HCl, 80 mM KCl, 10 % glycerol, 2 mM PMSF, pH 8.0, supplemented with 0.05 % (w/v) digitonin.

In parallel, isolated mitochondria were resuspended in 500 µL SH buffer and reisolated by centrifugation at 18,000 x g, 10 min, 4°C. After removing the supernatant, mitochondria were solubilized at 1 mg/mL with 1 % digitonin in 20 mM TRIS-HCl, 80 mM KCl, 10 % glycerol, 2 mM PMSF, pH 8.0 for 15 min at 4 °C on a rotating platform. Non-solubilized material was pelleted by ultracentrifugation at 124,500 x g, 20 min, 4 °C. Solubilized mitochondrial lysates were added to the antibodies prebound to Protein A-Sepharose beads and incubated for 45 min at 4 °C on a rotating platform. After incubation time, non-bound material in the supernatant (Sup) was collected and beads were washed three times with 20 mM TRIS-HCl, 80 mM KCl, 10 % glycerol, 2 mM PMSF, pH 8.0 supplemented with 0.05 % (w/v) digitonin. Beads were shortly centrifuged and bound proteins in the pelleted beads (Pellet) were eluted with 2x Laemmli (+/- β-Me) and cooked at 95 °C for 3 min. Samples were analysed by SDS-PAGE (2.4.1.2) and Western blotting (2.4.1.4).

2.4.4.3 *In organello* import experiments

2.4.4.3.1 Preparation of radioactive labelled precursor proteins

Precursor proteins were synthesized in the presence of ^{35}S methionine in a standard or a transcription and translation (TNT) coupled reticulocyte lysate system (Promega).

For the standard preparation of radioactive labelled precursor proteins, pGEM plasmids (from the Mokranjac group) encoding the indicated precursor proteins under the control of a Sp6 promotor were first transcribed for 1 h at 37 °C using following reagents in given quantities: 20 µL of 5x transcription buffer (200 mM Tris-HCl, pH 7.5, 50 mM NaCl, 30 mM $MgCl_2$, 10 mM spermidine), 10 µL of 0.1 M DTT, 4 µL RNAsin (40 U/µL), 20 µL rNTPs (10 mM each), 5.2 µL $m^7G(5')ppp(5')G$, 3 µL Sp6 polymerase, 10 µL plasmid DNA and sterile dH_2O to a total volume of 100 µL. After incubation, 10 µL of 10 M LiCl and 300 µL of ethanol were added and the reaction mix was incubated for 30 min at

– 20 °C. RNA was pelleted at 36,700 x g, 20 min, RT and after discarding the supernatant, the RNA pellet was washed with 70 % (v/v) ice-cold ethanol. RNA was recovered by adding 100 µL dH_2O containing 1 µL RNAsin and stored at -80 °C until use. For *in vitro* translation of radioactive labelled precursor proteins, RNA was translated for 1 h at 30 °C using following reagents in given quantities: 100 µL of reticulocyte lysate, 3.5 µL amino acid mix (1 mM each, except methionine), 1 µL RNAsin, 7 µL of 15 mM Mg-acetate, 12 µL of ^{35}S-methionine and 25 µL of RNA. After incubation, 12 µL of 58 mM unlabelled methionine and 24 µL of 1.5 M sucrose were added to stop incorporation of radioactive labelled methionine into the polypeptide chains. Reaction mix was ultracentrifuged at 124,500 x g, 30 min, 4 °C, supernatant was aliquoted for single-use and stored at -80 °C until use.

Some radioactive labelled precursor proteins were generated using the TNT coupled reticulocyte lysate system (Promega) instead. A reaction mix was pipetted using following reagents in given quantities: 25 µL TNT rabbit reticulocyte lysate, 2 µL of TNT reaction buffer, 1 µL of TNT Sp6 RNA polymerase, 1 µL of amino acid mix (without methionine), 2 µL of ^{35}S-methionine, 1 µL RNAsin (40 U/µL), 2 µL of plasmid DNA (~0.5 µg/µL) and dH_2O to a total volume of 50 µL. After incubation for 1.5 h at 30 °C, 4 µL of 58 mM unlabelled methionine and 8 µL of 1.5 M sucrose were added to stop incorporation of radioactive labelled methionine into the polypeptide chains. The reaction mix was ultracentrifuged at 124,500 x g, 30 min, 4 °C, supernatant was aliquoted for single-use and store at – 80 °C until use.

2.4.4.3.2 Import of radioactive precursor proteins into isolated mitochondria

Isolated mitochondria were resuspended at 0.5 mg/mL in SI buffer, supplemented with 1 mg/mL bovine serum albumin (BSA), 2.5 mM ATP, 3.75 mM NADH, 10 mM creatine phosphate, 100 µg/mL creatine kinase. Import of ^{35}S-labelled precursor proteins was performed at 25°C and the import reaction was stopped at indicated time points by diluting 90 µL of the samples in 810 µL of ice-cold SH buffer containing 1 µM valinomycin. Two samples were taken out at each time point. One half of the samples were treated with 35 µg/mL proteinase K (PK) for 15 min on ice. Protease treatment was stopped by adding 2 mM PMSF for 5 min on ice. Mitochondria were reisolated by centrifugation at 18,000 x g, 10 min, 4 °C, resuspended in 2x Laemmli (+ ß-Me), cooked at 95 °C for 5 min and analysed by SDS-PAGE (2.4.1.2), followed by autoradiography. Quantifications of the import experiments were done with the ImageJ software. The amount of the PK-protected mature form in the longest time point in the respective wild-type mitochondria was set to 100 %. Graphs were created with Python.

2.4.4.4 Chemical cross-linking of arrested precursor proteins

Isolated mitochondria were resuspended at 0.5 mg/mL in SI buffer, supplemented with 25 µM carbonyl cyanide m-chlorophenylhydrazone (CCCP), 8 µM oligomycin and 0.5 µM valinomycin and incubated for 15 min at 25 °C to dissipate membrane potential. ^{35}S-labelled precursor proteins were imported for 15 min at 25 °C and then transferred on ice. Cross-linking was performed with 50 µM homobifunctional, amino-group reactive agent 1,5-difluoro-2,4-dinitrobenzene (DFDNB) freshly dissolved in DMSO for 30 min on ice. Control samples were treated with DMSO. Cross-linking reaction was stopped by adding 0.1 M glycine, pH 8.8. Mitochondria were washed twice with SH buffer and reisolated by centrifugation at 18,000 x g, 10 min, 4 °C.

For subsequent immunoprecipitation, mitochondria were solubilized at 1 mg/mL with 1 % SDS in 50 mM Na-phosphate, 100 mM NaCl, 2 mM PMSF; pH 8.0 for 5 min at 25 °C on a rotating platform and diluted in the same buffer containing 0.2 % Triton X-100. Non-solubilized material was pelleted by ultracentrifugation at 124,500 x g, 20 min, 4 °C. Solubilized mitochondria (200 µL) were incubated with affinity purified antibodies against the N-terminal ($Tim50_N$) and C-terminal peptide ($Tim50_C$) of Tim50 prebound to Protein A-Sepharose beads (as described in 2.4.4.2, however equilibration of the beads was done in 50 mM Na-phosphate, 100 mM NaCl, pH 8.0 with 0.2 % Triton X-100) for 45 min at 4 °C. Pre-immune (PI) serum served as a negative control. After incubation, non-bound material was removed, beads were washed three times in the same buffer containing 0.2 % Triton X-100 and bound proteins were eluted with 2x Laemmli (+ ß-Me). Samples were analysed by SDS-PAGE (2.4.1.2) followed by autoradiography.

2.4.4.5 Accumulation of precursor proteins in the TOM complex

Isolated mitochondria (0.5 mg/mL) were resuspended in SI buffer containing 1 mg/mL BSA and incubated in the presence of 20 µM oligomycin and 1 µM valinomycin for 10 min at 25 °C to deplete the membrane potential or 2.5 mM ATP, 3.75 mM NADH, 10 mM creatine phosphate, 100 µg/mL creatine kinase for 3 min at 25 °C to generate membrane potential. Import of ^{35}S-labelled Oxa1 precursor was performed at 25 °C and the import reaction was stopped after 30 min (or indicated time points) by diluting the samples in 1 mL of ice-cold SH buffer and 1 µM valinomycin. Following reisolation by centrifugation at 18,000 x g, 10 min, 4 °C, mitochondria were washed once with SH buffer with 1 µM valinomycin. Mitochondria were solubilized at 1 mg/mL with 1 % digitonin in 20 mM TRIS, 0.1 mM EDTA, 50 mM NaCl, 10 % glycerol, 2 mM PMSF, pH 8.0 for 15 min at 4 °C on a rotating platform. Non-solubilized material was removed by centrifugation at 13,200 x g, 15 min, 4 °C

and samples were analysed by BN-PAGE (2.4.4.6) and SDS-PAGE (2.4.1.2) followed by autoradiography.

For the chase of Oxa1 precursor into the matrix, membrane potential was dissipated with 50 µM carbonyl cyanide m-chlorophenylhydrazone (CCCP) for 10 min at 25°C. After import of ^{35}S-labelled Oxa1 precursor for 30 min at 25 °C, mitochondria were reisolated in SHK buffer by centrifugation at 18,000 x g, 10 min, 4 °C. CCCP was washed away by resuspending the mitochondria in SI buffer containing 3 % BSA (w/v) and 5 mM DTT. Membrane potential was re-established by adding 2.5 mM ATP, 3.75 mM NADH, 10 mM creatine phosphate, 100 µg/mL creatine kinase at 25 °C and Oxa1 precursor was chased into the matrix. At indicated time points, 100 µL of each sample were taken out and import was stopped by diluting the samples in 900 µL of SH buffer with 1 µM valinomycin. The control sample was resuspended in SI buffer containing 1 µM valinomycin and kept on ice throughout the chase of the Oxa1 precursor. Samples were subsequently handled and analysed as described above.

2.4.4.6 Blue Native PAGE (BN-PAGE)

After solubilization of mitochondria (as described in 2.4.4.5), 1 µL of 5 % Coomassie Brilliant Blue-G were added to 20 µL of solubilized mitochondria. Samples were run according to manufacturer's instructions on a 4-16 % Native PAGE Bis-Tris Gel (Life Technologies) assembled in a gel running chamber. Briefly, the gel was first run at 150 V for 30 min at 4 °C with 1x NativePAGE dark blue cathode buffer (inside) and 1x NativePAGE running anode buffer (outside). Then, voltage was increased to 250 V and gel electrophoresis was continued until the dye front reached ca. 1/3 of the gel. At this point, the dark blue cathode buffer was exchanged with 1x NativePAGE light blue cathode buffer and the gel was run until the dye front reached the bottom of the gel. Finally, proteins were blotted onto a PVDF membrane at 130 mA, 7 V for 1 h and analysed by autoradiography.

2.4.4.7 Limited proteolysis with PK treatment

Isolated mitochondria were resuspended at 0.5 mg/mL in SI buffer, supplemented with 1 mg/mL BSA, 2.5 mM ATP, 3.75 mM NADH, 10 mM creatine phosphate, 100 µg/mL creatine kinase and incubated for 3 min at 25 °C. After putting the samples on ice and diluting them in 900 µL of SH buffer, 50 µg/mL of proteinase K (PK) was added to each sample. At indicated time points, reaction was stopped by adding 2 mM PMSF and incubating the samples for 5 min on ice. Mitochondria were reisolated by centrifugation at 18,000 x g, 10 min, 4 °C and washed with SH buffer once. After a final

centrifugation step, mitochondria were resuspended in 2x Laemmli (+ ß-Me), cooked at 95 °C for 5 min and analysed by SDS-PAGE (2.4.1.2) and Western blotting (2.4.1.4).

2.4.4.8 Oxidation assay

Isolated mitochondria were resuspended at 0.5 mg/mL in SI buffer, supplemented with 2 mM PMSF and 1 mM EDTA and incubated for 3 min at 25 °C. After putting the samples on ice, 2 mM of the oxidizing reagents 4,4'-dipyridyl disulfide (4-DPS), copper sulphate ($CuSO_4$) and copper phenanthroline (CuP) were added respectively and incubated for 10 min on ice. Oxidation was stopped by adding 50 mM iodoacetamide and further keeping the samples for 10 min on ice. After splitting the samples in half, mitochondria were reisolated in SH buffer by centrifugation at 18,000 x g, 10 min, 4 °C. Next, mitochondria were resuspended in SH buffer supplemented with or without 50 mM DTT and incubated for 15 min at 30 °C. After another centrifugation step at 18,000 x g, 10 min, 4 °C, mitochondria were resuspended in 2x Laemmli (+ ß-Me), cooked at 95 °C for 5 min and analysed by SDS-PAGE (2.4.1.2) and Western blotting (2.4.1.4).

For oxidation followed by import of precursor proteins, isolated mitochondria were resuspended at 0.5 mg/mL in SI buffer supplemented with 2.5 mM ATP, 3.75 mM NADH, 10 mM creatine phosphate, 100 µg/mL creatine kinase and incubated for 3 min at 25 °C. After putting the samples on ice, oxidizing conditions were implemented for 10 min by adding 0.5 mM of $CuSO_4$ Reaction was stopped by adding 50 mM iodoacetamide and keeping the samples another 10 min on ice. After reisolating mitochondria in SH buffer by centrifuging at 18,000 x g, 10 min, 4 °C, mitochondria were resuspended again in SI buffer supplemented with 2.5 mM ATP, 3.75 mM NADH, 10 mM creatine phosphate, 100 µg/mL creatine kinase and import of precursor proteins were performed as described in Chapter 2.4.4.3.2.

2.4.4.9 Chemical cross-linking

Mitochondria (0.5 mg/mL) were incubated in SI buffer containing 2 mM ATP, 2 mM NADH, 10 mM creatine phosphate and 100 µg/mL creatine kinase for 3 min at 25 °C. Cross-linking was performed with 0.45 mM 3,3'-dithiobis-succinimidylpropionate (DSP) for 30 min on ice. Cross-linking reaction was stopped by adding 0.1 M glycine, pH 8.8 and incubating for 15 min on ice. For cysteine-specific cross-linking, indicated concentrations of bismaleimidohexane (BMH) or bismaleimidoethane (BMOE) were used and the reaction stopped by adding 50 mM DTT. Mitochondria were washed with SH buffer and reisolated by centrifugation at 18,000 x g, 10 min, 4 °C.

For Ni-NTA pull-down of His-tagged Tom22, mitochondria were solubilized with 1 % SDS in 50 mM Na-phosphate, 100 mM NaCl, 10 mM imidazole, 2 mM PMSF, pH 8.0 for 5 min at 25 °C and diluted with the same buffer containing 0.2 % Triton X-100. Non-solubilized material was removed by ultracentrifugation at 124,500 x g, 20 min, 4 °C. In the meantime, Ni-NTA agarose beads were washed with dH_2O and equilibrated three times with the same buffer containing 0.2 % Triton X-100. Solubilized mitochondria were subsequently incubated for 45 min at 4 °C with equilibrated Ni-NTA agarose beads. After three washing steps, specifically bound proteins were eluted in 2x Laemmli (+ ß-Me) containing 300 mM imidazole to cleave the cross-links. Samples were analysed by SDS-PAGE (2.4.1.2) and Western blotting (2.4.1.4).

3. RESULTS

3.1 *In vitro* analysis of the two IMS domains of Tim50

Tim50 was identified as the main receptor of the TIM23 complex and contains a N-terminal presequence that is proteolytically removed after import, a short matrix-exposed stretch, a single transmembrane (TM) domain and a large segment exposed to the IMS which contains the highly conserved and crystallized core domain (Figure 1.5) (Geissler et al., 2002; Yamamoto et al., 2002; Mokranjac et al., 2003a). *In vitro* cross-linking experiments with the recombinantly expressed and purified IMS segment of Tim50 and presequence peptides revealed a distinct binding site for presequences in the C-terminal part of the IMS segment of Tim50, after the core domain (Schulz et al., 2011). This led to the proposal that the IMS segment of Tim50 consists of two domains – the core domain and the presequence-binding domain (PBD). The molecular understanding of how the two domains in the IMS individually contribute to the receptor function of Tim50 and how they interact with the TIM23 and TOM subunits is still missing.

In the first part of my thesis, I wanted to identify the interaction partners of the individual domains of Tim50 in the IMS, core and PBD, using recombinantly expressed and purified Tim50 variants.

3.1.1 Recombinant expression of His-tagged Tim50 variants in *E. coli* cells

To identify the specific interaction partners of the individual domains of Tim50 in the IMS, N-terminally His-tagged Tim50 variants corresponding to the IMS segment, Tim50(164-476), the core domain, Tim50(164-361), and the PBD, Tim50(366-476), were cloned into pET-Duet1 plasmids and transformed into *E. coli* BL21(DE3) cells for recombinant expression. The Tim50 variants were expressed at 18 °C overnight and bacterial cell lysates were analysed by SDS-PAGE and CBB staining (Figure 3.1). The IMS segment, the core domain and the PBD, all carrying a His-tag and a TEV cleavage site were all efficiently expressed in *E. coli* cells after addition of IPTG (+IPTG), as seen by the appearance of distinct protein bands at ca. 37 kDa (Tim50(164-476)), ca. 27 kDa (Tim50(164-361)) and ca. 15 kDa (Tim50(366-476)).

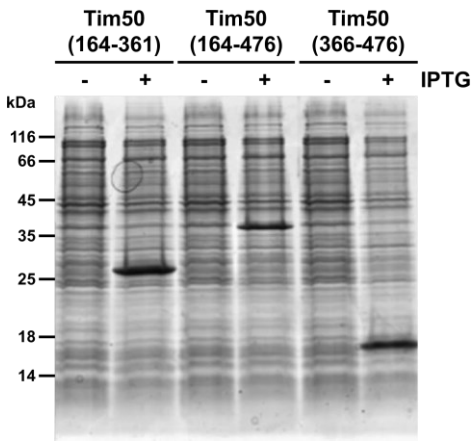

Figure 3.1 Recombinant expression of His-tagged Tim50 variants in *E. coli* cells. *E. coli* BL21(DE3) cells carrying pET-Duet1 plasmids encoding indicated Tim50 variants were grown in LB medium containing ampicillin. Cell extracts were made from cells taken before (- IPTG) and after (+ IPTG) induction with IPTG and were analysed by SDS-PAGE and CBB staining.

3.1.2 Purification of recombinant His-tagged Tim50 variants

Recombinantly expressed His-tagged Tim50 variants were purified using affinity- and size-exclusion chromatography. During the purification process of the three Tim50 variants, samples of each purification step were taken and analysed by SDS-PAGE and CBB staining. The following section describes the purification process of the His-tagged IMS segment of Tim50, Tim50(164-476), as an example.

E. coli cells were lysed using a cell microfluidizer and insoluble cell material was removed by centrifugation. The soluble part of the cell lysate was loaded on a Ni-NTA affinity chromatography column, in which the His-tagged IMS segment of Tim50 binds to the immobilized divalent cations. After a washing step to remove non-specifically bound proteins, the His-tagged IMS segment of Tim50 was eluted by a step elution with a buffer containing 300 mM imidazole (Figure 3.2). Ni-NTA fractions 3 and 4 were collected and pooled for further purification.

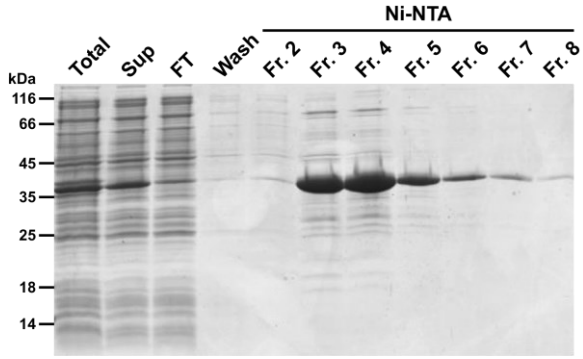

Figure 3.2 Ni-NTA purification step of recombinant His-tagged Tim50(164-476). His-tagged Tim50(164-476) was purified via Ni-NTA affinity chromatography column. Total, cell lysate of *E. coli* cells expressing Tim50(164-476) after cell lysis; Sup, supernatant of cell lysates after centrifugation; FT, flow-through fraction collected after loading the clarified cell lysate on the Ni-NTA column; Wash, fraction collected after washing the Ni-NTA column with washing buffer; Ni-NTA fractions 2-8, elution fractions collected with elution buffer. For each step, samples were taken and analysed by SDS-PAGE and CBB staining.

The IMS segment of Tim50 was further purified by size-exclusion chromatography (SEC), which separates proteins and other molecules based on their size and shape. The SEC column removed the remaining impurities and the IMS segment of Tim50 was eluted as a distinct protein band on a SDS-PA gel (Figure 3.3 A), which could also be visualized as a single symmetrical peak on the SEC chromatogram (Figure 3.3 B).

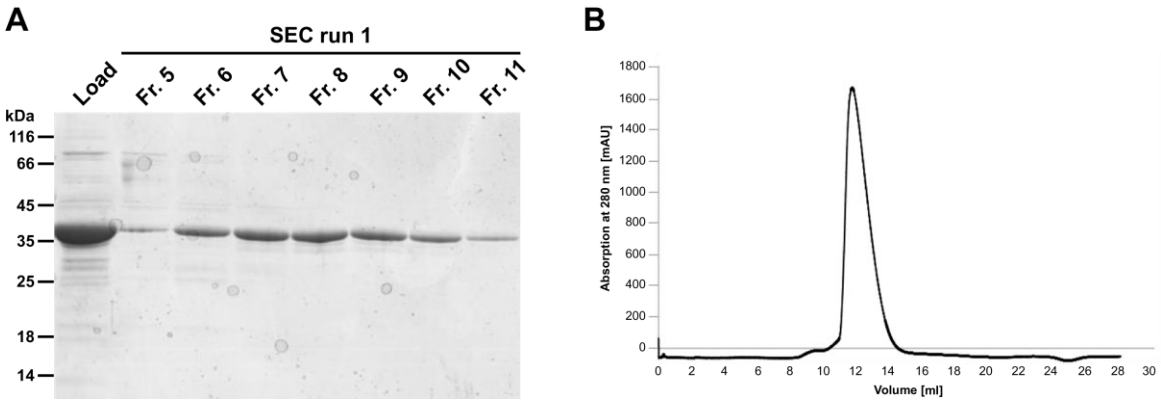

Figure 3.3 SEC purification step of recombinant His-tagged Tim50(164-476). (A) Tim50(164-476) was further purified via SEC column. Load, pooled Ni-NTA elution fractions were loaded on the SEC column; SEC run 1 (fractions 5-11), elution fractions collected after the SEC run. Samples were analysed by SDS-PAGE and CBB staining. (B) SEC chromatogram of Tim50(164-476). Y-axis, absorption at 280 nm [mAU]; x-axis, volume in [mL].

The three His-tagged Tim50 variants, the IMS segment, Tim50(164-476), the core domain, Tim50(164-361), and the PBD, Tim50(366-476) were purified in parallel following the same protocol. All three Tim50 variants were successfully expressed and purified with sufficient yield and purity for further experiments (Figure 3.4).

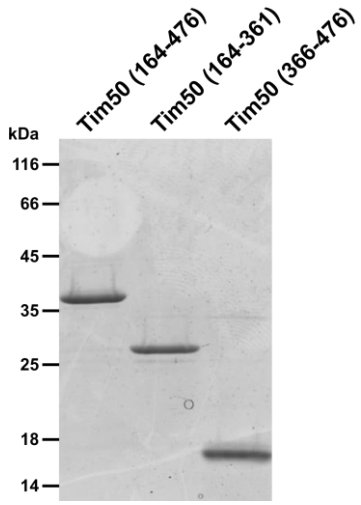

Figure 3.4 Overview of recombinantly expressed and purified Tim50 variants. Indicated purified Tim50 variants (5 µg loaded) were analysed by SDS-PAGE and CBB staining.

3.1.3 *In vitro* pull-down with immobilized Tim50 variants

To identify direct interaction partners of the individual domains of Tim50, the three recombinantly expressed and purified Tim50 variants were covalently coupled to CNBr-Sepharose beads and incubated with mitochondrial lysates of YPH499 wild-type cells in an *in vitro* pull-down experiment. CNBr-Sepharose beads with no coupled protein served as a negative control. Isolated wild-type mitochondria were solubilized in Triton X-100 containing buffer to dissociate the TIM23 complex into its individual subunits (except the stable Tim14-Tim16 subcomplex) and thus enables analysis of the direct interaction partners of the Tim50 variants. Analysis of the specifically bound material showed that both the IMS segment and the core domain of Tim50 stably interact with Tim23 (Figure 3.5), in agreement with the previously published data on Tim50-Tim23 interaction (Tamura et al., 2009; Qian et al., 2011; Schulz et al., 2011; Dayan et al., 2019). Notably, binding of Tim23 with the core domain of Tim50 seemed decreased, compared to its binding with the entire IMS segment. Surprisingly, all three Tim50 variants showed an interaction with Tim17. Whereas Tim17 bound with similar efficiencies to the IMS segment and core domain, the PBD of Tim50 only showed a weak binding to Tim17. Neither Tom22 nor Tom40 were efficiently binding to any of the Tim50 variants,

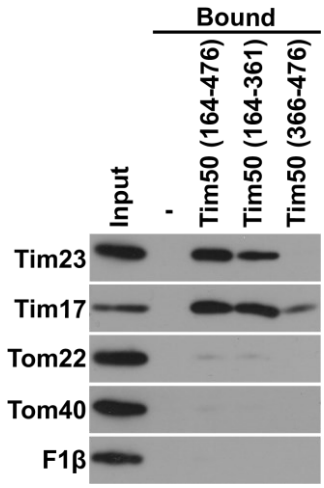

Figure 3.5 *In vitro* pulldown of immobilized Tim50 variants with solubilized mitochondrial lysates. Indicated recombinantly expressed and purified Tim50 variants were immobilized on CNBr-Sepharose beads and incubated with mitochondrial lysates from YPH499 wild-type cells, solubilized in Triton X-100 containing buffer. After extensive washing steps, specifically bound proteins were eluted with Laemmli buffer and analysed by SDS-PAGE and immunostaining. Input, mitochondrial lysate before incubating with CNBr-Sepharose beads; (-), CNBr-Sepharose beads without immobilized Tim50 variant, served as negative control.

with only a minor fraction of Tom22 seemed to bind to the IMS segment and core domain. F1β, used as a negative control, did not bind to any of the Tim50 variants, confirming the specificity of the *in vitro* pulldown experiment.

In conclusion, the *in vitro* pull-down experiment indicates that the core domain of Tim50 contains the main binding site for Tim23. Furthermore, Tim17 appears to be a novel interaction partner of Tim50 which binds to both the core domain and to a minor extent also the PBD of Tim50.

3.2 *In vivo* analysis of the individual domains of Tim50 in the IMS

Since most of our knowledge on the roles of the two domains of Tim50 in the IMS comes from the experiments performed *in vitro* (Schulz et al., 2011; Lytovchenko et al., 2013; Bajaj et al., 2014; Rahman et al., 2014), in the following part of my thesis I wanted to functionally dissect the roles of the core and PBD *in vivo*.

3.2.1 Both domains of Tim50 in the IMS are essential for cell viability

To gain molecular insight into the functions of the two domains of Tim50 in the IMS, the ability of the individual domains to support the function of the full-length Tim50 was analysed. For this, two Tim50 variants were generated and cloned into yeast centromeric plasmids under the control of endogenous *TIM50* promoter and 3´-UTR (Figure 3.6 A).

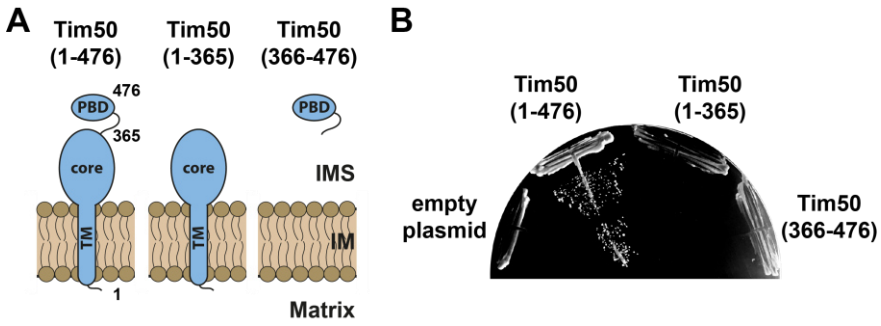

Figure 3.6 Both domains of Tim50 in the IMS are essential for cell viability. (A) Schematic representation of the domain structure of Tim50 and the variants analysed. 1 and 476 indicate the first and the last amino acid residue of Tim50 precursor and 365 the last residue of the core domain. TM, transmembrane segment; PBD, presequence-binding domain; IMS, intermembrane space; IM, inner membrane. (B) A Tim50 shuffling strain was transformed with centromeric plasmids encoding indicated variants of Tim50 under control of the endogenous promoter and 3'UTR. The ability of the Tim50 variants to support the function of the full-length protein was analysed on plates containing 5-FOA. Empty plasmid and a plasmid encoding a wild-type copy of Tim50 were used as negative and positive controls, respectively.

In the first variant, Tim50(1-365), Tim50 was truncated from the C-terminus, deleting the PBD. In the second one, Tim50(366-476), only the PBD of Tim50 was present. Since the targeting information of Tim50 is located in the N-terminal segments that are absent in the second variant, the PBD was preceded by the first 167 residues of yeast cytochrome b_2, which targets the PBD to the IMS. As deletion of *TIM50* is lethal, all rescue experiments were done in a Tim50 shuffling strain, a haploid yeast strain with a deleted chromosomal copy of *TIM50* but made viable by the presence of a wild-type copy of Tim50 encoded on a URA plasmid. The ability of the individual Tim50 variants to rescue the function of the full-length Tim50 was analysed on medium containing 5-fluoroorotic acid (5-FOA) that selects against the URA plasmids. An empty plasmid and one containing the full-length Tim50 were used as negative and positive controls, respectively. Whereas cells transformed with the plasmid encoding the wild-type Tim50, Tim50(1-476), grew on the 5-FOA medium, neither the core nor the PBD of Tim50 gave viable clones, like the empty plasmid which was used as a negative control (Figure 3.6 B). This result shows that both domains of Tim50 in the IMS are essential for yeast cell viability, and that neither of the two domains is sufficient to take over the function of Tim50 on its own.

The inability of the PBD to rescue the function of Tim50 could potentially be due to the absence of the endogenous Tim50 presequence, matrix and TM segments in the Tim50(366-476) variant. To exclude this possibility, another Tim50 variant, Tim50(Δ131-365), was generated. In this Tim50 variant only the core domain was deleted, anchoring the PBD with the endogenous TM of Tim50 to the IM (Figure 3.7 A). However, also cells transformed with this Tim50 variant did not give any viable colonies on 5-FOA medium (Figure 3.7 B), demonstrating that the PBD is indeed not sufficient to rescue the function of the full-length Tim50, even when it is anchored to the IM with the endogenous TM of Tim50.

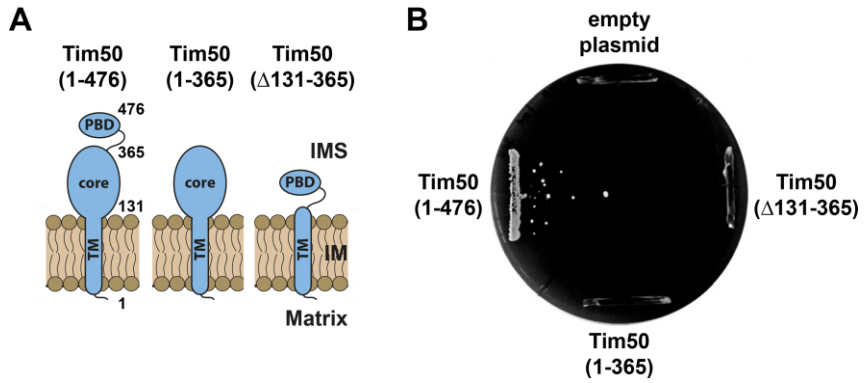

Figure 3.7 Anchoring the PBD to the IM is not sufficient to rescue the function of Tim50. (A) Schematic representation of Tim50 variants analysed. TM, transmembrane segment; PBD, presequence-binding domain; IMS, intermembrane space; IM, inner membrane. (B) A Tim50 shuffling strain was transformed with centromeric plasmids carrying indicated Tim50 variants under control of the endogenous promoter and 3'UTR. The ability of the Tim50 variants to support the function of the full-length protein was analysed on plates containing 5-FOA. Empty plasmid and a plasmid encoding a wild-type copy of Tim50 were used as negative and positive controls, respectively.

To confirm that the inability of the Tim50 variants to support the function of Tim50 is not due to their instability, the Tim50 variants were expressed from a GPD overexpression promoter in YPH499 wild-type yeast cells, in the background of the endogenous Tim50. Transformed cells were grown in SD medium and total cell extracts were made and analysed by SDS-PAGE and immunoblotting (Figure 3.8). Antibodies against Tim50 gave distinct additional bands for all three transformed Tim50 variants which correspond to their molecular weights. Thus, the inability of the Tim50 variants to rescue the function of the full-length Tim50 is not due to a lack of protein expression but rather a consequence of both domains of Tim50 in the IMS being essential for the viability of yeast cells.

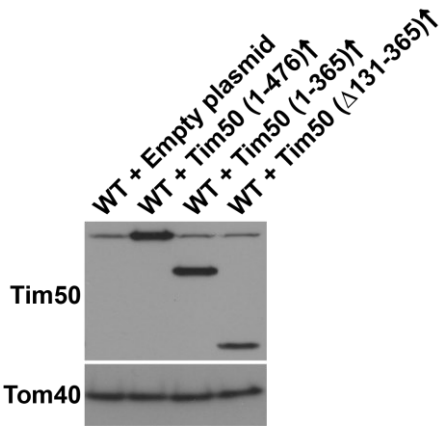

Figure 3.8 Expression of Tim50 variants in the background of YPH499 wild-type cells. YPH499 yeast cells carrying indicated Tim50 variants were grown in SD medium at 30 °C and total cell extracts were made and analysed by SDS-PAGE and immunostaining.

To exclude the further possibility that the IM anchored PBD is not able to rescue the function of the full-length Tim50 because it cannot reach the TOM complex, an additional Tim50 variant, Tim50(Δ164-365)+15flex, was generated. Here, the core domain was exchanged with a flexible linker sequence (Chen et al., 2013; Patel et al., 2022) of 15 amino acids to cover the distance of the deleted core domain (Figure 3.9 A). When this Tim50 variant was transformed into the Tim50 shuffling strain and selected on 5-FOA containing plates, no viable colonies were obtained (Figure 3.9 B). Taken together, neither a soluble PBD nor an IM-anchored PBD is sufficient to rescue the function of Tim50 on its own, confirming that both the core and the PBD of Tim50 are essential for cell viability.

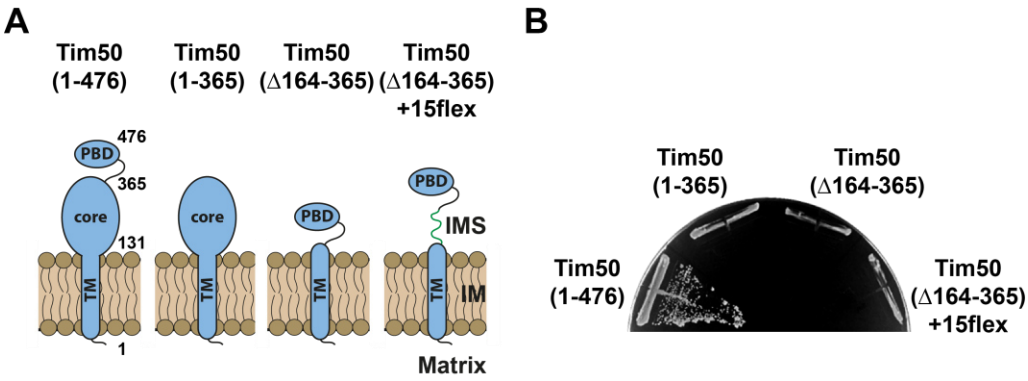

Figure 3.9 Introducing a flexible linker between the PBD and the TM is not sufficient to rescue the function of Tim50. (A) Schematic representation of Tim50 and its variants analysed. TM, transmembrane segment; PBD, presequence-binding domain; IMS, intermembrane space; IM, inner membrane. (B) A Tim50 shuffling strain was transformed with centromeric plasmids carrying indicated variants of Tim50 under control of the endogenous promoter and 3'UTR. The ability of the Tim50 variants to support the function of the full-length protein was analysed on plates containing 5-FOA. A plasmid encoding a wild-type copy of Tim50 was used as a positive control.

3.2.2 The function of Tim50 can be rescued by its two domains in the IMS expressed *in trans*

Since neither of the two domains of Tim50 in the IMS was able to rescue the function of Tim50 on its own, I tested whether the function of Tim50 could be reconstituted *in vivo* by co-expressing the core and PBD *in trans* (Figure 3.10 A). For this, the IM-anchored core domain, Tim50(1-365), and the PBD, Tim50(366-476), were transformed individually or together in the Tim50 shuffling strain. A wild-type copy of Tim50, Tim50(1-476) and an empty plasmid were transformed as positive and negative controls, respectively. The ability of yeast cells to grow using the transformed Tim50 variants was analysed on 5-FOA containing plates, as described before. Like shown above, cells transformed with the full-length Tim50 were growing on 5-FOA containing plates, whereas the individual Tim50 variants on their own as well as the empty plasmid produced no viable clones. Unexpectedly, when the core and the PBD of Tim50 were co-transformed, viable colonies were recovered after 5-FOA chase (Figure 3.10 B).

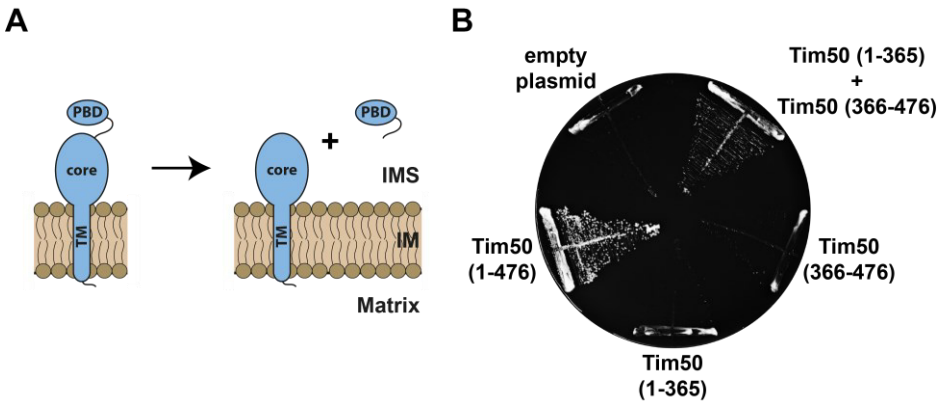

Figure 3.10 The function of Tim50 can be rescued by its two domains, core and PBD, expressed *in trans*. (A) Schematic representation of the core and PBD of Tim50 expressed *in trans*. TM, transmembrane segment; PBD, presequence-binding domain; IMS, intermembrane space; IM, inner membrane. (B) A Tim50 shuffling strain was transformed with centromeric plasmids carrying the indicated Tim50 variants under control of endogenous promoter and 3'UTR. The ability of the Tim50 variants, alone or upon co-expression, to support the function of the full-length protein was analysed on plates containing 5-FOA at 24°C. Empty plasmid and a plasmid encoding a wild-type copy of Tim50 were used as negative and positive controls, respectively.

To confirm that the full-length Tim50 is indeed absent in the co-expression strain, isolated mitochondria were analysed by SDS-PAGE and immunoblotting. While the wild-type Tim50 strain had a protein band corresponding to the full-length Tim50, this band was absent in the co-expression strain (Figure 3.11). Instead, three faster migrating protein bands were observed which correspond to

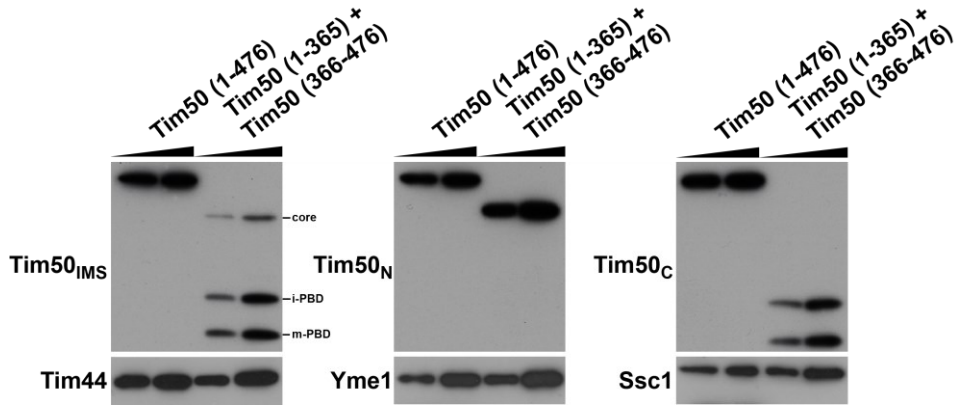

Figure 3.11 Protein expression of the Tim50 variants in isolated mitochondria. Isolated mitochondria (10 and 20 µg) were analysed by SDS-PAGE, followed by immunoblotting against depicted mitochondrial proteins. i-PBD and m-PBD as intermediate and mature forms of the PBD.

the core domain and PBD of Tim50. The IM anchored core domain of Tim50, Tim50(1-365), with its matrix exposed segment, was specifically detected using the $Tim50_N$ antibodies, while the $Tim50_C$ antibodies specifically recognized the two faster migrating protein species that correspond to the two processing forms of the IMS targeted PBD. This demonstrates that the full-length Tim50 is indeed not required for viability of yeast cells and that the function of Tim50 can be reconstituted *in vivo* from its individual domains co-expressed *in trans*.

To analyse the membrane association of the Tim50 variants in the co-expression strain, carbonate extraction was performed with isolated mitochondria. After treating mitochondria with 0.1 M sodium carbonate, integral membrane proteins were separated from soluble and peripheral membrane proteins by centrifugation and the pellet and supernatant fractions were subsequently analysed by SDS-PAGE and immunoblotting (Figure 3.12). Mge1 and Tim17 were used as markers for soluble and integral membrane proteins, respectively. While Mge1 was solely recovered in the supernatant, Tim17 was exclusively found in the pellet fraction, confirming the specificity of the assay. The full-length Tim50 was mainly recovered in the pellet fraction, even though a portion of Tim50 was also observed in the supernatant, in agreement with the previously observed partial extraction of α-helical single-spanning integral membrane proteins under used conditions (Mokranjac et al., 2003b). In the co-expression strain, the core domain of Tim50 was recovered exclusively in the pellet fraction, while the two forms of the PBD behaved differently. The slower migrating species was recovered mainly in the pellet fraction, demonstrating that it is still membrane integrated. The faster migrating species was however, found mainly in the supernatant fraction, indicating that it is present soluble in the IMS.

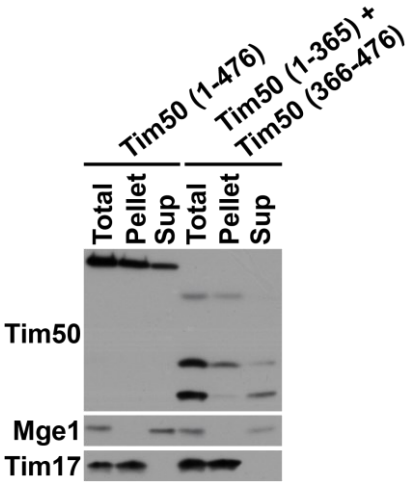

Figure 3.12 Membrane association of the Tim50 variants analysed by carbonate extraction. Isolated mitochondria from indicated cells were treated with 0.1 M sodium carbonate. Supernatant (Sup) and pellet fractions were separated by centrifugation. Total, sample before carbonate extraction, sup and pellet fractions were analysed by SDS-PAGE and immunoblotting. Mge1 and Tim17 were used as markers for soluble and integral membrane proteins, respectively.

These results validate the notion that the PBD is present in two forms, an intermediate form that is still membrane-integrated and the fully processed, mature form that is soluble in the IMS. The presence of the two forms is most likely due to incomplete processing of the cytochrome b_2 targeting signal.

Next, serial dilution spot assay was performed to compare the growth of the Tim50 co-expression strain, Tim50(1-365) + Tim50(366-476), to the strain carrying the wild-type copy of Tim50, Tim50(1-476). Cells were spotted on plates containing rich medium with glucose (YPD) or lactate (YPLac), as fermentable or non-fermentable carbon sources, respectively, and incubated at three different temperatures (24, 30 and 37 °C). While on glucose-containing medium yeast cells are able to produce energy through glycolysis, on non-fermentable medium like YPLac, they are fully dependent on mitochondria to produce ATP through the oxidative phosphorylation, making growth phenotypes of mitochondrial mutants usually more prominent in the latter medium. The Tim50 co-expression strain already showed a strong growth defect on YPD plates at 24 and 30 °C, compared to the wild-type strain (Figure 3.13). Moreover, on the same carbon source at an elevated temperature (37 °C), as well as on YPLac plates at all temperatures tested, the co-expression strain of Tim50 was virtually dead. Therefore, the two domains of Tim50 in the IMS when expressed *in trans* can rescue the function of the full-length Tim50 but only rather poorly.

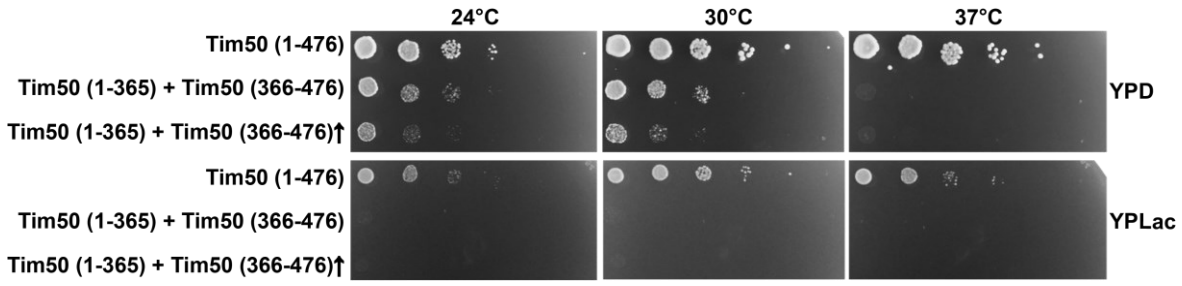

Figure 3.13 Growth phenotype of the co-expression strain of Tim50. Growth of indicated yeast strains was analysed by ten-fold serial dilution spot assay on plates containing rich medium with glucose (YPD) or lactate (YPLac), as fermentable and non-fermentable carbon sources, respectively. Plates were incubated on indicated temperatures.

Since the PBD is present in two processing forms in the co-expression strain of Tim50, this may limit the availability of the functional PBD. Therefore, it was tested whether overexpression of the PBD in the context of the co-expression strain of Tim50 may improve growth of yeast cells. For this, the PBD was cloned into a yeast plasmid with a GPD overexpression promoter and co-transformed with the core domain into the Tim50 shuffling strain. After obtaining viable colonies of the Tim50(1-365) + Tim50(366-476)↑ strain through 5-FOA selection, serial dilution spot assay was performed to compare the growth of yeast cells. Overexpression of the PBD in the context of the co-expression strain of Tim50 impaired the growth of yeast cells on fermentable medium at 24 and 30 °C even more severely than the initial co-expression strain of Tim50 (Figure 3.13).

3.2.3 Viability of the co-expression strain of Tim50 strictly depends on distinct segmentation of the two domains of Tim50

It was previously reported that the soluble IMS segment on its own is sufficient to support the function of the full-length Tim50 (Mokranjac et al., 2009). Thus, it was analysed in more detail how important the TM segment of Tim50 is in the context of the co-expression strain of Tim50.

First, a Tim50 variant, Tim50(132-365), was generated in which the core domain alone was targeted into the IMS using the cytochrome b_2 targeting signal (Figure 3.14 A). This Tim50 variant was transformed into the Tim50 shuffling strain, either alone or together with the PBD and its ability to rescue the function of Tim50 analysed on 5-FOA containing plates, as described before. The soluble core domain, neither on its own, nor upon co-expression with the PBD, generated any viable colonies on 5-FOA plates (Figure 3.14 B).

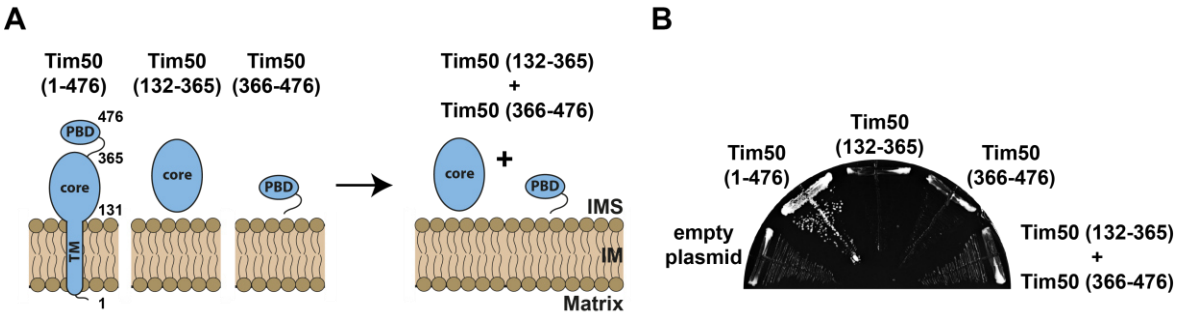

Figure 3.14 Co-expression of a soluble core and PBD is not sufficient to rescue the function of Tim50. (A) Schematic representation of Tim50 and its variants expressed *in trans*. TM, transmembrane segment; PBD, presequence-binding domain; IMS, intermembrane space; IM, inner membrane. (B) A Tim50 shuffling strain was transformed with centromeric plasmids carrying indicated protein variants of Tim50 under control of endogenous promoter and 3'UTR. The ability of the individual or co-expressed Tim50 variants to support the function of the full-length protein was analysed on plates containing 5-FOA. Empty plasmid and a plasmid encoding a wild-type copy of Tim50 were used as negative and positive controls, respectively.

Furthermore, the same core domain, together with the IM-anchored PBD generated above, Tim50(132-365) + Tim50(Δ164-365) (Figure 3.15 A), was also not sufficient to produce any viable yeast cells on 5-FOA medium (Figure 3.15 B).

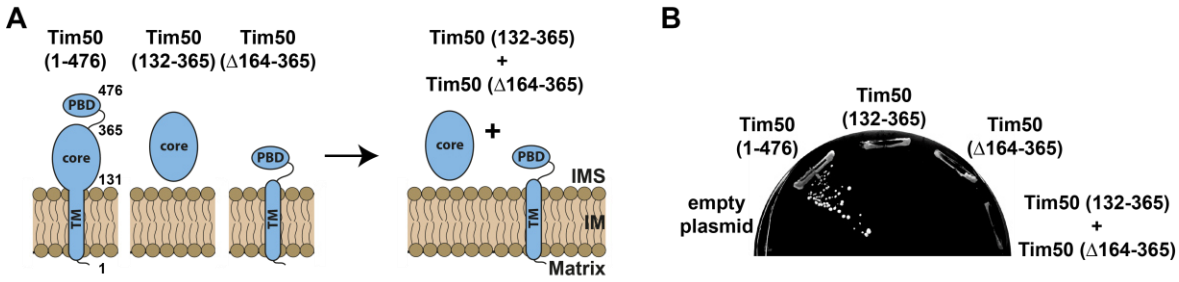

Figure 3.15 Co-expression of a soluble core and an IM anchored PBD is not sufficient to rescue the function of Tim50. (A) Tim50 variants expressed *in trans* are schematically illustrated. TM, transmembrane segment; PBD, presequence-binding domain; IMS, intermembrane space; IM, inner membrane. (B) Centromeric plasmids carrying indicated protein variants of Tim50 under control of endogenous promoter and 3'UTR were transformed into a Tim50 shuffling strain. The ability of the individual or co-expressed Tim50 variants to support the function of the full-length protein was analysed on 5-FOA plates. Empty plasmid and a plasmid encoding a wild-type copy of Tim50 were used as negative and positive controls, respectively.

Lastly, cells that were co-transformed with the Tim50 variants in which both the core domain and PBD were anchored to the IM with the endogenous TM segments of Tim50, Tim50(1-365) + Tim50(Δ164-365) (Figure 3.16 A), were also not able to produce viable clones on 5-FOA medium (Figure 3.16 B).

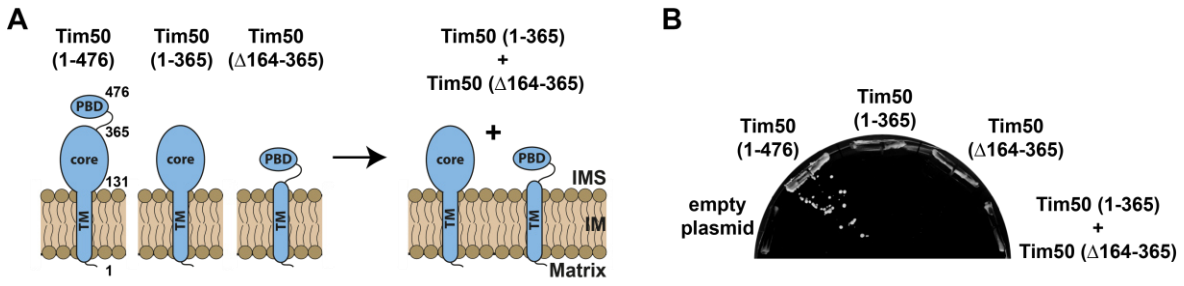

Figure 3.16 Co-expression of an IM anchored core and PBD is not sufficient to rescue the function of Tim50. (A) Schematic illustration of Tim50 variants expressed *in trans*. TM, transmembrane segment; PBD, presequence-binding domain; IMS, intermembrane space; IM, inner membrane. (B) A Tim50 shuffling strain was transformed with centromeric plasmids carrying indicated Tim50 variants under control of endogenous promoter and 3'UTR. The ability of the individual or co-expressed Tim50 variants to support the function of the full-length protein was analysed on plates containing 5-FOA. Empty plasmid and a plasmid encoding a wild-type copy of Tim50 were used as negative and positive controls, respectively.

In conclusion, the rescue of the function of Tim50 by co-expression of its two domains *in trans* strictly depends on anchoring the core domain to the IM on the one hand, and on targeting the PBD to the IMS without the presence of another TM segment of Tim50, on the other. The latter result may suggest that the endogenous TM segment of Tim50 specifically interacts with the TM segments of other TIM23 subunits. The presence of additional TM segments of Tim50 may therefore interfere with the assembly of the TIM23 complex and/or the recruitment of Tim50 to the complex.

3.2.4 The co-expression strain of Tim50 with an extended core domain rescues the growth of yeast cells more efficiently

Currently available literature has defined the boundaries of the core domain from residues 164-365 (Qian et al., 2011; Schulz et al., 2011; Rahman et al., 2014). To analyse the C-terminal boundary of the core domain and its flanking linker segment in an unbiased approach, extended versions of the core domain from the C-terminus were generated (Tim50(1-365), (1-370), (1-380), (1-390) and Tim50(1-394)) (Figure 3.17).

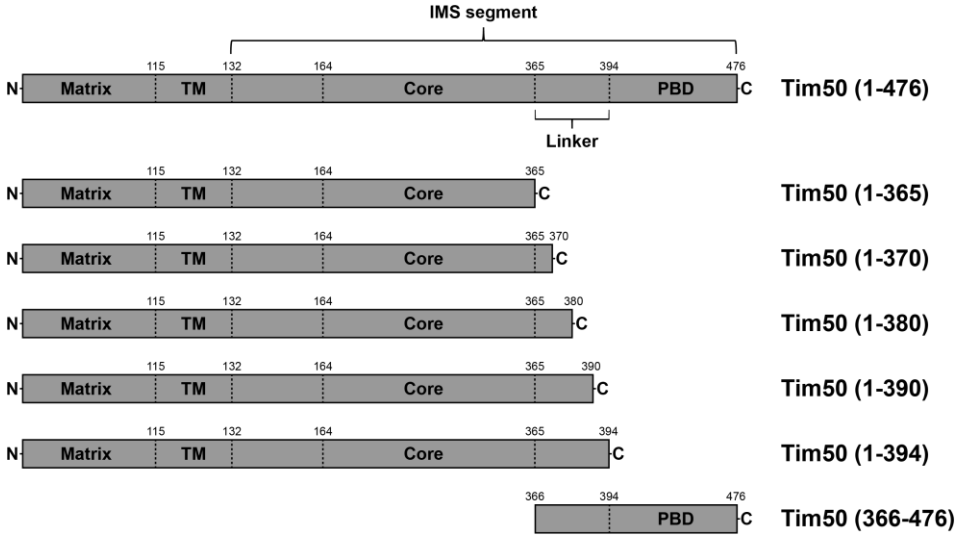

Figure 3.17 Extending the core domain of Tim50. Schematic representation of the domain structure of mature Tim50 and the variants analysed. Tim50 segments are indicated: Matrix, aa 45-114; transmembrane (TM), aa 115-131; core, aa 164-365; linker, aa 366-394; presequence-binding domain (PBD), aa 395-476. IMS, intermembrane space.

The ability of these Tim50 extended core domains to rescue the function of the full-length Tim50 was analysed by transforming them, alone or together with the PBD, into a Tim50 shuffling strain and streaking the obtained transformants on 5-FOA containing plates (Figure 3.18). The wild-type copy of Tim50, Tim50(1-476), and an empty plasmid were used as positive and negative controls, respectively. While cells transformed with the full-length Tim50 were growing on 5-FOA plates, none of the individual Tim50 variants produced any viable colonies, just like the empty plasmid used as a negative control.

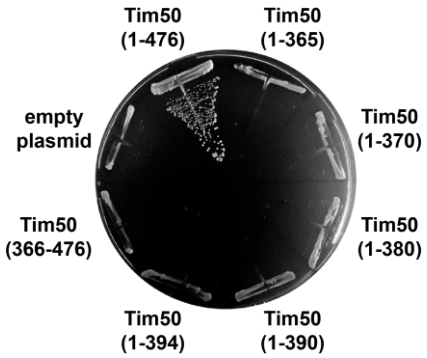

Figure 3.18 Extending the core domain of Tim50 is not sufficient to rescue the function of Tim50. Centromeric plasmids carrying indicated Tim50 variants under control of endogenous promoter and 3'UTR were transformed into a Tim50 shuffling strain. The ability of the individual Tim50 variants to support the function of the full-length protein was analysed on plates containing 5-FOA on 30 °C. Empty plasmid and a plasmid encoding a wild-type copy of Tim50 were used as negative and positive controls, respectively.

Interestingly, when the plasmids encoding the extended core domains of Tim50 were co-transformed with the PBD, viable yeast colonies were obtained on 5-FOA containing plates even at 30 °C (Figure 3.19). On this temperature, the initial co-expression strain of Tim50, Tim50(1-365) + Tim50(366-476), with the currently defined core domain was essentially dead.

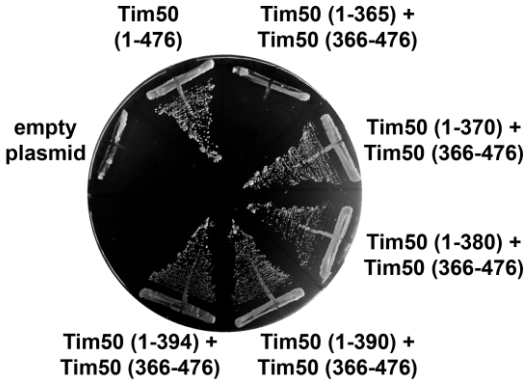

Figure 3.19 Extending the core domain of Tim50 by just five residues upon co-expression with the PBD produced viable yeast cells on 5-FOA plates even at 30 °C. A Tim50 shuffling strain was transformed with centromeric plasmids carrying indicated protein variants of Tim50 under control of endogenous promoter and 3'UTR. The ability of the co-expressed Tim50 variants to support the function of the full-length protein was analysed on plates containing 5-FOA on 30 °C. Empty plasmid and a plasmid encoding a wild-type copy of Tim50 were used as negative and positive controls, respectively.

Thus, extension of the core domain by just five residues results in a co-expression strain that grows much better than the initial co-expression strain of Tim50 (Figure 3.20).

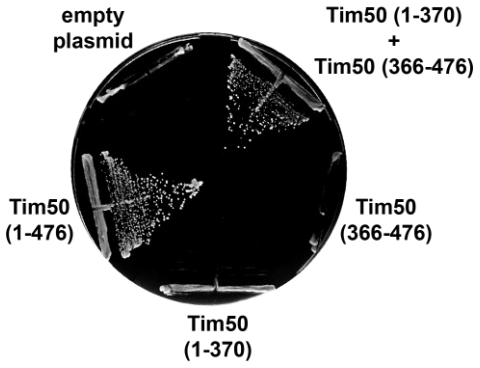

Figure 3.20 The function of Tim50 can be reconstituted *in vivo* more efficiently by co-expressing the extended core domain with the PBD. Centromeric plasmids carrying indicated protein variants of Tim50 under control of endogenous promoter and 3'UTR were transformed into a Tim50 shuffling strain. The ability of the individual or co-expressed Tim50 protein variants to support the function of the full-length protein was analysed on 5-FOA plates on 30 °C. Empty plasmid and a plasmid encoding a wild-type copy of Tim50 were used as negative and positive controls, respectively.

To visualize the difference in growth between the initial co-expression strain of Tim50, Tim50(1-365) + Tim50(366-476), and the one in which the core domain was extended by five residues, Tim50(1-370) + Tim50(366-476), serial dilution spot assay was performed (Figure 3.21). Compared to the initial co-expression strain which only grew very poorly on fermentable medium at 24 °C and 30 °C and was virtually dead on all other conditions, the co-expression strain of Tim50 with the extended core domain, Tim50(1-370) + Tim50(366-476), grew like wild type on both fermentable and non-fermentable medium at 24 °C and 30 °C. Even at 37 °C this co-expression strain grew almost like wild type on fermentable medium and only had an obvious growth defect on nonfermentable medium at 37 °C.

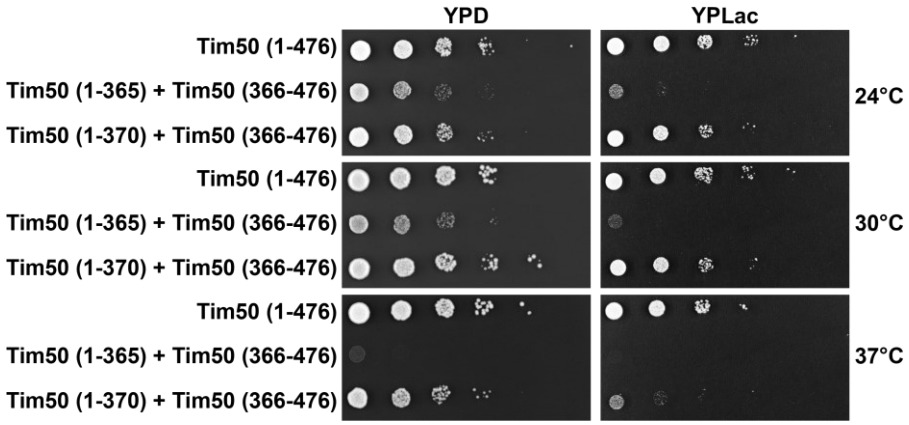

Figure 3.21 Co-expression of the two domains of Tim50 with the extended core domain rescues the function of Tim50 more efficiently. Growth of indicated yeast strains was analysed by ten-fold serial dilution spot assay on plates containing rich medium with glucose (YPD) or lactate (YPLac), as fermentable and non-fermentable carbon sources, respectively. Plates were incubated on indicated temperatures.

In conclusion, the function of Tim50 can be reconstituted *in vivo* from its two IMS domains expressed *in trans*. Extending the core domain by just 5 amino acids, compared to the previously defined boundary, results in a more efficient rescue, offering the opportunity to dissect the functional roles of the two domains of Tim50 in the IMS. For simplicity reasons, the co-expression strain of Tim50 with the extended core domain, Tim50(1-370) + Tim50(366-476), was defined as “50split” and this name will be used hereafter, in comparison to “50FL”, the corresponding wild-type strain expressing the full-length version of Tim50, Tim50(1-476).

3.2.5 Expression levels of mitochondrial proteins in 50split cells

To analyse the expression levels of the two domains of Tim50 in the IMS and of other mitochondrial proteins, mitochondria were isolated from 50FL and 50split cells and the mitochondrial protein profiles compared using SDS-PAGE and immunoblotting. Like in the initial co-expression strain of Tim50, affinity-purified antibodies raised against N-terminal ($Tim50_N$) and C-terminal ($Tim50_C$) peptides of Tim50 revealed that the full-length Tim50 was absent in 50split cells (Figure 3.22).

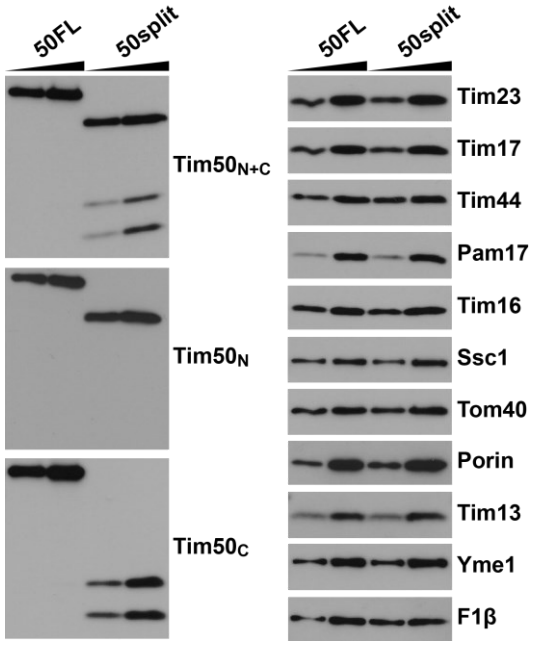

Figure 3.22 Expression of mitochondrial proteins is not affected in 50split cells. Isolated mitochondria (10 and 20 µg loaded) from 50FL and 50split cells grown in YPD at 24 °C were analysed by SDS-PAGE, followed by immunoblotting against depicted mitochondrial proteins.

In 50split mitochondria, three faster migrating proteins were present, corresponding to the IM anchored core domain, Tim50(1-370), and the two processing forms of the IMS targeted PBD, Tim50(1-370), as elaborated above (see Chapter 3.2.2 and Figure 3.11). The expression of the two Tim50 variants in 50split was comparable to that of the full-length Tim50 in 50FL, indicating that splitting Tim50 into its two domains did not affect Tim50 levels. Furthermore, splitting of Tim50 did not affect the expression of other subunits of the TIM23 complex analysed (Tim23, Tim17, Tim44, Pam17, Tim16 and Ssc1). Example proteins of other mitochondrial subcompartments, the OM (Tom40, porin), IMS (Tim13), IM (Yme1) and the matrix (F1β), also did not show any obvious difference in protein levels between the two types of mitochondria. To conclude, the growth of yeast cells can be supported by co-expression of the two domains of Tim50 in the IMS and this does not affect the expression levels of Tim50 and other mitochondrial proteins.

3.2.6 The membrane-integrated form of the PBD is sufficient in the context of 50split cells

Targeting of the PBD of Tim50 into the IMS using the cytochrome b_2 sorting signal results in the presence of two processing forms of the PBD. Carbonate extraction experiments shown above (Figure 3.12) confirmed the presence of a membrane integrated intermediate form and a predominantly soluble mature form of the PBD. However, it remained unclear which of the two processing forms, or both, are functionally relevant version(s) of the PBD.

To understand whether the membrane-integrated form of the PBD is sufficient to support growth in 50split cells, a further Tim50 variant of the PBD was generated, in which the IMP processing site in the cytochrome b_2 sorting signal was mutated so that no fully processed, soluble form can be produced. This Tim50 variant was co-transformed with the core domain, leading to a co-expression strain of Tim50, 50split+IMPmut, in which only the intermediate form of the PBD should be present. The 50FL, 50split and 50split+IMPmut strains were grown in YPD medium and their total cell extracts analysed by SDS-PAGE and immunoblotting. While the 50split strain contained both processing forms of the PBD, in the 50split+IMPmut cells essentially only the intermediate form of the PBD was present (Figure 3.23 A). Virtually the same result was obtained when isolated mitochondria from these cells were analysed (Figure 3.23 B).

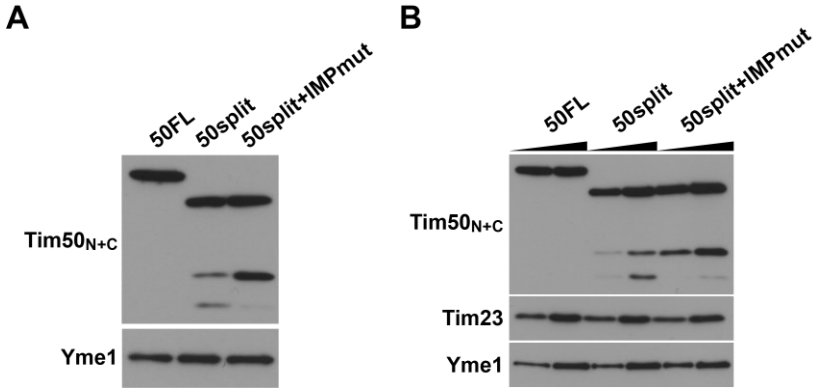

Figure 3.23 Mutation of the IMP processing site in 50split increases the intermediate form of the PBD variant. (A) Total cell extracts of the indicated strains grown in YPD at 24 °C were made and protein levels of the different Tim50 variants were analysed by SDS-PAGE and immunoblotting. (B) Isolated mitochondria (10 and 20 µg loaded) from indicated cells grown in YPD at 24 °C were analysed by SDS-PAGE, followed by immunoblotting against depicted mitochondrial proteins.

If the soluble form of the PBD is the functionally relevant protein species in 50split cells, then 50split+IMPmut cells, in which this version of the PBD is virtually absent, should grow worse than

50split cells. To test this hypothesis, growth of 50split and 50split+IMPmut cells was compared by serial dilution spot assay. Surprisingly, 50split+IMPmut cells were growing essentially the same as 50split on both fermentable and non-fermentable media and at all three tested temperatures (Figure 3.24). This indicates that the intermediate, membrane-integrated form of PBD is the functionally relevant one and that the soluble form may not be necessary in the context of 50split cells.

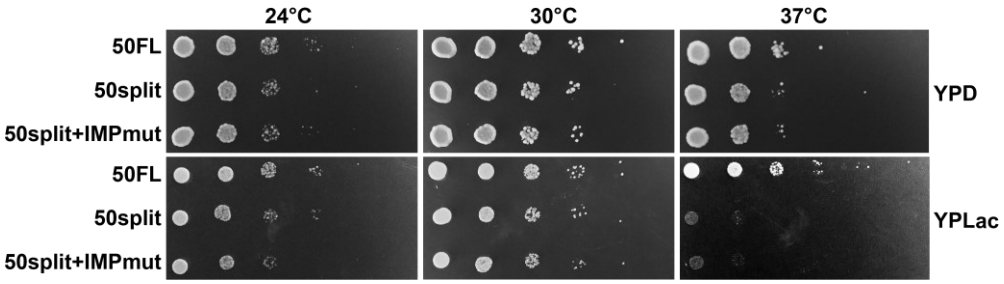

Figure 3.24 Increasing the intermediate form of the PBD variant in context of 50split cells does not affect growth of yeast cells. Growth of indicated yeast strains was analysed by ten-fold serial dilution spot assay on plates containing rich medium with glucose (YPD) or lactate (YPLac), as fermentable and non-fermentable carbon sources, respectively. Plates were incubated at indicated temperatures.

3.2.7 Tim50 is recruited to the TIM23 complex mainly through its core domain

To analyse how Tim50 is recruited to the TIM23 complex in 50split cells and whether the two individually expressed domains of Tim50 are interacting with each other, coimmunoprecipitation experiment was performed. Isolated mitochondria from 50FL and 50split cells were solubilized in digitonin-containing buffer, and affinity-purified $Tim50_N$, $Tim50_C$ and Tim23 antibodies were used for coimmunoprecipitation. Pre-immune serum was used as a negative control. Both $Tim50_N$ and $Tim50_C$ antibodies essentially depleted the full-length Tim50 and coprecipitated Tim23 and Tim17 to similar extents from solubilized 50FL mitochondria (Figure 3.25). With affinity-purified antibodies against Tim23, both Tim23 and Tim17 were depleted from the supernatant and Tim50 was coprecipitated, as described before (Mokranjac et al., 2009). When solubilized 50split mitochondria were used, affinity-purified $Tim50_N$ antibodies depleted the Tim50 variant containing the core domain, however, the PBD was not coprecipitated. Similarly, $Tim50_C$ antibodies depleted the PBD of Tim50 from the lysate, without coprecipitating the core domain. This suggests that even under the mild solubilization conditions used in the experiment, the two domains of Tim50 do not seem to stably interact with each other. Interestingly, Tim23 and Tim17 were only found in the bound fraction when $Tim50_N$ antibodies were used for coimmunoprecipitation and not with $Tim50_C$ antibodies. Likewise, affinity-purified Tim23 antibodies only coprecipitated the Tim50 variant with the core domain and not the PBD of

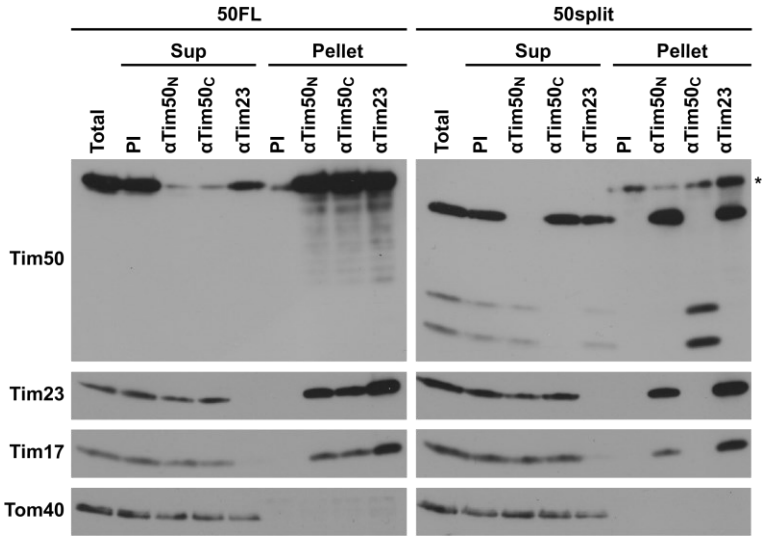

Figure 3.25 Tim50 is recruited to the TIM23 complex mainly through its core domain. Isolated mitochondria from 50FL and 50split cells were solubilized with digitonin-containing buffer and subjected to immunoprecipitation with affinity-purified antibodies against $Tim50_N$, $Tim50_C$ and Tim23 prebound to Protein A-Sepharose beads. Antibodies from preimmune serum (PI) were used as a negative control. After three washing steps, specifically bound proteins were eluted with Laemmli buffer. Total (20 %), supernatant (Sup, 20 %), and bound (Pellet, 100 %) fractions were analysed by SDS-PAGE and immunoblotting with indicated antibodies. (*) indicates the heavy chains of the IgGs.

Tim50. The interaction between Tim17 and Tim23 was not affected in 50split mitochondria. It is possible that an interaction of one of the two Tim50 domains with the TOM complex is masked in the context of the full-length protein and may therefore be revealed in 50split cells. However, neither in 50split nor in 50FL mitochondria was Tom40 coprecipitated with any of the Tim50 antibodies. In conclusion, the coimmunoprecipitation experiment demonstrates that the two domains of Tim50 in the IMS do not stably interact with each other, that Tim50 is recruited to the TIM23 complex mainly through its core domain and that neither of the two domains of Tim50 interacts stably with the TOM complex.

It is in principle possible that the interaction of Tim23 with the Tim50 variant carrying the core domain is mediated through the matrix and TM segments of Tim50, rather than through the core domain. To analyse this possibility, Tim50(1-365)↑ and Tim50(Δ131-365)↑ strains, that carry these Tim50 variants under an overexpression promoter in the background of wild-type Tim50 and which were described above (see Figure 3.8), were used. Mitochondria from WT+Tim50(1-365)↑ and WT+Tim50(Δ131-365)↑ cells were isolated and the expression of these Tim50 variants in the background of the wild-type Tim50 visualized by SDS-PAGE followed by immunoblotting (Figure 3.26 A).

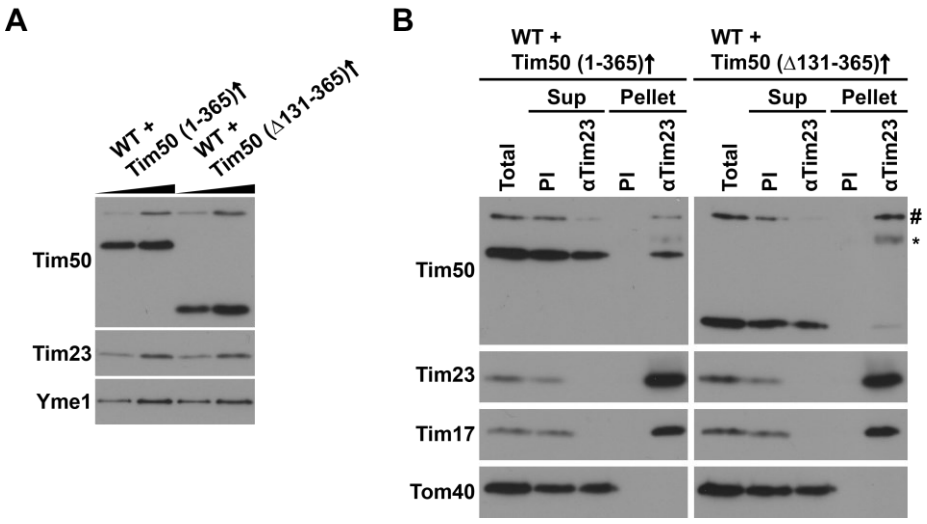

Figure 3.26 In the absence of the core domain of Tim50, Tim23-Tim50 interaction is disrupted. (A) Isolated mitochondria (10 and 20 µg) from indicated cells grown in YPD at 30 °C were analysed by SDS-PAGE, followed by immunoblotting against depicted mitochondrial proteins. (B) Isolated mitochondria from indicated cells were solubilized with digitonin-containing buffer and subjected to immunoprecipitation with affinity-purified antibodies against Tim23 prebound to Protein A-Sepharose beads. As a negative control, antibodies from preimmune serum (PI) were used. After three washing steps, specifically bound proteins were eluted with Laemmli buffer. Total (20 %), supernatant (Sup, 20 %), and bound (Pellet, 100 %) fractions were analysed by SDS-PAGE and immunoblotting with indicated antibodies. (#) indicates the endogenous wild-type version of Tim50. (*) indicates the heavy chains of the IgGs.

Subsequently, coimmunoprecipitation experiments were performed with affinity-purified Tim23 antibodies (Figure 3.26 B). In digitonin-solubilized WT+Tim50(1-365)↑ mitochondria, affinity-purified Tim23 antibodies depleted both Tim23 and Tim17 from the lysate and coprecipitated the full-length Tim50, in agreement with the coimmunoprecipitation results above. The Tim50 variant lacking the PBD, which was overexpressed compared to the full-length Tim50, was also found in the bound fraction to a higher extent compared to Tim50, suggesting that it was precipitated as efficiently as the full-length Tim50. Similarly, affinity-purified Tim23 antibodies depleted Tim23 and Tim17 from the WT+Tim50(Δ131-365)↑ lysate and coprecipitated full-length Tim50. The amount of the Tim50 variant that lacks the core domain was, however, strongly decreased in the bound fraction, compared to the full-length protein, even though it was present in higher levels in the lysate. This unambiguously demonstrates that the core domain of Tim50 contains the main binding site for Tim23.

3.2.8 Protein import via the TIM23 complex is impaired in 50split

As the main receptor of the TIM23 complex, Tim50 recognizes and binds precursor proteins, and therefore has an essential role during protein import into mitochondria. Thus, it was analysed

how co-expression of the two domains of Tim50 *in trans* in 50split cells affects protein translocation into mitochondria *in vivo* and *in organello*. The accumulation of the precursor form of the matrix targeted protein, Mdj1, which uses the TIM23 complex for its import into mitochondria, is frequently used as a marker for *in vivo* protein import efficiency (Yamamoto et al., 2002; Banerjee et al., 2015). 50FL and 50split cells were grown in non-fermentable medium and total cell extracts were prepared and analysed by SDS-PAGE and immunoblotting (Figure 3.27 A). While in 50FL cells only the mature form of Mdj1 was observed, in 50split cells a slower migrating form, which corresponds to the

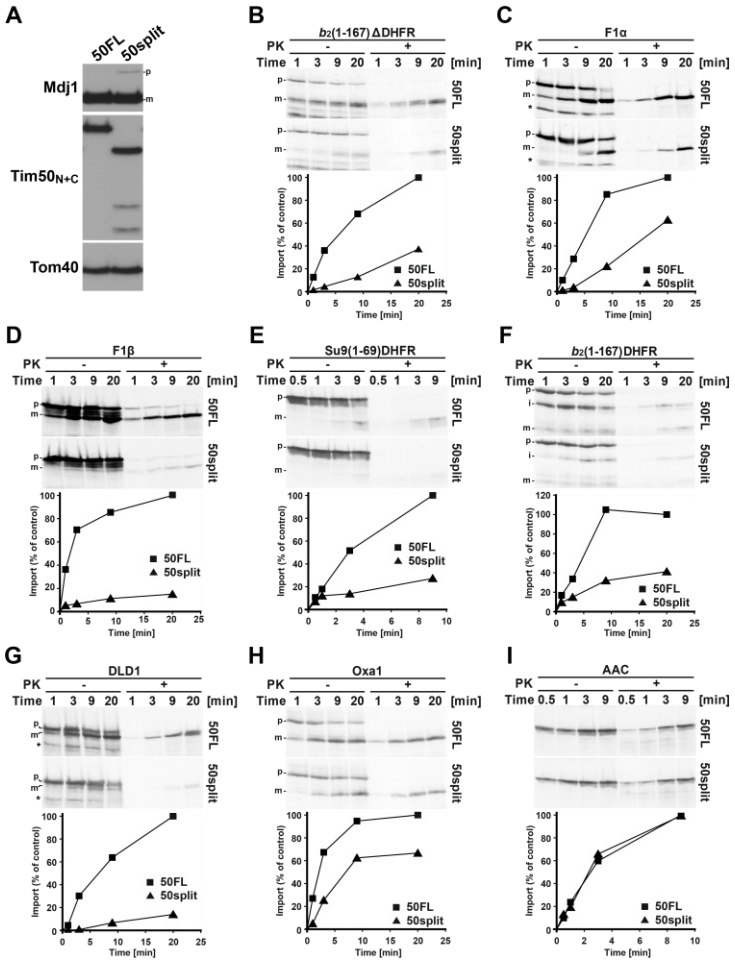

Figure 3.27 Protein import via the TIM23 complex is impaired in 50split. (A) Indicated yeast cells were grown in YPLac at 30 °C and total cell extracts were analysed by SDS-PAGE and immunostaining. p, precursor form; m, mature form. (B-I) ^{35}S-labelled mitochondrial precursor proteins were imported into mitochondria isolated from 50FL and 50split cells. After indicated time periods, aliquots were removed, import was stopped and Proteinase K (PK) was added, where indicated. Mitochondria were reisolated and analysed by SDS-PAGE and autoradiography (upper panels). Quantifications of PK-protected mature forms of imported proteins are shown in the lower panels. The amount of the PK-protected mature form of imported proteins in the longest time point in 50FL mitochondria was set to 100 %. p, precursor; i, intermediate; m, mature forms of imported proteins. (*), indicates translation products synthesized from an internal methionine.

precursor form of Mdj1, was additionally revealed. This suggests an impaired import of proteins in 50split cells via the TIM23 complex *in vivo*.

Protein import was also analysed *in organello* by synthesizing a series of artificial and endogenous precursor proteins *in vitro* in the presence of ^{35}S-methione and subsequently importing them into 50split and 50FL mitochondria (Figure 3.27 B-I). Samples were taken at indicated time points and, after stopping the import reactions, mitochondria were treated with Proteinase K (PK) to degrade all nonimported precursor proteins. Protein import of matrix targeted precursor proteins (b_2(1-167)ΔDHFR, Su9(1-69)DHFR, F1α and F1β) that require the TIM23 complex was strongly impaired in 50split compared to 50FL mitochondria. Similarly, proteins that are laterally inserted via the TIM23 complex (b_2(1-167)DHFR and DLD1), as well as the presequence-containing precursor protein Oxa1, which contains multiple TM segments, were imported less efficiently into 50split mitochondria. The ATP/ADP carrier (AAC) that uses another protein translocase for its import into mitochondria and is therefore TIM23 complex independent, was imported with comparable efficiencies in 50split mitochondria as in 50FL, suggesting an overall functional and structural integrity of mitochondria. Taken together, these *in vivo* and *in organello* results demonstrate an impaired protein import of TIM23 dependent precursor proteins in 50split cells.

3.2.9 Binding of precursors by Tim50 is affected in 50split

Tim50 is the first component of the TIM23 complex that interacts with incoming presequences as soon as they appear at the outlet of the TOM complex. In the absence of membrane potential, the presequence is translocated through the TOM complex, however most of the precursor protein is still outside of mitochondria. Already at this stage presequences can be cross-linked to Tim50 (Yamamoto et al., 2002; Mokranjac et al., 2003a; Mokranjac et al., 2009).

To investigate whether splitting of Tim50 in 50split cells affects receptor function of the protein and which of the two domains in the IMS recognizes presequences, ^{35}S-labelled Oxa1 precursor was imported into 50FL and 50split mitochondria in the absence of membrane potential, followed by cross-linking with the amino-group-specific chemical cross-linking reagent 1,5-Difluor-2,4-dinitrobenzol (DFDNB). After quenching the excess of cross-linker, mitochondria were solubilized with SDS to dissociate all noncovalent interactions. Subsequently, mitochondrial lysates were subjected to immunoprecipitation with affinity-purified Tim50$_N$ and Tim50$_C$ antibodies and with antibodies from a preimmune serum as a negative control. In 50FL mitochondria cross-linking adduct between Oxa1

precursor and the full-length Tim50 was efficiently precipitated with both $Tim50_N$ and $Tim50_C$ antibodies (Figure 3.28 A).

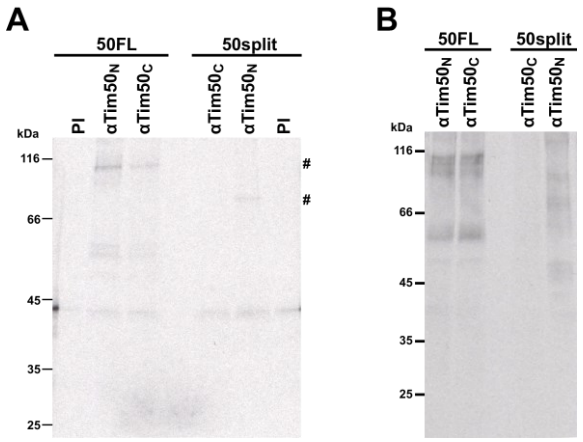

Figure 3.28 Binding of precursors by Tim50 is affected in 50split. ^{35}S-labelled Oxa1 precursor (A) and b_2(1–167)ΔDHFR$_{K5}$ (B) was imported into isolated 50FL and 50split mitochondria in the absence of membrane potential. Samples were subjected to cross-linking with 1,5-Difluor-2,4-dinitrobenzol (DFDNB). After quenching of excess cross-linker, mitochondria were reisolated and solubilized in SDS-containing buffer. Samples were diluted in Triton X-100-containing buffer and subjected to immunoprecipitation with affinity-purified antibodies against N- ($Tim50_N$) and C-terminal peptides ($Tim50_C$) of Tim50 prebound to Protein A-Sepharose. Antibodies from pre-immune serum (PI) were used as a negative control. The immunoprecipitates were analysed by SDS-PAGE and autoradiography. (#) indicate the immunoprecipitated cross-linking adducts.

In 50split mitochondria, however, a faster migrating cross-linking adduct was detected exclusively when $Tim50_N$ antibodies were used for immunoprecipitation, indicating Oxa1 precursor binding to the core domain of Tim50. Comparing the signal intensities of the cross-linking adducts precipitated with $Tim50_N$ antibodies, cross-linking efficiency in 50split was decreased compared to 50FL mitochondria. Essentially the same results were obtained when another ^{35}S-labelled precursor protein, b_2(1-167)ΔDHFR$_{K5}$, was analysed (Figure 3.28 B). While in 50FL mitochondria the cross-linking adducts between b_2(1-167)ΔDHFR$_{K5}$ and Tim50 were precipitated with both $Tim50_N$ and $Tim50_C$ antibodies, faster migrating cross-links which were also generated with less efficiency, were precipitated only with $Tim50_N$ antibodies in 50split. In conclusion, these results indicate that the core domain of Tim50 is the primary binding-site for presequences, however, the PBD seems to contribute to the receptor function of Tim50 as well.

3.2.10 Association of precursor proteins with the TOM complex is already affected in 50split

Since splitting the two domains of Tim50 affects binding of precursor proteins to Tim50 at the stage when only presequences appear at the outlet of the TOM complex while most of the precursor protein is still outside of mitochondria, it was analysed whether the association of precursor proteins with the TOM complex is already affected in 50split mitochondria. For this, ^{35}S-labelled Oxa1 precursor protein was imported into 50FL and 50split mitochondria in the presence and absence of membrane potential. After reisolation, mitochondria were solubilized in digitonin-containing buffer and analysed by SDS- and BN-PAGE. In the presence of membrane potential Oxa1 precursor was processed to its mature form in both 50FL and 50split mitochondria (Figure 3.29, lower panel). Processing efficiency was, however, decreased in 50split mitochondria, in agreement with the import defects of TIM23 dependent precursor proteins observed above. In both 50FL and 50split mitochondria, Oxa1 was accumulated in its precursor form in the absence of membrane potential. This precursor form of Oxa1 generates a ca. 500 kDa intermediate in the TOM complex that can be visualized on BN-PAGE (Frazier et al., 2003; Chacinska et al., 2005). Formation of this Oxa1-TOM complex intermediate was dependent on the presence of a functional Tim50, without it being a component of the intermediate (Chacinska et al., 2005). In 50split, the Oxa1-TOM complex intermediate was formed less efficiently, compared to 50FL mitochondria (Figure 3.29, upper panel). Notably, in the presence of membrane

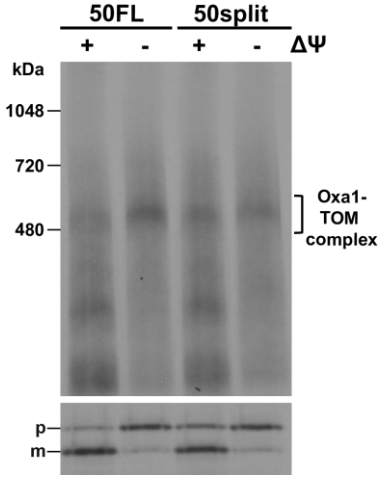

Figure 3.29 Association of precursor proteins with the TOM complex is already affected in 50split. ^{35}S-labelled Oxa1 precursor was imported into 50FL and 50split mitochondria at 25 °C in the presence or in the absence of membrane potential (ΔΨ), as indicated. Mitochondria were reisolated, solubilized in digitonin-containing buffer and samples were analysed by BN-PAGE (upper panel) and SDS-PAGE (bottom panel) followed by autoradiography. p, precursor; m, mature forms of Oxa1.

potential the Oxa1-TOM complex intermediate is more abundant in 50split than in 50FL mitochondria, consistent with the import defects and thus accumulation of Oxa1 precursor in the TOM complex.

To analyse the kinetics of the formation of the Oxa1-TOM complex intermediate, Oxa1 precursor was imported in the absence of membrane potential into 50FL and 50split mitochondria and samples were taken at indicated time points and analysed by BN-PAGE (Figure 3.30 A). In 50split mitochondria the Oxa1-TOM complex intermediate was formed more slowly and after 30 minutes reached only about 50 % of the intermediate formed in 50FL mitochondria (Figure 3.30 B).

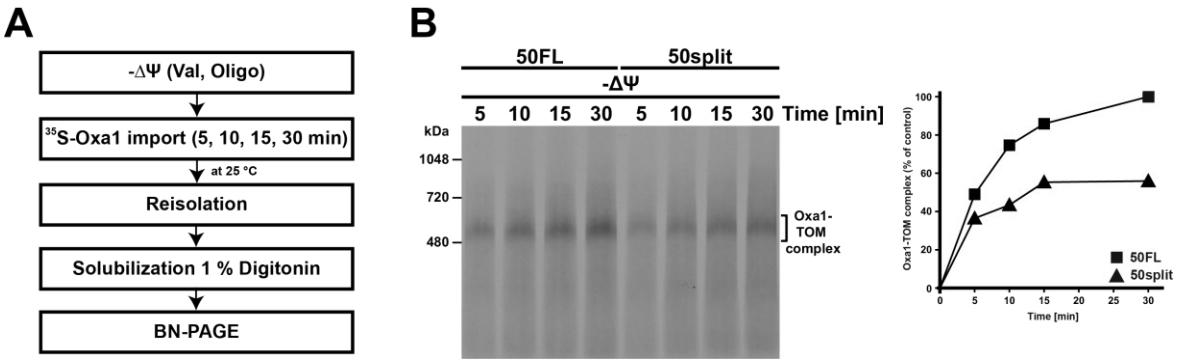

Figure 3.30 The Oxa1-TOM complex intermediate is formed more slowly in 50split. (A) Schematic representation of the major experimental steps and conditions. (B) ^{35}S-labelled Oxa1 precursor was imported into 50FL and 50split mitochondria in the absence of membrane potential (ΔΨ). Samples were taken at indicated time points, mitochondria were reisolated, solubilized with digitonin and samples were analysed on BN-PAGE and autoradiography (left panel). Right panel, quantification of the Oxa1-TOM complex intermediate. The amount of the intermediate at the latest time point in 50FL was set to 100 %.

Precursor proteins that were previously bound to mitochondria in the absence of membrane potential can be chased across the inner membrane via the TIM23 complex by re-energizing mitochondria (Kanamori et al., 1999). For this, membrane potential was reversibly dissipated with carbonyl cyanide m-chlorophenylhydrazone (CCCP) and Oxa1 precursor was imported into 50FL and 50split mitochondria. After reisolation, CCCP was washed away with DTT and BSA-containing buffer, the membrane potential was re-established and Oxa1 precursor was chased into mitochondria (Figure 3.31 A). The chase of Oxa1 precursor was slower in 50split compared to 50FL mitochondria (Figure 3.31 B), though this effect was less evident compared to the formation of the Oxa1-TOM complex intermediate.

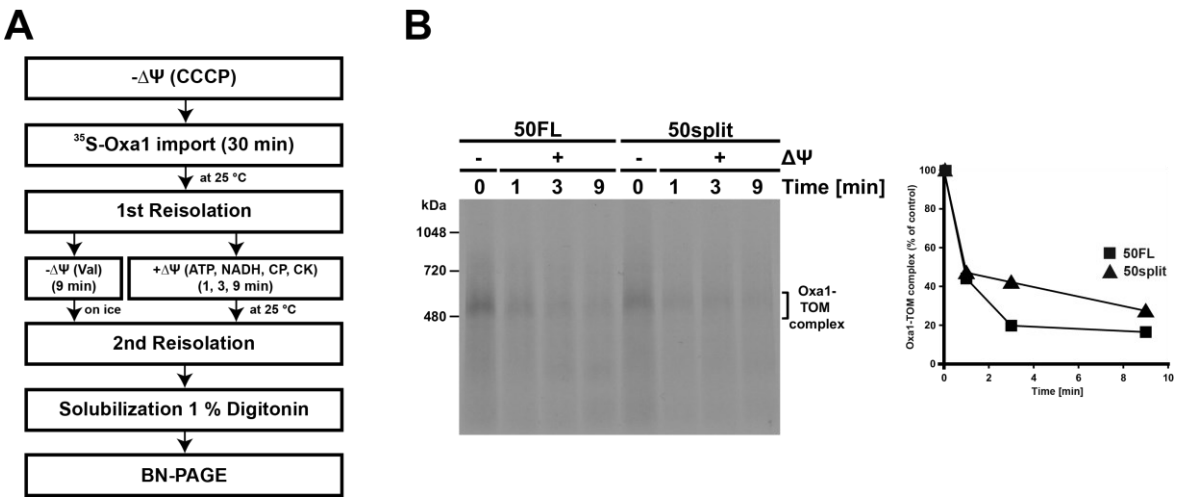

Figure 3.31 Chasing Oxa1 precursor into the matrix after accumulation in the TOM complex, is affected in 50split. (A) Schematic representation of the major experimental steps and conditions. (B) ^{35}S-labelled Oxa1 precursor was imported into 50FL and 50split mitochondria in which the membrane potential (ΔΨ) was dissipated with CCCP. After reisolation, mitochondria were either kept with dissipated ΔΨ or were energized to chase Oxa1 into the mitochondria. At indicated time points, mitochondria were reisolated again, solubilized in digitonin-containing buffer and then analysed as in Figure 3.30. The amounts of Oxa1-TOM complex intermediate at timepoint 0 in 50FL and 50split were set to 100 %.

In conclusion, these results indicate that splitting of Tim50 in 50split not only affects binding of precursor proteins to Tim50, but already impairs the association of precursor proteins with the TOM complex, as well as their subsequent transfer to the TIM23 complex.

3.2.11 Coordination between TIM23 and TOM complexes is affected in 50split

Since splitting of Tim50 already impairs association of precursor proteins with the TOM complex, it is possible that the coordination between TIM23 and TOM complexes is also affected in 50split. Another lab member, Shalini Roy Chowdhury, obtained genetic evidence that the cooperation between TIM23 and TOM complexes is impaired in 50split cells. Here, TOM *trans* site mutants (*tom22ΔC*, *tom40ΔC* and *Δtom7*), that are implicated in cooperation between the two complexes, showed strong negative genetic interactions with 50split on serial dilution spot assay (Genge et al., 2023). To further explore the influence of splitting Tim50 on the coordination between the TOM and TIM23 complexes, the unique two-membrane spanning topology of Tim23 was analysed. The accessibility of the N-terminal segment of Tim23 to externally added proteases in intact mitochondria (Donzeau et al., 2000), the so-called “clipping” of Tim23, is modulated by the Tim50-Tim23 interaction, import of precursor proteins and additionally by the assembly of the TOM complex (D. Popov-Celeketić et al., 2008; Gevorkyan-Airapetov et al., 2009; Waegemann et al., 2015). Thus, it facilitates

transfer of proteins between the two complexes and hence may serve as a marker for the efficient coordination of TOM and TIM23 complexes.

To understand how splitting Tim50 affects the exposure of Tim23 to the cytosol, isolated mitochondria from 50FL and 50split cells were incubated in the presence and absence of proteinase K (PK) and samples were taken at indicated time points and analysed by SDS-PAGE. In 50FL mitochondria, the N-terminal segment of Tim23 was degraded by PK generating the faster migrating, clipped version of Tim23 (Figure 3.32). Clipping of Tim23 was, however, virtually absent in 50split mitochondria. Tom70 served as a control for an OM protein and was degraded by PK in both 50FL and 50split mitochondria. Yme1 and Tim44 served as controls for IM and matrix proteins, respectively, and were unaffected by the addition of PK, demonstrating the integrity of mitochondria. In conclusion, splitting of Tim50 into its two domains in 50split cells affects the exposure of Tim23 to the cytosol which likely additionally impairs the cooperation of TOM and TIM23 complexes.

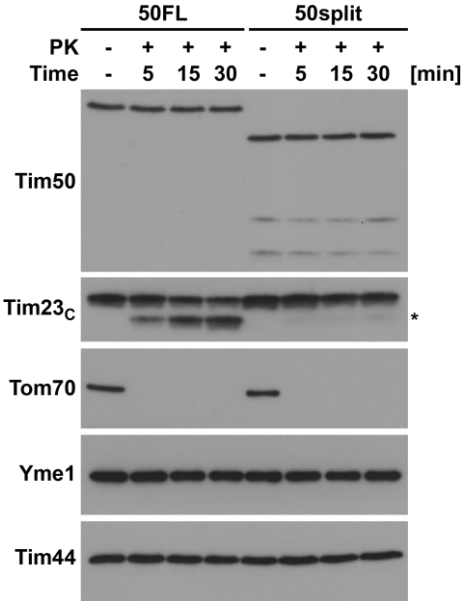

Figure 3.32 Exposure of Tim23 into the cytosol is affected in 50split. Isolated mitochondria from 50FL and 50split cells were incubated in the presence and absence of Proteinase K (PK) for the indicated time and subsequently analysed by SDS-PAGE and immunoblotting. (*) indicates the clipped version of Tim23.

3.3 Analysis of the interaction between the core and PBD in the context of the full-length Tim50

The results of the 50split strain suggest that, although it is possible to rescue the function of the full-length Tim50 by co-expression of its two domains *in trans*, binding of precursor proteins to

Tim50 and coordination between TOM and TIM23 complexes are impaired in these cells. The experiments shown so far also demonstrate that the core domain of Tim50 contains both the main binding site for presequences and the main recruitment point to the TIM23 complex. However, previously reported interactions between the core and PBD (Rahman et al., 2014) could not be recapitulated.

Thus, in the last part of my thesis, I wanted to analyse how the two domains of Tim50, core and PBD, cooperate with each other to fulfil the function of Tim50.

3.3.1 Introducing a disulfide bond between core and PBD of Tim50

To explore the notion that the two domains of Tim50 interact with each other, the idea was to introduce cysteine residues in the core and PBD, respectively, and lock the two domains together through a disulfide bond. With the help of the Alphafold structural prediction of yeast Tim50 (Figure 3.33 A) and a disulfide prediction software (Gao et al., 2020), two positions in the core and PBD were chosen that are in close proximity and fulfil the criteria for a disulfide bond formation. The identified endogenous residues were replaced by cysteine residues (A257C and I413C) in the context of the full-length Tim50 (Figure 3.33 B). This new Tim50 variant, defined as 50FL_2xC, was generated and cloned into yeast centromeric plasmids under the control of endogenous *TIM50* promoter and 3´-UTR.

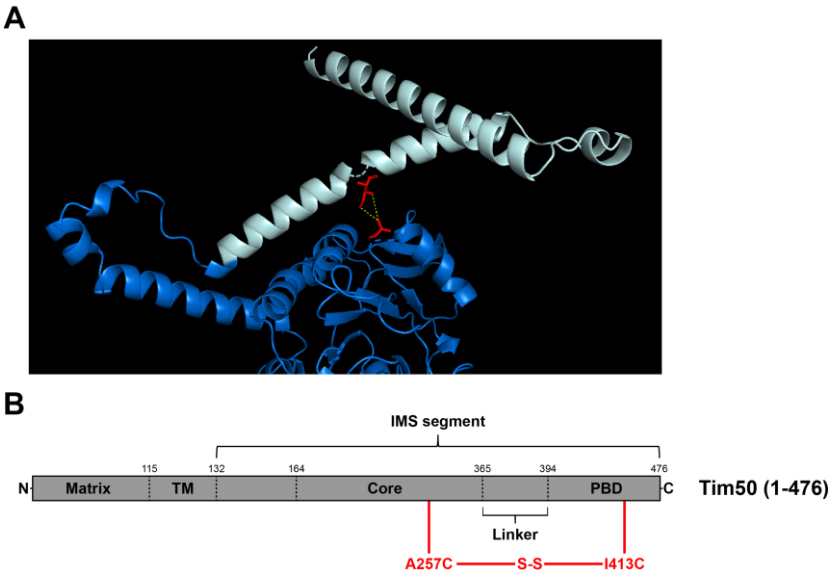

Figure 3.33 Locking the PBD to the core domain in Tim50 through a disulfide bond. (A) Alphafold2 structure prediction of Tim50. Marine blue, core domain; pale cyan, PBD. The two cysteine mutations in the core and PBD are depicted in red. (B) Schematic representation of the domain structure of Tim50 and the two cysteine mutations in the core and PBD of Tim50. Tim50 segments are indicated: Matrix, aa 45-114; transmembrane (TM), aa 115-131; core, aa 164-365; linker, aa 366-394; presequence-binding domain (PBD), aa 395-476. IMS, intermembrane space.

After plasmid shuffling, the expression levels of Tim50 and other mitochondrial proteins were tested by isolating mitochondria from 50FL and 50FL_2xC cells and analysing them by SDS-PAGE and immunoblotting. Expression of the Tim50 cysteine variant in 50FL_2xC was identical to that of the wild-type Tim50 in 50FL mitochondria (Figure 3.34). Furthermore, protein levels of other subunits of the TIM23 complex analysed (Tim23 and Tim17) or example mitochondrial proteins of the OM (Tom40) and IM (Yme1) also did not show any obvious differences between 50FL and 50FL_2xC mitochondria.

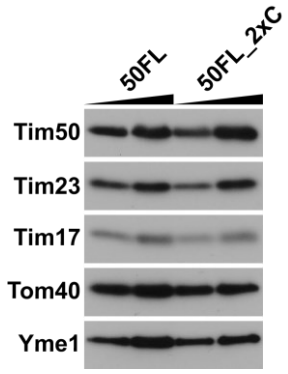

Figure 3.34 Expression levels of Tim50 and other mitochondrial proteins are not affected in 50FL_2xC cells. Isolated mitochondria (10 and 20 µg loaded) from 50FL and 50FL_2xC cells grown in YPD at 30 °C were analysed by SDS-PAGE, followed by immunostaining against depicted mitochondrial proteins.

Next, serial dilution spot assay was performed to analyse whether introducing two cysteines in the core and PBD affects growth of yeast cells. Cells of 50FL_2xC and the corresponding wild-type Tim50 strain, 50FL, were serially diluted and spotted on plates containing fermentable (YPD) or non-fermentable (YPLac) carbon sources at two different temperatures (30 and 37 °C). 50FL_2xC cells did not show any growth phenotype compared to the 50FL strain under any of the conditions tested (Figure 3.35). Therefore, a Tim50 strain carrying two cysteine residues in the core and PBD was generated and these mutations did not affect growth of yeast cells and levels of various mitochondrial proteins.

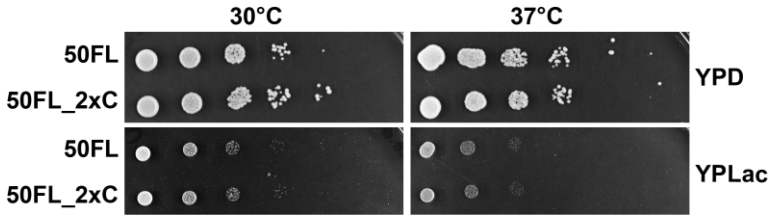

Figure 3.35 Cysteine mutations in Tim50 do not affect the growth of yeast cells. Cell growth of indicated yeast strains was analysed by ten-fold serial dilution spot assay on plates containing rich medium with glucose (YPD) or lactate (YPLac), as fermentable and non-fermentable carbon sources, respectively. Plates were incubated on indicated temperatures.

3.3.2 Growth analysis of 50FL and 50FL_2xC cells under oxidizing conditions

Oxidizing reagents, such as 4,4'-dipyridyl disulfide (4-DPS), copper sulfate ($CuSO_4$) and copper phenanthroline (CuP) are commonly used to induce oxidizing conditions (Qiu et al., 2013; Doerner and Sousa, 2017; Höhr et al., 2018). Upon oxidation, two cysteines form a disulfide bond, when in close proximity and right orientation. To investigate whether locking of the PBD to the core domain through oxidation affects growth of yeast cells, growth curves of 50FL and 50FL_2xC cells in the presence of an oxidizing reagent were analysed. Cells were grown in SLac medium (+ 0.1 % Glc) supplemented with different concentrations of 4-DPS and their cell growth was continuously monitored by measuring the absorbance at 600 nm in a plate reader. As a control, both strains were also grown in the same medium without any oxidizing reagent. Growth of both 50FL and 50FL_2xC cells was impaired by increasing the concentration of the oxidizing reagent (Figure 3.36). At the highest concentration of 4-DPS, both strains were virtually dead. Under tested oxidizing conditions, however, 50FL_2xC cells did not show any additional growth impairment compared to the 50FL strain. This indicates, that even though at a certain concentration the oxidizing reagent 4-DPS seems to impair the growth of yeast cells in general, oxidation did not additionally affect 50FL_2xC cell growth.

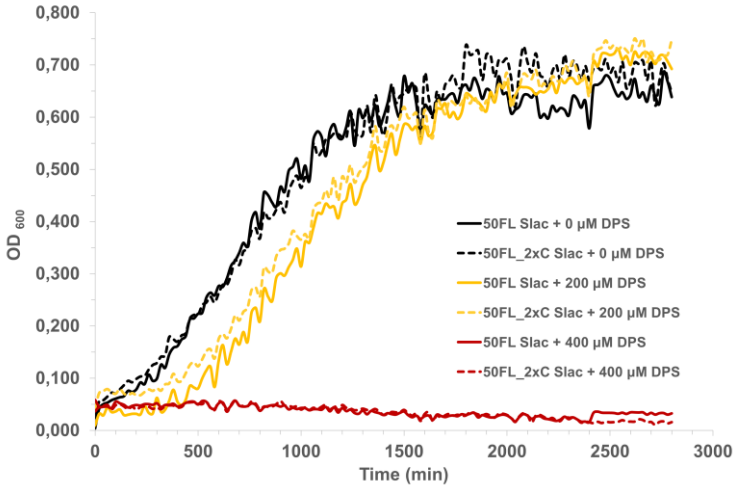

Figure 3.36 Growth analysis of 50FL and 50FL_2xC cells under oxidizing conditions. Cells of indicated yeast strains were grown in SLac medium without or with different concentrations of 4-DPS and constant agitation at 30 °C. Cell growth was continuously monitored by measuring the absorbance at 600 nm.

3.3.3 Disulfide bond formation between core and PBD of Tim50 under oxidizing conditions in 50FL_2xC

To analyse whether on protein level the Tim50 cysteine variant in 50FL_2xC is able to form a disulfide bond between the core and PBD under oxidizing conditions, isolated mitochondria from 50FL and 50FL_2xC cells were incubated with the oxidizing reagents 4-DPS, $CuSO_4$ and CuP. After oxidation, samples were treated with or without DTT and analysed by SDS-PAGE followed by immunoblotting. One sample of each strain was incubated without oxidizing reagent as a negative control. Whereas immunoblotting with Tim50 antibodies gave a single protein band for Tim50 in 50FL mitochondria under oxidizing conditions, 50FL_2xC revealed an additional, faster migrating protein band, most likely corresponding to the oxidized form of Tim50 in which the core and PBD are disulfide-bonded (Figure 3.37). The efficiency of generating the oxidized form of Tim50 seemed to depend on the oxidizing reagent and reached a maximum of ca. 50 % when mitochondria were treated with $CuSO_4$ or CuP. During the establishment of the experimental procedure, different concentrations (0.1 – 10 mM) of oxidizing reagents and incubation durations (10 – 30 min) were tested. However, the efficiency of generating the oxidized form of Tim50 stayed more or less constant under all the different conditions and it was never possible to reach 100 % efficiency. Tom40, which was previously reported to be affected by oxidizing reagents due to its endogenous cysteines (Qiu et al., 2013), similarly showed a faster migrating, oxidized form of Tom40 upon oxidation with $CuSO_4$ or CuP. The running behaviour of Tim17, on the other hand, remained unchanged, in agreement with the previous findings that its disulfide bond is not affected under these conditions (Ramesh et al., 2016).

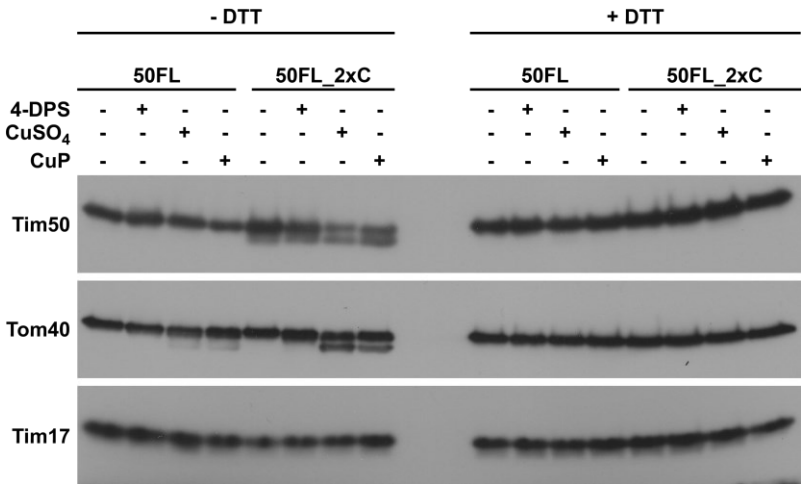

Figure 3.37 Formation of an oxidized, disulfide-linked Tim50 under oxidizing conditions in 50FL_2xC. Isolated mitochondria from 50FL and 50FL_2xC cells were incubated with 2 mM of indicated oxidizing reagents, respectively, and subsequently treated with or without DTT.

Importantly, when oxidized samples were subsequently treated with DTT, the oxidized forms of Tim50 and Tom40 disappeared, validating the specificity and reversibility of the disulfide bond formation in the Tim50 cysteine variant and Tom40. Notably, the oxidized form of the Tim50 cysteine variant was generated in 50FL_2xC mitochondria even without any treatment with oxidizing reagents. One possible explanation is that the conditions used during isolation of mitochondria are already sufficient to oxidize the Tim50 cysteine variant. The efficiency of generating the oxidized form of the Tim50 cysteine variant was, however, higher upon oxidation with $CuSO_4$ or CuP. In conclusion, a form of Tim50 in which the PBD is disulfide-bonded to the core domain could be generated, though not very efficiently.

3.3.4 Import of precursor proteins into isolated YPH499 wild-type mitochondria under oxidizing conditions

In vitro import experiments are able to detect even minor import defects that are not obvious from growth analyses and therefore, it was analysed next whether import of precursor proteins is affected when an oxidized form of Tim50 is present. For this, *in organello* import experiments under oxidizing conditions in YPH499 wild-type mitochondria were tested first, to determine the suitable concentration of oxidizing reagents and to investigate whether oxidation affects protein import into mitochondria in general. Since in cultivated yeast cells 0.4 mM of 4-DPS already impaired cell growth in general (see Figure 3.36), it was tested whether concentrations of 0.1 or 0.5 mM of the three previously mentioned oxidizing reagents already affect import of precursors into isolated mitochondria. Thus, isolated mitochondria from YPH499 wild-type yeast cells were incubated with 4-DPS, $CuSO_4$ and CuP, respectively, followed by the import of ^{35}S-labelled Oxa1 precursor. Samples were subsequently analysed by SDS-PAGE and autoradiography (Figure 3.38). One sample was not

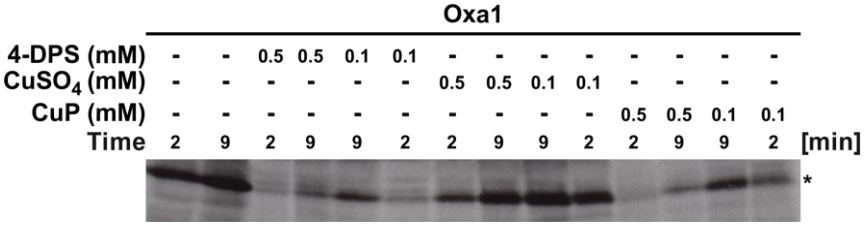

Figure 3.38 Import of Oxa1 precursor under oxidizing conditions into YPH499 wild-type mitochondria. ^{35}S-labelled Oxa1 precursor was imported into mitochondria isolated from YPH499 wild-type cells, treated with different concentrations of oxidizing reagents prior to import. After indicated time periods, aliquots were removed and import was stopped by diluting the samples in ice-cold SH buffer containing 1 µM valinomycin. Mitochondria were reisolated and analysed by SDS-PAGE and autoradiography. (*) indicates the mature form of Oxa1.

treated with any oxidizing reagent prior to the import of Oxa1 precursor and served as a control. Whereas Oxa1 precursor was efficiently imported in the control sample, treating the mitochondria with 4-DPS or CuP beforehand strongly impaired the import of Oxa1. Upon oxidation with $CuSO_4$, Oxa1 precursor was imported with similar efficiency like in the control sample. Thus, treating isolated mitochondria with oxidizing reagents 4-DPS and CuP already affects protein import into wild-type mitochondria and 0.5 mM $CuSO_4$ seems to be the most suitable to induce oxidizing conditions prior to import and to compare import efficiencies between 50FL and 50FL_2xC cells.

3.3.5 Protein import into 50FL_2xC under oxidizing conditions

To analyse whether locking the PBD to the core domain of Tim50 affects protein import via the TIM23 complex, ^{35}S-labelled precursor proteins were incubated with isolated mitochondria from 50FL and 50FL_2xC cells after treatment with $CuSO_4$ (Figure 3.39). Samples were taken at indicated time points and after stopping the import reaction, mitochondria were treated with Proteinase K (PK)

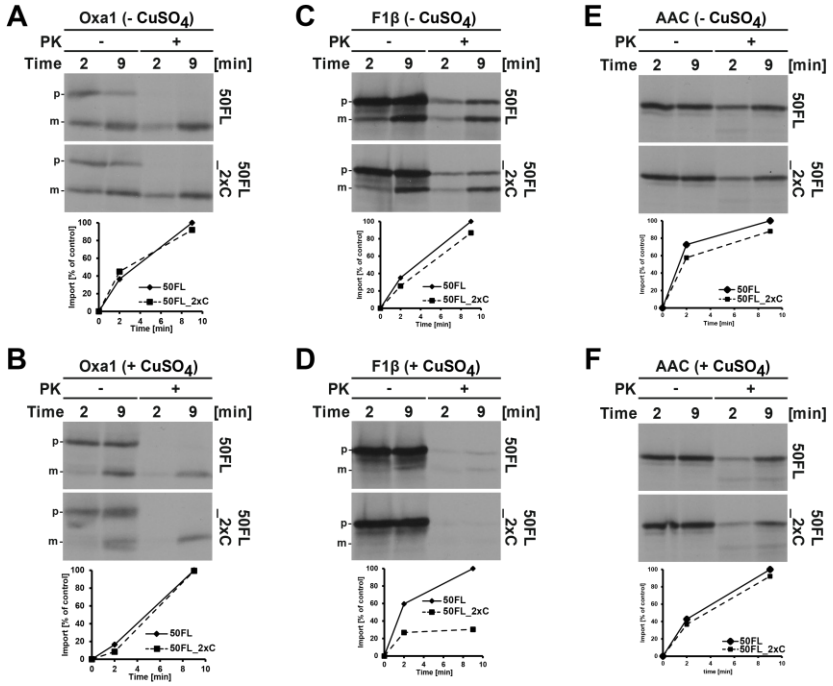

Figure 3.39 Import of precursor proteins under oxidizing conditions. ^{35}S-labelled Oxa1 (A and B), F1β (C and D) and AAC (E and F) precursors were imported into mitochondria isolated from 50FL and 50FL_2xC cells without (A, C and E) or with $CuSO_4$ (B, D and F) oxidation prior to import. After indicated time periods, aliquots were removed, import was stopped and Proteinase K (PK) was added, where indicated. Mitochondria were reisolated and analysed by SDS-PAGE and autoradiography (upper panels). Quantifications of PK-protected mature forms of imported proteins are shown in the lower panels. The amount of the PK-protected mature form of imported proteins in the longest time point in 50FL mitochondria was set to 100 %. p, precursor; m, mature forms of imported proteins.

to degrade all nonimported precursor proteins. Subsequently, mitochondria were reisolated and analysed by SDS-PAGE and autoradiography.

Under non-oxidizing conditions (- $CuSO_4$), all three precursor proteins were imported with similar efficiencies into 50FL_2xC compared to the imports into 50FL mitochondria (Figure 3.39 A, C and E), indicating that the Tim50 cysteine variant does not affect protein import under normal conditions. However, while import of the Oxa1 precursor into 50FL_2xC did not show any import defect under oxidizing conditions (Figure 3.39 B), F1β precursor protein was imported with ca. 60 % lower efficiency into 50FL_2xC compared to its import into 50FL mitochondria (Figure 3.39 D). The TIM23-independent precursor AAC, was imported with similar efficiency into 50FL and 50FL_2xC mitochondria upon oxidation with $CuSO_4$ (Figure 3.39 F). Thus, locking the core and PBD of Tim50 upon oxidation seems to affect protein import via the TIM23 complex, however, the degree of impairment appears to be precursor dependent. Since no complete locking of the PBD to the core of Tim50 was ever achieved, these results are rather inconclusive, until the oxidation assay is optimized to generate the oxidized form of Tim50 with 100 % efficiency.

3.3.6 Locking the core and PBD of Tim50 in 50FL_2xC with cysteine-specific cross-linkers

Since locking of the PBD and core of Tim50 via the disulfide bond did not lead to conclusive results due to incomplete oxidation of the cysteine residues, another approach to covalently link two cysteine residues using cysteine-specific chemical cross-linkers, like bismaleimidohexane (BMH) or bismaleimidoethane (BMOE) (Shiota et al., 2015; Höhr et al., 2018), was tested. The sulfhydryl group of a cysteine specifically reacts with the maleimide group of the cross-linker, resulting in the formation of a stable thioether linkage that cannot be cleaved by reducing agents.

To analyse whether the core and PBD of Tim50 with their cysteine residues in 50FL_2xC cells can also be covalently locked through cross-linking, isolated 50FL and 50FL_2xC mitochondria were incubated on ice with different concentrations of BMH and BMOE. One sample was incubated without cross-linker, as a control. After quenching the excess of cross-linkers, samples were analysed by SDS-PAGE and immunoblotting. Whereas the wild-type Tim50 in 50FL mitochondria did not generate any cross-linked product, the Tim50 cysteine variant in 50FL_2xC mitochondria formed a cross-linked product below the non-cross-linked Tim50 under all tested concentrations of both BMH and BMOE (Figure 3.40). This faster migrating cross-linked adduct was not present in the sample which was

incubated without cross-linker. However, the efficiency of cross-linked adduct formation of the Tim50 cysteine variant did not significantly change with different concentrations of cross-linker. Tim14, used as a negative control, did not generate any cysteine-specific cross-linked products. Thus, cysteine-specific cross-linking could in principle be used as another approach to covalently lock the core and PBD through the introduced cysteines in Tim50 in 50FL_2xC cells, however, since it also did not generate a locked form of Tim50 with a sufficiently high efficiency, no further experiments were done.

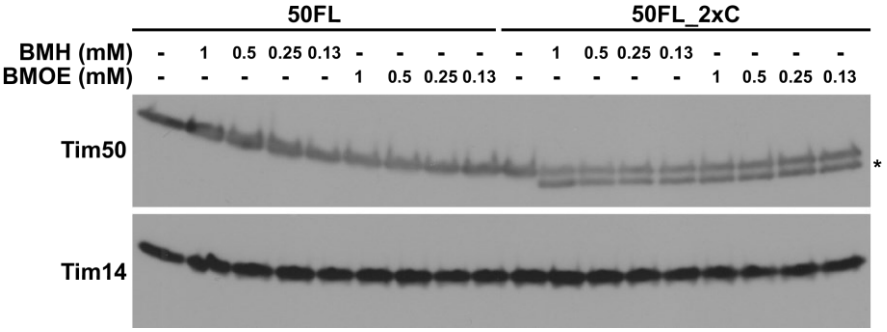

Figure 3.40 Core and PBD of Tim50 can be cross-linked in 50FL_2xC mitochondria by using cysteine-specific cross-linkers. Isolated mitochondria from 50FL and 50FL_2xC cells were incubated on ice in the absence or presence of cysteine-specific cross-linkers, BMH or BMOE, respectively. Following quenching of the cross-linker and reisolation of mitochondria by centrifugation, the samples were analysed by SDS-PAGE and immunostaining. (*) indicates the cross-linked adduct of Tim50.

3.3.7 Introducing artificial linkers between the core and PBD of Tim50

As the attempt to artificially lock together the two domains of Tim50 in the IMS did not lead to conclusive results due to the inefficient linking, in a complementary approach it was tested whether it is possible to artificially separate the core and the PBD of Tim50.

To this end, Tim50 linker variants were generated in which the endogenous Tim50 sequence between the core and PBD was replaced by either 15 amino acid residues long flexible or rigid linker sequences (Kümmel et al., 2011; Chen et al., 2013; Patel et al., 2022) (Figure 3.41 A). These artificial linkers were previously reported to keep two domains of a single polypeptide chain either in a flexible conformation relative to each other or strictly separated them from each other both *in vivo* and *in vitro*. After transforming the Tim50 linker variants into the Tim50 shuffling strain and subsequent 5-FOA chase, total cell extracts were made and the protein levels of Tim50 analysed by SDS-PAGE and immunoblotting. The Tim50 linker variants were expressed at the essentially same level as the wild-type Tim50, merely migrating slightly differently on the SDS-PA gel depending on the introduced linker

sequence (Figure 3.41 B). Expression of control proteins, Tom40 and Tim23, was also not affected in the Tim50 linker variants.

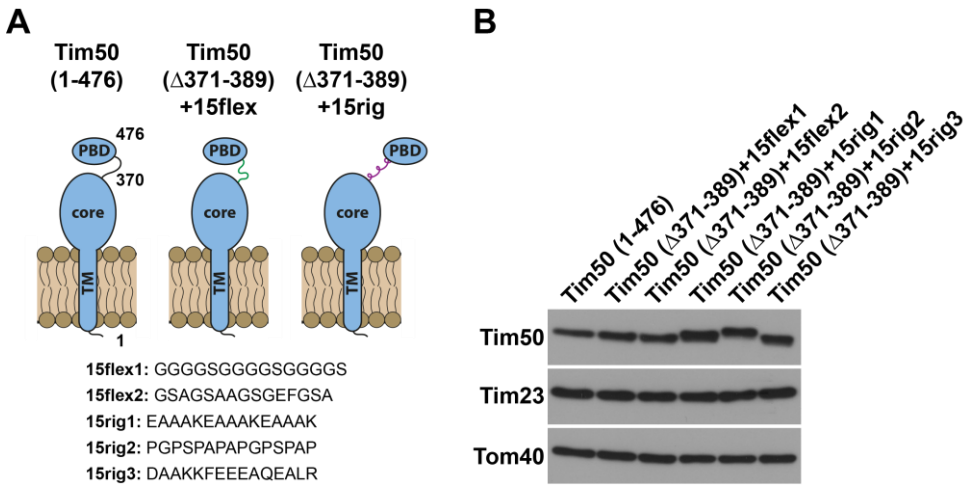

Figure 3.41 Introducing artificial linkers between the core and PBD of Tim50. (A) Schematic representation of Tim50 and its artificial linker variants analysed, are depicted above. Amino acid sequences of the different flexible and rigid linkers are written below. TM, transmembrane segment; PBD, presequence-binding domain. (B) Indicated yeast cells were grown in YPD at 30 °C and total cell extracts were analysed by SDS-PAGE and immunoblotting

3.3.8 Separating core and PBD of Tim50 with rigid linkers impairs the growth of yeast cells

Next, serial dilution spot assay was performed to analyse whether growth of yeast cells is affected by the Tim50 linker variants. Yeast cells expressing either of the two Tim50 flexible linker variants grew comparable to the wild-type Tim50 on the fermentable medium and only had a slight growth defect when the non-fermentable carbon source was used (Figure 3.42). On the other hand, all three Tim50 rigid linker variants severely reduced growth of yeast cells on the fermentable medium

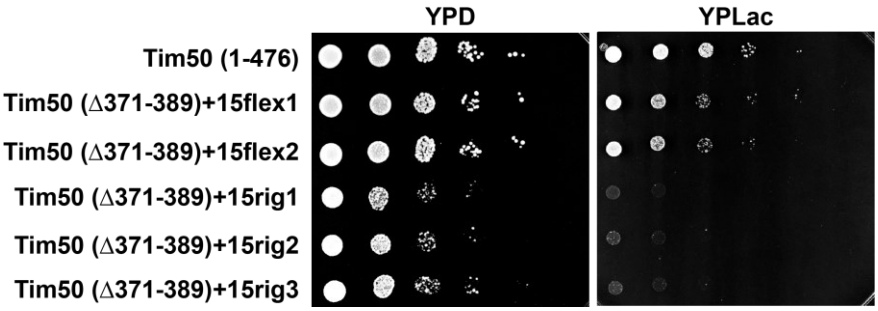

Figure 3.42 Separating the core and PBD of Tim50 with rigid linkers impairs the growth of yeast cells. Growth of indicated yeast strains was analysed by ten-fold serial dilution spot assay on plates containing rich medium with glucose (YPD) or lactate (YPLac), as fermentable and non-fermentable carbon sources, respectively. Plates were incubated at 30 °C.

and were virtually unable to support growth on the non-fermentable medium. Thus, artificially separating the core and PBD of Tim50 within the same polypeptide chain impairs growth of yeast cells.

3.3.9 Separation of the two domains of Tim50 in the IMS affects interaction of Tim50 with Tom22

Since splitting Tim50 into two separate polypeptide chains in 50split cells, as described above, affects the receptor function of Tim50 and cooperation of TOM and TIM23 complexes, I analysed whether artificially separating the core and PBD with a rigid linker within one polypeptide chain recapitulates these findings. To this end, Tim50 linker variants were generated in the background of a C-terminally His-tagged Tom22 (Tom22His+Tim50flex1 and Tom22His+Tim50rig1) in order to analyse the interaction between Tim50 and Tom22. Mitochondria were isolated and incubated with the amino-group specific and cleavable cross-linker di-thiobis-succinimidylpropionate (DSP), followed by Ni-NTA pulldown of the His-tagged Tom22 and its cross-linking partners. As previously reported (Waegemann et al., 2015), the wild-type Tim50 was efficiently cross-linked to Tom22 and found in the bound fraction together with the His-tagged Tom22 (Figure 3.43). While the cross-link of Tom22 with the Tim50 flexible linker variant was recovered with a similar efficiency like with the wild-type Tim50, the cross-linking of Tom22 was strongly decreased with the Tim50 rigid linker variant. Taken together, by artificially separating the core and PBD of Tim50 with a rigid linker, the interaction between TOM and TIM23 complexes is strongly affected, just as it is when Tim50 is split into two polypeptide chains.

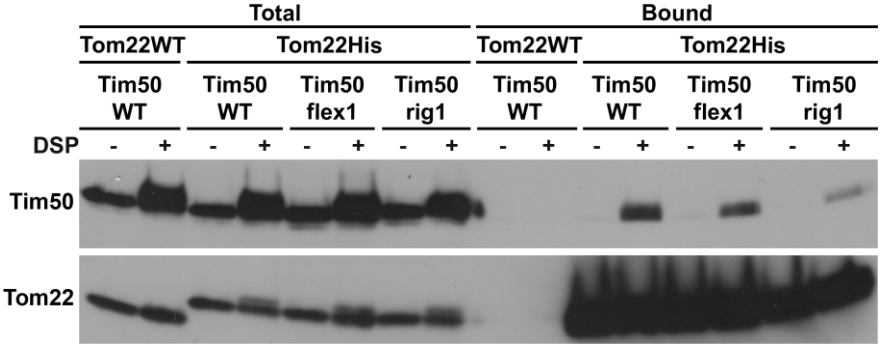

Figure 3.43 Separating the core and PBD of Tim50 with a rigid linker affects the interaction between Tim50 and Tom22. Isolated mitochondria from indicated cells were incubated on ice in the absence or presence of the amino-group-specific and cleavable cross-linker DSP, respectively. After quenching of excess cross-linker, mitochondria were reisolated, solubilized in SDS-containing buffer, diluted with Triton X-100 containing buffer and subsequently incubated with NiNTA-Agarose beads. After three washing steps, specifically bound proteins were eluted with Laemmli buffer containing 300 mM imidazole and β-mercaptoethanol to cleave the cross-links. Total (5 %) and bound fractions (100 %) were analysed by SDS-PAGE and immunoblotting with the indicated antibodies.

4. Discussion

One of the major unresolved questions of protein import into mitochondria is how the TOM and TIM23 complexes in the OM and IM, respectively, coordinate translocation of proteins across two mitochondrial membranes. Tim50 was identified as the main receptor of the TIM23 complex, binding presequence-containing precursor proteins in the IMS and transferring them from TOM to TIM23 complex. With Tom22, Tom40 and Tom7, from the TOM side, and Tim23 and Tim21, from the TIM23 side, Tim50 is one of the major players in the coordination of protein import into mitochondria along the presequence pathway. Most of the functions of Tim50 were analysed assuming that Tim50 contains only a single domain in the IMS. However, understanding the molecular mechanisms of how Tim50 is involved in protein import became even more complicated when *in vitro* experiments with recombinantly expressed and purified Tim50 variants suggested that Tim50 has two distinct domains in the IMS – the core and the so-called presequence-binding domain (PBD). How the core and PBD of Tim50 interact with each other, with the various subunits of the TOM and TIM23 complexes and with precursor proteins therefore remained unknown. In this thesis, I have dissected the functional roles of the two domains of Tim50 in the IMS and how they coordinate the transfer of presequence-containing precursor proteins from TOM to TIM23 complex.

4.1 Deletion of either of the two domains of Tim50 in the IMS is lethal, however, co-expressing them *in trans* rescues cell viability

In vivo analysis shown here demonstrated that the deletion of the PBD is lethal for yeast cells, in agreement with the previously published results (Schulz et al., 2011; Lytovchenko et al., 2013). This led to the question whether the PBD on its own could be sufficient to carry out the function of Tim50. Data presented here showed that this is not the case, indicating that both domains of Tim50 in the IMS have essential roles that are necessary for the viability of yeast cells. One of the key findings in this thesis was the unexpected observation that the function of Tim50 can be reconstituted from its two domains expressed *in trans* (50split strain). The rescue was strictly dependent on anchoring the core domain to the IM with the endogenous TM of Tim50 and targeting the PBD to mitochondria with the cytochrome b_2 targeting signal. Expressing a soluble core domain together with the PBD of Tim50 was not sufficient to rescue the function of Tim50, most likely due to the fact that the endogenous TM also contributes to the recruitment of Tim50 to the TIM23 complex (Malhotra et al., 2017).

Interestingly, anchoring of both core and PBD with a TM segment of Tim50 also did not generate any viable yeast cells, indicating that the endogenous TM segment of Tim50 may specifically interact with the TM segments of other TIM23 subunits and that therefore the presence of multiple such segments may interfere with the assembly of the TIM23 complex and/or the recruitment of Tim50 to the complex.

One interesting observation made with the 50split strain is the presence of two protein species of the PBD, the intermediate and mature forms. They most likely result from an incomplete processing of the cytochrome b_2 targeting signal by IMP, generating both an intermediate, membrane-anchored version of the PBD as well as a fully processed mature form that is soluble in the IMS. Introducing a point mutation in the IMP processing site (50split+IMPmut strain) and thereby changing the ratio of the two forms by increasing the levels of the intermediate form of the PBD did not affect the growth of yeast cells, suggesting that a membrane anchored PBD may be the functionally important form. Targeting of passenger proteins into the IMS by means of fusing them to the cytochrome b_2 targeting signal has been successfully used in a number of publications before (Mokranjac et al., 2009; Popov-Čeleketić et al., 2011). However, since this approach to target proteins into the IMS is dependent on the functional TIM23 complex, the incomplete processing of PBD in 50split cells may actually be due to splitting of Tim50 into its two domains. An alternative approach could be to target the PBD of Tim50 into the IMS by using the mitochondrial intermembrane space sorting (MISS) signal. Previous studies have identified this specific sorting signal as sufficient to import radioactively labelled passenger proteins to the IMS via the MIA pathway in isolated mitochondria (Milenkovic et al., 2009; Sideris et al., 2009). Whether the MISS signal can also efficiently target passenger proteins into the IMS *in vivo* has not been analysed yet. However, if it does, then expressing the PBD with the MISS signal *in vivo* would be an elegant way to circumvent the import via the TIM23 complex and to obtain exclusively a soluble version of the PBD in the IMS. Should this work, it would be possible to establish whether membrane anchoring of PBD is necessary or an exclusively soluble form of PBD could also support the growth in the context of 50split cells.

The serendipitous observation that extending the core domain by just five residues resulted in a more efficient rescue than the initial co-expression strain of Tim50 genetically identified a novel boundary for the core domain. The previously assumed C-terminal end of the core domain was set at residue 365 and was based on the finding that the stable domain, obtained upon trypsin treatment of the recombinantly expressed IMS segment of Tim50, ended with this residue (Qian et al., 2011).

However, the last four residues (aa 362-365) of the core domain were not resolved in the final crystal structure. By predicting the structure of the full-length yeast Tim50 using the in the meantime developed tool Alphafold2 (Figure 4.1), it is now possible to give a structural explanation for this observation.

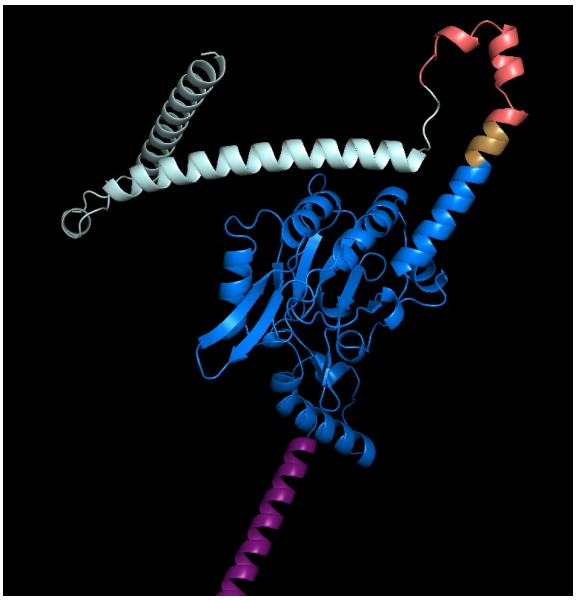

Figure 4.1 Structural prediction of yeast Tim50 by Alphafold2. Core domain ending at 365 is shown in marine blue and the extension of the core domain to 370 is shown in sand, transmembrane domain is in purple, linker sequence in deep salmon and PBD in pale cyan.

As shown in Figure 4.1, after the TM segment, the core domain of Tim50 folds into a compact structure consisting of five α-helices and nine β-sheets. Interestingly, the structure of the core domain ends with a distinct α-helix protruding away from the domain. While ending the core domain at residue 365 would disturb the formation of this α-helix, truncating it at residue 370 would include essentially the whole α-helix. Even though the individual core domains ending at either residue 365 or 370 did not rescue the function of Tim50 when expressed on their own, the strong difference in growth phenotype when co-expressed with the PBD may suggest that this α-helix and the last five residues are important for the stability and integrity of the core domain of Tim50, especially when one considers binding of the long helix of the PBD that interacts with this and the additional two helices on top of the core domain (in the orientation shown).

4.2 The core domain contains the main recruitment point to the TIM23 complex and the main binding site for precursor proteins

One outstanding question of this thesis was which of the two domains of Tim50 in the IMS interact with TIM23 and TOM subunits. Initial *in vitro* pull-down experiments with recombinantly expressed and purified Tim50 variants in this study showed that the IMS segment as well as the core domain of Tim50 stably interact with Tim23. This result could nicely be recapitulated *in organello* through co-immunoprecipation experiments with isolated mitochondria of 50split cells, which showed that the core domain is the main recruitment point of Tim50 to the TIM23 complex, in agreement with the previous findings (Tamura et al., 2009; Qian et al., 2011; Schulz et al., 2011; Dayan et al., 2019). The PBD may however, directly or indirectly, support this interaction, which could explain the observation of two previous articles. NMR studies suggested that the PBD is required for an efficient complex formation of the recombinantly expressed and purified IMS segments of Tim50 and Tim23 (Bajaj et al., 2014). Furthermore, a cross-link between the PBD and Tim23 was identified through chemical cross-linking with isolated and purified TIM23 complexes and mass spectrometric analyses (Gomkale et al., 2021), indicating that the PBD is in close proximity to Tim23. A direct interaction between the PBD and Tim23, however, could neither be shown through *in vitro* pull-down, nor by co-immunoprecipitation experiments with isolated 50split mitochondria in this study. Instead, *in vitro* pull-down experiments revealed Tim17 as a specific and novel interaction partner of the PBD, even though the binding efficiency was quite weak compared to that of the IMS segment or the core domain of Tim50. Since this interaction could not be recapitulated *in organello*, further experiments are required to demonstrate the biological relevance of this finding. So far, Tim17 is assumed to interact with Tim50 indirectly through Tim23 via the stable heterodimer of Tim17-Tim23 (Mokranjac et al., 2003b; Mokranjac et al., 2009). Giving the recent findings that Tim17 forms the cavity used for protein translocation and Tim23 contributing in a rather scaffold-like manner (Fielden et al., 2023; Im Sim et al., 2023), it is tempting to speculate that Tim50 may directly interact with Tim17 to transfer precursor proteins, after recognition in the IMS, into the lipid exposed cavity for further import into the matrix.

Both Tom22 and Tom40 were shown to be cross-linked to Tim50 using chemical and site-specific UV cross-linking in intact mitochondria (Shiota et al., 2011; Waegemann et al., 2015; Araiso et al., 2019), suggesting that Tim50 is in close proximity to the *trans* site of the TOM complex. When a C-terminally truncated variant of Tim50, lacking the PBD, was expressed in the background of a wild-

type version of Tim50, chemical cross-linking of Tom22 to the truncated Tim50 was abolished (Waegemann et al., 2015), suggesting that the PBD is either directly or indirectly involved in Tim50-Tom22 interaction. In this study, in *in vitro* pull-down and co-immunoprecipitation experiments in isolated mitochondria, neither the full-length Tim50 nor its individual domains were stably interacting with Tom40 or Tom22. One possibility is that the affinity-purified antibody against the C-terminal peptide of Tim50 used to specifically precipitate the PBD in the co-immunoprecipitation experiment may potentially mask the binding site for TOM subunits on the rather small PBD and therefore disrupt the interaction between the two proteins. Performing the co-immunoprecipitation experiment in isolated 50split mitochondria with Tom40 or Tom22 antibodies directed against the cytosol-exposed segments of these proteins could potentially circumvent this problem and thus reveal whether the PBD is a binding partner of Tom40 or Tom22. It is however also possible that the full-length Tim50, in a single polypeptide chain, may be required for a stable interaction or that Tim50 interacts with the TOM subunits only in a very transient manner and that the conditions used in the pull-down or co-immunoprecipitation experiments are too harsh and disrupt these interactions, in contrast to cross-linking performed in intact cells or mitochondria. For the latter point, it may be interesting to perform the co-immunoprecipitation experiment in isolated mitochondria from 50split cells in the presence of an arrested precursor protein, which has been previously reported to stabilize the interactions of the two protein translocases in a TOM-TIM23 supercomplex intermediate (Chacinska et al., 2003; Gomkale et al., 2021). Since in this case the two complexes in the OM and IM are additionally fixed together by the two-membrane spanning precursor protein, the interactions of the two domains of Tim50 with Tom22 and/or Tom40 may be additionally stabilized.

The data presented in this study also show that, in intact mitochondria, the main binding site for the incoming precursor proteins is present within the core domain of Tim50. However, the receptor function of Tim50 is impaired in 50split cells, judging by the decreased cross-linking efficiency of the core domain to precursor proteins compared to the one of the full-length Tim50. This suggests that the PBD contributes, directly or indirectly, to the receptor function of Tim50 as well. It is possible that the PBD and the core domain each contribute to a part of the presequence-binding site or that the presequences are initially recognized by the PBD and then transferred to the core domain. For the latter scenario, it could be that the cross-linking experiment in the absence of membrane potential only captures binding of precursors when they were already transferred from the PBD to the core domain, thus not showing any cross-linking adducts between the precursor and the PBD of Tim50. It is, however, also possible that the PBD helps the core to adopt the conformation conducive to

recognition of presequences. Previous NMR studies with recombinantly expressed and purified Tim50 variants indeed suggested an interaction between the core and PBD of Tim50 (Rahman et al., 2014). The data in this thesis point to a similar direction, since an artificial separation of the two domains of Tim50, either through co-expression *in trans* or by introducing an artificial rigid linker between them, impairs the function of the protein, suggesting that the two domains in the IMS need to interact, dynamically or not, with each other.

4.3 Both domains of Tim50 need to associate during transfer of precursor proteins between TOM and TIM23 complexes

Both the genetic and biochemical evidence presented here suggest that the coordination of the TOM and TIM23 complexes is particularly sensitive to the separation of the two domains of Tim50 in the IMS. Separation of the core and PBD of Tim50, in 50split cells, impairs accumulation of presequence-containing proteins in the TOM complex and their subsequent transfer to the TIM23 complex. These results are probably caused by an impaired interaction of Tim50 with the TOM complex, since cross-linking of Tom22 to Tim50 was strongly affected when the two domains are separated by a rigid linker. The observed decrease of Oxa1-TOM complex intermediate formed in 50split cells, however, does not resolve whether precursor proteins are not able to accumulate in the TOM channel due to an impaired precursor binding at the *trans* site of the TOM complex or whether binding to the TOM complex from the cytosolic side is already affected. One way to address this question could be to perform cross-linking experiments of precursor proteins to the receptors of the TOM complex, Tom20 or Tom22, which recognize precursor proteins on the *cis* site of the TOM complex in the cytosol (Kanamori et al., 1999; Yamamoto et al., 2011). If already binding to the cytosolic surface of the TOM complex is affected, this could suggest that splitting the two domains of Tim50 in the IMS not only affects the TOM-TIM23 coordination, but that the assembly and/or function of the TOM complex may also be affected. It is tempting to speculate that this could also indicate a crosstalk between the TOM and TIM23 complexes that senses the impairment of the downstream protein import by the TIM23 complex due to the Tim50split mutation and thus already transduces a signal to the surface of the organelle, suppressing binding of precursor proteins to the TOM complex. A previous publication from our group suggested a similar mechanism for the intrinsically disordered IMS segment of Tim23, that interacts with several subunits of the TOM and TIM23 complexes and serves as an organizational hub in the IMS (Günsel et al., 2020). On the one hand, mutations in the IMS segment of Tim23 were shown to be transduced to the matrix side of the IM, impairing its

interaction with Pam17. On the other hand, further mutations in the IMS segment of Tim23 were also signaled to the cytosolic side of the OM through increased exposure of the N-terminal segment of Tim23 on the mitochondrial surface. Interestingly, the exposure of Tim23 on the mitochondrial surface was strongly impaired when the core and PBD in the IMS are separated in 50split cells. This suggests that the exposure of Tim23 on the mitochondrial surface is dependent on even more dynamic processes in the IMS than the ones uncovered so far. That the dynamics of the TOM-TIM23 cooperation are affected in 50split cells is further supported by the finding made by Shalini Roy Chowdhury in our group that the 50split strain shows very strong negative genetic interactions with all segments of the TOM complex exposed to the IMS (Genge et al., 2023). These newly revealed negative genetic interactions of 50split with TOM *trans* site mutants are far stronger than any other TOM-TIM23 contact previously analysed (Waegemann et al., 2015). Thus, the essential function of Tim50 is not only to serve as the receptor of the TIM23 complex but also to coordinate translocation across two mitochondrial membranes and this function is strongly dependent on the association of the core and PBD of Tim50 in the IMS. Still, it remains unclear how the expression of the PBD in the 50split strain supports growth of yeast cells. One possibility is that the PBD promotes protein transport already at the TOM complex. This possibility was partially addressed with a Tim50 variant in which the PBD was targeted to the TIM23 complex with the endogenous TM segment of Tim50 and which carried a flexible linker in between, to span the IMS and allow the PBD to reach the TOM complex. This mutant, however, did not rescue the function of the full-length Tim50. Even though this study could not reveal a direct interaction between the PBD and TOM subunits, another idea may be to generate a fusion variant of Tom22 carrying the PBD of Tim50 at the C-terminus. Should this chimera be able to support the function of Tom22, it will be interesting to see whether it can also rescue, on its own or together with the core domain, the function of Tim50.

Splitting the two domains of Tim50, either by co-expressing them *in trans* or by artificially separating them by the rigid linker, impairs the function of Tim50, indicating that the two domains need to interact with each other, particularly for the coordination of the TOM and TIM23 complexes in the IMS. The previously reported interactions between the core and PBD with recombinantly expressed and purified Tim50 variants (Rahman et al., 2014), however, could not be observed in co-immunoprecipitation experiments in isolated mitochondria of 50split cells. Possible explanation could be a transient interaction between the two domains or that even the mild solubilization condition with digitonin is sufficient to disrupt the interaction between the core and PBD of Tim50. To further analyse the interaction between the two domains of Tim50 in the IMS, cysteine residues were

introduced in the core and PBD of Tim50, respectively, to lock the two domains together through a disulfide bond. Similar disulfide bond formation experiments were previously reported for Tom40 and Sam50, subunits of the TOM and SAM complex, respectively, to monitor the β-barrel formation of newly imported precursor proteins *in vivo* and *in organello* (Qiu et al., 2013; Höhr et al., 2018). The idea behind this was, that if separation of the two domains impairs the function of Tim50 because they need to interact with each other, then locking them together by a disulfide bond should not have such a drastic effect, unless the interaction between the two domains is dynamic and they also need to separate at one stage. Using different oxidizing reagents, it was possible to reversibly generate an oxidized, disulfide-linked form of Tim50 exclusively in the Tim50 cysteine mutant. The efficiency of the disulfide bond formation, however, only reached a maximum of ca. 50 %, irrespective of the oxidizing reagent or conditions used. Furthermore, oxidizing reagents affected import of proteins into wild-type mitochondria, further complicating the analysis. It appears that the oxidizing reagents specifically affect translocation across the inner membrane as similar effects were not previously observed when insertion into the OM was analyzed (Qiu et al., 2013; Höhr et al., 2018). Whether oxidizing conditions affect the membrane potential and/or ATP levels is currently unclear. An alternative approach to lock the two domains of Tim50 via the introduced cysteine residues by means of the cysteine specific cross-linkers also did not result in more than ca. 50 % efficiency of cross-linking, irrespective of the conditions used. Therefore, the obtained results were in the end not conclusive as it was not possible to differentiate between lack of an effect due to incomplete locking of the domains or due to an actual absence of the effect. Even though different oxidizing reagents, cross-linkers, concentrations and incubation durations were already tested during the establishment of the experimental procedure, further optimization of the conditions may be still required to find the "sweet spot" of increasing the amount of the domain-locked Tim50.

With the available structural prediction of yeast Tim50 by Alphafold2 and the biochemical data on the interaction between the core and PBD presented in this study and in a previous publication (Rahman et al., 2014), a potentially interesting approach to study the interaction between the two domains of Tim50 in the IMS would be Förster resonance energy transfer (FRET). FRET was previously used in our research group in collaboration with the Don C. Lamb laboratory to analyse the conformational dynamics of the mtHsp70 (Ssc1 in yeast) in ensemble or even on single molecule level *in vitro* and *in organello* (Mapa et al., 2010; Sikor et al., 2013). Here the intrinsic dynamic movements of the substrate-binding domain (SBD) and the dynamic interactions between the SBD and the nucleotide-binding domain (NBD) of Ssc1 in response to nucleotides and interacting proteins was

monitored by FRET. Attaching donor and acceptor fluorophores on specifically introduced cysteines in the core and PBD of Tim50 for FRET assays would potentially clarify whether the two domains of Tim50 interact rather dynamically or are constantly associated with each other. If monitoring the interaction between the two domains of Tim50 by FRET would work out, analysing their dynamics during precursor binding at different stages of protein import, would further help to understand how the two domains dynamically coordinate import of proteins into mitochondria.

4.4 Evolutionary conservation of the core and PBD of Tim50

One major puzzling aspect about Tim50 is the evolutionary conservation of its two domains in the IMS. Previous articles have noted that the core domain of Tim50 is ubiquitously present among eukaryotes, but the PBD has only been identified in Fungi so far (Rahman et al., 2014; Callegari et al., 2020). The results in this study suggest that the core domain is the main contributor to the receptor function of Tim50, with the PBD having a supporting role and being involved in the TOM-TIM23 cooperation. Still, the deletion of the PBD is lethal in yeast, which questions its evolutionary conservation among different species.

To further address this unresolved question about Tim50, an extensive bioinformatic analysis of the evolutionary conservation of Tim50 was performed together with the group of Pavel Dolezal. The analysis revealed clear Tim50 orthologues among virtually all sequenced eukaryotic genomes in the various eukaryotic supergroups (Figure 4.2). The only exception was the supergroup of Metamonada, which are adapted to anoxic environments and, instead of mitochondria, possess mitochondria-related organelles with greatly reduced metabolic capacity (Muñoz-Gómez, 2023). The PBD was however only identified among Fungi. In this bioinformatic analysis, a hidden Markov model specific PBD was used to search UniProtKB and EukProt3 databases. The positive hits were only fungal species, including microsporidia and other early branching fungi, which indicates that the PBD may have evolved early in the evolution of Fungi. It is possible that the PBD may be present in non-fungal eukaryotes as a separate polypeptide. This would possibly be supported by the results shown in this study, that the PBD can be separated from the rest of Tim50 and yeast still being viable. However, the bioinformatic analysis with the currently available tools were not able to recognize such an ORF, possibly due to the very limited length and relatively poor sequence conservation even among Fungi. Another possibility is that Tim50 in Fungi may have undergone a potential domain-swap event. However, a PBD-like extension on any other TOM or TIM23 subunit was also not identified.

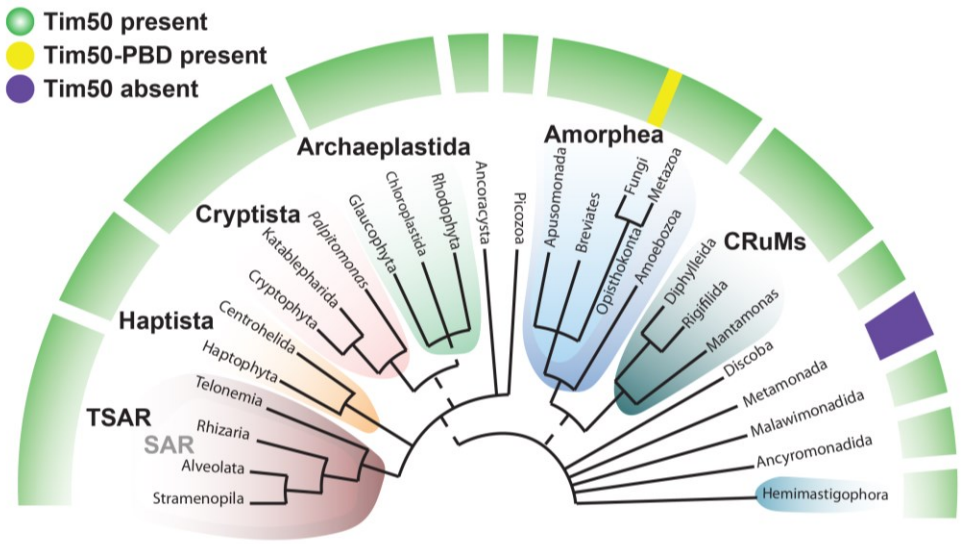

Figure 4.2 The distribution of Tim50 and PBD among eukaryotes. Orthologues of Tim50 could be identified in all eukaryotic groups except Metamonada that include only unicellular eukaryotes (protists). The schematic tree corresponds to recent summary of phylogenomic studies (Burki et al., 2020) where the coloured groups represent the recognized eukaryotic supergroups and dashed lines depict unsure monophyletic origin. Note that the PBD of Tim50 could be detected only in Fungi. (Figure made in collaboration with Vitek Dohnalek and Pavel Dolezal and adapted from (Genge et al., 2023))

Throughout the eukaryotic kingdom, the components of the TIM23 complex are extremely well conserved and the majority of them are essential for the cell viability in yeast (Mokranjac et al., 2003a; Ahting et al., 2009; Demishtein-Zohary and Azem, 2017). Still, there are exceptions and some components carry distinct extensions in yeast. For example, both Tim23 and Tim14 possess N-terminal extensions that are actively involved in protein import. However, removal of these parts does not majorly affect the growth of yeast cells (Donzeau et al., 2000; Chacinska et al., 2003; Mokranjac et al., 2007; D. Popov-Celeketić et al., 2008; Popov-Čeleketić et al., 2011; Günsel et al., 2020). The PBD of Tim50 is an intriguing example of the differences among the components of the TIM23 complex on the evolutionary scale. Even though it seems to be present only in Fungi, the PBD has an essential role there and its deletion is lethal for yeast cells.

One of the major results presented in this study is that when the PBD is separated from the core domain, either by co-expressing them *in trans* or by artificially separating them through a rigid linker, this appears to have minor effects on the recruitment of Tim50 to the TIM23 complex, while the TOM-TIM23 cooperation is strongly affected. Could it be that the ability of Tim50 to coordinate the cooperation of TOM and TIM23 complexes between the two mitochondrial membranes is

particularly important for faster growing species, including the ones within Fungi? Yeast cells double their mass, including their mitochondrial content, under optimal growth conditions within 90 minutes. Some *Kluyveromyces* species can even double their mass faster (within ca. 70 min) (Groeneveld et al., 2009). Thus, it is tempting to speculate that these faster growing eukaryotes may have developed adaptions for a more efficient mitochondrial protein import, than the slower growing ones. One adaption may have included the critical, rate-limiting steps during protein translocation across two mitochondrial membranes that needed to be optimized for extreme import efficiency. The PBD of Tim50 may be one adaption to optimize the TOM-TIM23 cooperation for a more efficient transfer of precursor proteins in the IMS. Along the same lines, the data from the group of Toshiya Endo, with whom we collaborated on this project, further suggests that yeast Tim50 dimerizes through its PBD (Genge et al., 2023). This would enable the recruitment of two TIM23 complexes to a dimeric TOM complex and may represent a further adaption towards increasing import efficiency. Previous studies have reported a similar mechanism for Tim23, that has been shown to dimerize as well (Bauer et al., 1996; Alder et al., 2008b; D. Popov-Celeketić et al., 2008; Günsel et al., 2020). Dimerization of both receptors of the TIM23 complex, Tim50 and Tim23, may thus increase the occupancy at the *trans* site of the TOM complex but also allow a higher frequency of precursor recognition and, overall, a higher efficiency of protein import through the TIM23 complex.

Based on all the available data, this study suggests that the core domain of Tim50, being ubiquitously present among eukaryotes, serves both as the main presequence-recognition and -binding element of Tim50 as well as the main recruitment point to the TIM23 complex. The PBD on the other hand has, directly or indirectly, an important role in TOM-TIM23 cooperation, which is potentially an adaption of faster growing organisms to increase protein import efficiency.

5. Summary

Mitochondria, though commonly known as 'powerhouses of the cell', are not only involved in the energy production but rather represent a central biosynthetic and signalling hub for many essential cellular processes, ranging from metabolite synthesis and degradation to apoptosis. Even though mitochondria possess their own genome, this genome only encodes for a very limited number of proteins and therefore mitochondrial biogenesis requires import of over 1000 different nuclear-encoded proteins from the cytosol. The vast majority of these proteins carry cleavable, N-terminal presequences that target proteins to the mitochondrial matrix in a process mediated by two highly specific protein translocases, the TOM and TIM23 complexes in the outer and inner membranes, respectively. Several components of the TOM and TIM23 complexes form an intricate network of protein–protein interactions in the intermembrane space (IMS) that coordinates transfer of precursor proteins from the outer to the inner mitochondrial membrane. Through interactions with incoming precursor proteins and multiple subunits of both translocases, Tim50 is the central player in this network and as the major receptor subunit of the TIM23 complex involved in the recognition and coordinated transfer of precursor proteins. The functionally relevant part of Tim50, its IMS-exposed segment, was proposed to consist of two domains – the core and the presequence-binding domain (PBD). Understanding how the two domains of Tim50 in the IMS contribute to the function of Tim50 is very limited. This study provides new molecular insights into the functions and interaction partners of the individual domains of Tim50, as well as their interplay in the IMS and how they coordinate the translocation of proteins across two mitochondrial membranes.

In vivo analysis performed in this thesis demonstrated that the deletion of either the core domain or PBD of Tim50 is lethal for yeast cells, showing that both domains of Tim50 in the IMS have a role essential for cell viability. Surprisingly, when expressed *in trans*, the two domains of Tim50 reconstituted the function of the full-length protein. Biochemical and genetic experiments performed with this 50split strain revealed that the core domain contains the main presequence-binding site and is the main recruitment point of Tim50 to the TIM23 complex, with a supporting role of the PBD. On the other hand, a critical role of the PBD appears to be in coordinating, directly or indirectly, the cooperation of the TOM and TIM23 complexes. Therefore, the two domains of Tim50 in the IMS both have essential but distinct roles during translocation of proteins into mitochondria.

In summary, this study provides a compelling example of how to use experimental domain splitting to analyse functions and interactions of membrane proteins within multi-subunit complexes.

A combination of genetic and biochemical assays made it possible to assign the critical functions of Tim50 to its individual domains and show that, together, they coordinate translocation of proteins across two mitochondrial membranes.

6. Zusammenfassung

Mitochondrien, die gemeinhin als „Kraftwerke der Zelle“ bezeichnet werden, sind nicht nur an der Energieerzeugung beteiligt. Vielmehr stellen sie eine zentrale Biosynthese- und Signaltransduktionsdrehscheibe für viele wichtige zelluläre Prozesse dar, die von der Synthese sowie dem Abbau von Metaboliten bis hin zur Apoptose reichen. Obwohl Mitochondrien ein eigenes Genom besitzen, kodiert dieses nur für eine sehr begrenzte Anzahl von Proteinen, sodass die mitochondriale Biogenese den Import von über 1000 verschiedenen im kern-kodierten Proteinen aus dem Zytosol erfordert. Die überwiegende Mehrheit dieser Proteine trägt ab spaltbare N-terminale Präsequenzen, die die Proteine in die mitochondriale Matrix dirigieren. Dieser Vorgang wird durch zwei hochspezifische Proteintranslokasen, die TOM- und TIM23-Komplexe in der äußeren sowie inneren Mitochondrienmembran, vermittelt. Mehrere Komponenten der TOM- und TIM23-Komplexe bilden ein kompliziertes Netzwerk aus Protein-Protein-Interaktionen im Intermembranraum, welches die Übergabe von Vorläuferproteinen von der äußeren zur inneren Mitochondrienmembran koordiniert. Durch Interaktionen mit ankommenden Vorläuferproteinen und mehreren Untereinheiten beider Proteintranslokasen ist Tim50 der zentrale Akteur in diesem Netzwerk und als wichtigste Rezeptoruntereinheit des TIM23-Komplexes an der Erkennung und der koordinierten Übergabe von Vorläuferproteinen beteiligt. Es wurde vorgeschlagen, dass der funktionell relevante Teil von Tim50, sein Intermembran-exponiertes Proteinsegment, aus zwei Domänen besteht - die Kern- und die Präsequenz-bindende Domäne (PBD). Das Verständnis darüber, wie die beiden Domänen im Intermembranraum zur Funktion von Tim50 beitragen, ist sehr begrenzt. Diese Studie liefert neue molekulare Erkenntnisse über die Funktionen und Interaktionspartner der einzelnen Domänen von Tim50 sowie über ihr Zusammenspiel im Intermembranraum und darüber, wie sie die Translokation von Proteinen durch zwei mitochondriale Membranen koordinieren.

In vivo-Analysen im Rahmen dieser Arbeit, haben gezeigt, dass die Deletion der Kerndomäne oder der PBD von Tim50 für Hefezellen tödlich ist, was darauf hindeutet, dass beide Domänen von Tim50 im Intermembranraum eine für die Lebensfähigkeit der Zellen wichtige Rolle spielen. Überraschenderweise konnte die Koexpression beider Tim50 Domänen *in trans* die Funktion des Volllängenproteins wiederherstellen. Biochemische und genetische Experimente mit dem sogenannten 50split-Stamm zeigten, dass die Kerndomäne die Hauptbindestelle für Präsequenzen enthält und für Tim50 der Hauptrekrutierungsort zum TIM23-Komplex ist, wobei die PBD dabei eine unterstützende Rolle besitzt. Andererseits scheint die PBD direkt oder indirekt bei der Koordinierung

der Zusammenarbeit der TOM- und TIM23-Komplexe beteiligt zu sein. Die beiden Domänen von Tim50 im Intermembranraum spielen also beide eine wesentliche, aber unterschiedliche Rolle bei der Translokation von Proteinen in die Mitochondrien.

Zusammengefasst liefert diese Arbeit ein überzeugendes Beispiel, wie die experimentelle Aufspaltung von Proteindomänen zur Analyse der Funktionen und Interaktionen von Membranproteinen innerhalb von Proteinkomplexen mit mehreren Untereinheiten eingesetzt werden kann. Durch eine Kombination aus genetischen und biochemischen Experimenten konnten die kritischen Funktionen von Tim50 seinen einzelnen Domänen zugeordnet werden, und gezeigt werden, dass sie zusammen die Translokation von Proteinen durch zwei mitochondriale Membranen koordinieren.

7. References

Abe, Y., Shodai, T., Muto, T., Mihara, K., Torii, H., Nishikawa, S., et al. (2000). Structural basis of presequence recognition by the mitochondrial protein import receptor Tom20. *Cell* 100, 551–560. doi: 10.1016/s0092-8674(00)80691-1

Ahting, U., Floss, T., Uez, N., Schneider-Lohmar, I., Becker, L., Kling, E., et al. (2009). Neurological phenotype and reduced lifespan in heterozygous Tim23 knockout mice, the first mouse model of defective mitochondrial import. *Biochim Biophys Acta* 1787, 371–376. doi: 10.1016/j.bbabio.2008.12.001

Ahting, U., Thieffry, M., Engelhardt, H., Hegerl, R., Neupert, W., and Nussberger, S. (2001). Tom40, the pore-forming component of the protein-conducting TOM channel in the outer membrane of mitochondria. *J Cell Biol* 153, 1151–1160. doi: 10.1083/jcb.153.6.1151

Alberts, B. (2022). *Molecular biology of the cell*. New York: W.W. Norton and Company.

Albrecht, R., Rehling, P., Chacinska, A., Brix, J., Cadamuro, S. A., Volkmer, R., et al. (2006). The Tim21 binding domain connects the preprotein translocases of both mitochondrial membranes. *EMBO Rep* 7, 1233–1238. doi: 10.1038/sj.embor.7400828

Alder, N. N., Jensen, R. E., and Johnson, A. E. (2008a). Fluorescence mapping of mitochondrial TIM23 complex reveals a water-facing, substrate-interacting helix surface. *Cell* 134, 439–450. doi: 10.1016/j.cell.2008.06.007

Alder, N. N., Sutherland, J., Buhring, A. I., Jensen, R. E., and Johnson, A. E. (2008b). Quaternary structure of the mitochondrial TIM23 complex reveals dynamic association between Tim23p and other subunits. *Mol Biol Cell* 19, 159–170. doi: 10.1091/mbc.E07-07-0669

Araiso, Y., Imai, K., and Endo, T. (2022). Role of the TOM Complex in Protein Import into Mitochondria: Structural Views. *Annu Rev Biochem* 91, 679–703. doi: 10.1146/annurev-biochem-032620-104527

Araiso, Y., Tsutsumi, A., Qiu, J., Imai, K., Shiota, T., Song, J., et al. (2019). Structure of the mitochondrial import gate reveals distinct preprotein paths. *Nature* 575, 395–401. doi: 10.1038/s41586-019-1680-7

Backes, S., Bykov, Y. S., Flohr, T., Räschle, M., Zhou, J., Lenhard, S., et al. (2021). The chaperone-binding activity of the mitochondrial surface receptor Tom70 protects the cytosol against mitoprotein-induced stress. *Cell Rep* 35, 108936. doi: 10.1016/j.celrep.2021.108936

Backes, S., Hess, S., Boos, F., Woellhaf, M. W., Gödel, S., Jung, M., et al. (2018). Tom70 enhances mitochondrial preprotein import efficiency by binding to internal targeting sequences. *Journal of Cell Biology* 217, 1369–1382. doi: 10.1083/jcb.201708044

Bajaj, R., Jaremko, Ł., Jaremko, M., Becker, S., and Zweckstetter, M. (2014). Molecular basis of the dynamic structure of the TIM23 complex in the mitochondrial intermembrane space. *Structure* 22, 1501–1511. doi: 10.1016/j.str.2014.07.015

Baker, K. P., Schaniel, A., Vestweber, D., and Schatz, G. (1990). A yeast mitochondrial outer membrane protein essential for protein import and cell viability. *Nature* 348, 605–609. doi: 10.1038/348605a0

Banerjee, R., Gladkova, C., Mapa, K., Witte, G., and Mokranjac, D. (2015). Protein translocation channel of mitochondrial inner membrane and matrix-exposed import motor communicate via two-domain coupling protein. *Elife* 4, e11897. doi: 10.7554/eLife.11897

Bauer, M. F., Sirrenberg, C., Neupert, W., and Brunner, M. (1996). Role of Tim23 as voltage sensor and presequence receptor in protein import into mitochondria. *Cell* 87, 33–41. doi: 10.1016/s0092-8674(00)81320-3

Baumann, F., Neupert, W., and Herrmann, J. M. (2002). Insertion of bitopic membrane proteins into the inner membrane of mitochondria involves an export step from the matrix. *Journal of Biological Chemistry* 277, 21405–21413. doi: 10.1074/jbc.M201670200

Becker, T., Pfannschmidt, S., Guiard, B., Stojanovski, D., Milenkovic, D., Kutik, S., et al. (2008). Biogenesis of the mitochondrial TOM complex: Mim1 promotes insertion and assembly of signal-anchored receptors. *Journal of Biological Chemistry* 283, 120–127. doi: 10.1074/jbc.M706997200

Becker, T., Song, J., and Pfanner, N. (2019). Versatility of Preprotein Transfer from the Cytosol to Mitochondria. *Trends Cell Biol* 29, 534–548. doi: 10.1016/j.tcb.2019.03.007

Blobel, G. (2000). Protein Targeting (Nobel Lecture). *ChemBioChem* 1, 86–102. doi: 10.1002/1439-7633(20000818)1:2<86:AID-CBIC86>3.0.CO;2-A

Brix, J., Rüdiger, S., Bukau, B., Schneider-Mergener, J., and Pfanner, N. (1999). Distribution of binding sequences for the mitochondrial import receptors Tom20, Tom22, and Tom70 in a presequence-carrying preprotein and a non-cleavable preprotein. *J Biol Chem* 274, 16522–16530. doi: 10.1074/jbc.274.23.16522

Burki, F., Roger, A. J., Brown, M. W., and Simpson, A. G. B. (2020). The New Tree of Eukaryotes. *Trends Ecol Evol* 35, 43–55. doi: 10.1016/j.tree.2019.08.008

Busch, J. D., Fielden, L. F., Pfanner, N., and Wiedemann, N. (2023). Mitochondrial protein transport: Versatility of translocases and mechanisms. *Mol Cell* 83, 890–910. doi: 10.1016/j.molcel.2023.02.020

Bykov, Y. S., Rapaport, D., Herrmann, J. M., and Schuldiner, M. (2020). Cytosolic Events in the Biogenesis of Mitochondrial Proteins. *Trends Biochem Sci* 45, 650–667. doi: 10.1016/j.tibs.2020.04.001

Callegari, S., Cruz-Zaragoza, L. D., and Rehling, P. (2020). From TOM to the TIM23 complex - handing over of a precursor. *Biol Chem* 401, 709–721. doi: 10.1515/hsz-2020-0101

Casadaban, M. J., and Cohen, S. N. (1980). Analysis of gene control signals by DNA fusion and cloning in Escherichia coli. *J Mol Biol* 138, 179–207. doi: 10.1016/0022-2836(80)90283-1

Caumont-Sarcos, A., Moulin, C., Poinot, L., Guiard, B., van der Laan, M., and Ieva, R. (2020). Transmembrane Coordination of Preprotein Recognition and Motor Coupling by the Mitochondrial Presequence Receptor Tim50. *Cell Rep* 30, 3092-3104.e4. doi: 10.1016/j.celrep.2020.02.031

Chacinska, A., Lind, M., Frazier, A. E., Dudek, J., Meisinger, C., Geissler, A., et al. (2005). Mitochondrial presequence translocase: switching between TOM tethering and motor recruitment involves Tim21 and Tim17. *Cell* 120, 817–829. doi: 10.1016/j.cell.2005.01.011

Chacinska, A., Pfannschmidt, S., Wiedemann, N., Kozjak, V., Sanjuán Szklarz, L. K., Schulze-Specking, A., et al. (2004). Essential role of Mia40 in import and assembly of mitochondrial intermembrane space proteins. *EMBO J* 23, 3735–3746. doi: 10.1038/sj.emboj.7600389

Chacinska, A., Rehling, P., Guiard, B., Frazier, A. E., Schulze-Specking, A., Pfanner, N., et al. (2003). Mitochondrial translocation contact sites: separation of dynamic and stabilizing elements in formation of a TOM-TIM-preprotein supercomplex. *EMBO J* 22, 5370–5381. doi: 10.1093/emboj/cdg532

Chen, X., Zaro, J. L., and Shen, W.-C. (2013). Fusion protein linkers: property, design and functionality. *Adv Drug Deliv Rev* 65, 1357–1369. doi: 10.1016/j.addr.2012.09.039

Craig, E. A. (2018). Hsp70 at the membrane: driving protein translocation. *BMC Biol* 16, 11. doi: 10.1186/s12915-017-0474-3

Dayan, D., Bandel, M., Günsel, U., Nussbaum, I., Prag, G., Mokranjac, D., et al. (2019). A mutagenesis analysis of Tim50, the major receptor of the TIM23 complex, identifies regions that affect its interaction with Tim23. *Sci Rep* 9, 2012. doi: 10.1038/s41598-018-38353-1

Dekker, P. J., Ryan, M. T., Brix, J., Müller, H., Hönlinger, A., and Pfanner, N. (1998). Preprotein translocase of the outer mitochondrial membrane: molecular dissection and assembly of the general import pore complex. *Mol Cell Biol* 18, 6515–6524. doi: 10.1128/MCB.18.11.6515

Demishtein-Zohary, K., and Azem, A. (2017). The TIM23 mitochondrial protein import complex: function and dysfunction. *Cell Tissue Res* 367, 33–41. doi: 10.1007/s00441-016-2486-7

Demishtein-Zohary, K., Günsel, U., Marom, M., Banerjee, R., Neupert, W., Azem, A., et al. (2017). Role of Tim17 in coupling the import motor to the translocation channel of the mitochondrial presequence translocase. *Elife* 6. doi: 10.7554/eLife.22696

Demishtein-Zohary, K., Marom, M., Neupert, W., Mokranjac, D., and Azem, A. (2015). GxxxG motifs hold the TIM23 complex together. *FEBS J* 282, 2178–2186. doi: 10.1111/febs.13266

Doerner, P. A., and Sousa, M. C. (2017). Extreme Dynamics in the BamA β-Barrel Seam. *Biochemistry* 56, 3142–3149. doi: 10.1021/acs.biochem.7b00281

Dolezal, P., Likic, V., Tachezy, J., and Lithgow, T. (2006). Evolution of the molecular machines for protein import into mitochondria. *Science* 313, 314–318. doi: 10.1126/science.1127895

Donzeau, M., Káldi, K., Adam, A., Paschen, S., Wanner, G., Guiard, B., et al. (2000). Tim23 links the inner and outer mitochondrial membranes. *Cell* 101, 401–412. doi: 10.1016/s0092-8674(00)80850-8

D'Silva, P. D., Schilke, B., Walter, W., Andrew, A., and Craig, E. A. (2003). J protein cochaperone of the mitochondrial inner membrane required for protein import into the mitochondrial matrix. *Proc Natl Acad Sci U S A* 100, 13839–13844. doi: 10.1073/pnas.1936150100

D'Silva, P. R., Schilke, B., Walter, W., and Craig, E. A. (2005). Role of Pam16's degenerate J domain in protein import across the mitochondrial inner membrane. *Proc Natl Acad Sci U S A* 102, 12419–12424. doi: 10.1073/pnas.0505969102

Esaki, M., Kanamori, T., Nishikawa, S.-I., Shin, I., Schultz, P. G., and Endo, T. (2003). Tom40 protein import channel binds to non-native proteins and prevents their aggregation. *Nat Struct Biol* 10, 988–994. doi: 10.1038/nsb1008

Esaki, M., Shimizu, H., Ono, T., Yamamoto, H., Kanamori, T., Nishikawa, S.-I., et al. (2004). Mitochondrial protein import. Requirement of presequence elements and tom components for precursor binding to the TOM complex. *J Biol Chem* 279, 45701–45707. doi: 10.1074/jbc.M404591200

Fielden, L. F., Busch, J. D., Merkt, S. G., Ganesan, I., Steiert, C., Hasselblatt, H. B., et al. (2023). Central role of Tim17 in mitochondrial presequence protein translocation. *Nature*. doi: 10.1038/s41586-023-06477-8

Frazier, A. E., Chacinska, A., Truscott, K. N., Guiard, B., Pfanner, N., and Rehling, P. (2003). Mitochondria use different mechanisms for transport of multispanning membrane proteins

through the intermembrane space. *Mol Cell Biol* 23, 7818–7828. doi: 10.1128/MCB.23.21.7818-7828.2003

Fukasawa, Y., Oda, T., Tomii, K., and Imai, K. (2017). Origin and Evolutionary Alteration of the Mitochondrial Import System in Eukaryotic Lineages. *Mol Biol Evol* 34, 1574–1586. doi: 10.1093/molbev/msx096

Gao, S.-P., Sun, H.-F., Jiang, H.-L., Li, L.-D., Hu, X., Xu, X.-E., et al. (2016). Loss of TIM50 suppresses proliferation and induces apoptosis in breast cancer. *Tumour Biol* 37, 1279–1287. doi: 10.1007/s13277-015-3878-0

Gao, X., Dong, X., Li, X., Liu, Z., and Liu, H. (2020). Prediction of disulfide bond engineering sites using a machine learning method. *Sci Rep* 10, 10330. doi: 10.1038/s41598-020-67230-z

Geissler, A., Chacinska, A., Truscott, K. N., Wiedemann, N., Brandner, K., Sickmann, A., et al. (2002). The mitochondrial presequence translocase: an essential role of Tim50 in directing preproteins to the import channel. *Cell* 111, 507–518. doi: 10.1016/s0092-8674(02)01073-5

Genge, M. G., and Mokranjac, D. (2021). Coordinated Translocation of Presequence-Containing Precursor Proteins Across Two Mitochondrial Membranes: Knowns and Unknowns of How TOM and TIM23 Complexes Cooperate With Each Other. *Front Physiol* 12, 806426. doi: 10.3389/fphys.2021.806426

Genge, M. G., Roy Chowdhury, S., Dohnálek, V., Yunoki, K., Hirashima, T., Endo, T., et al. (2023). Two domains of Tim50 coordinate translocation of proteins across the two mitochondrial membranes. *Life Sci Alliance* 6. doi: 10.26508/lsa.202302122

Gevorkyan-Airapetov, L., Zohary, K., Popov-Celeketic, D., Mapa, K., Hell, K., Neupert, W., et al. (2009). Interaction of Tim23 with Tim50 Is essential for protein translocation by the mitochondrial TIM23 complex. *J Biol Chem* 284, 4865–4872. doi: 10.1074/jbc.M807041200

Gomkale, R., Linden, A., Neumann, P., Schendzielorz, A. B., Stoldt, S., Dybkov, O., et al. (2021). Mapping protein interactions in the active TOM-TIM23 supercomplex. *Nat Commun* 12, 5715. doi: 10.1038/s41467-021-26016-1

Grevel, A., Pfanner, N., and Becker, T. (2019). Coupling of import and assembly pathways in mitochondrial protein biogenesis. *Biol Chem* 401, 117–129. doi: 10.1515/hsz-2019-0310

Groeneveld, P., Stouthamer, A. H., and Westerhoff, H. V. (2009). Super life--how and why 'cell selection' leads to the fastest-growing eukaryote. *FEBS J* 276, 254–270. doi: 10.1111/j.1742-4658.2008.06778.x

Guna, A., Stevens, T. A., Inglis, A. J., Replogle, J. M., Esantsi, T. K., Muthukumar, G., et al. (2022). MTCH2 is a mitochondrial outer membrane protein insertase. *Science* 378, 317–322. doi: 10.1126/science.add1856

Günsel, U., Paz, E., Gupta, R., Mathes, I., Azem, A., and Mokranjac, D. (2020). InVivo Dissection of the Intrinsically Disordered Receptor Domain of Tim23. *J Mol Biol* 432, 3326–3337. doi: 10.1016/j.jmb.2020.03.031

Gupta, A., and Becker, T. (2021). Mechanisms and pathways of mitochondrial outer membrane protein biogenesis. *Biochim Biophys Acta Bioenerg* 1862, 148323. doi: 10.1016/j.bbabio.2020.148323

Hansen, K. G., and Herrmann, J. M. (2019). Transport of Proteins into Mitochondria. *Protein J* 38, 330–342. doi: 10.1007/s10930-019-09819-6

Harner, M., Mokranjac, D., and Neupert, W. (2012). Die molekulare Architektur der Mitochondrien. *Biospektrum* 18, 576–581. doi: 10.1007/s12268-012-0230-8

Hell, K., Neupert, W., and Stuart, R. A. (2001). Oxa1p acts as a general membrane insertion machinery for proteins encoded by mitochondrial DNA. *EMBO J* 20, 1281–1288. doi: 10.1093/emboj/20.6.1281

Herrmann, J. M., Neupert, W., and Stuart, R. A. (1997). Insertion into the mitochondrial inner membrane of a polytopic protein, the nuclear-encoded Oxa1p. *EMBO J* 16, 2217–2226. doi: 10.1093/emboj/16.9.2217

Höhr, A. I. C., Lindau, C., Wirth, C., Qiu, J., Stroud, D. A., Kutik, S., et al. (2018). Membrane protein insertion through a mitochondrial β-barrel gate. *Science* 359. doi: 10.1126/science.aah6834

Hwang, S., Jascur, T., Vestweber, D., Pon, L., and Schatz, G. (1989). Disrupted yeast mitochondria can import precursor proteins directly through their inner membrane. *J Cell Biol* 109, 487–493. doi: 10.1083/jcb.109.2.487

Ieva, R., Schrempp, S. G., Opaliński, L., Wollweber, F., Höß, P., Heißwolf, A. K., et al. (2014). Mgr2 functions as lateral gatekeeper for preprotein sorting in the mitochondrial inner membrane. *Mol Cell* 56, 641–652. doi: 10.1016/j.molcel.2014.10.010

Im Sim, S., Chen, Y., Lynch, D. L., Gumbart, J. C., and Park, E. (2023). Structural basis of mitochondrial protein import by the TIM23 complex. *Nature*. doi: 10.1038/s41586-023-06239-6

Kanamori, T., Nishikawa, S., Nakai, M., Shin, I., Schultz, P. G., and Endo, T. (1999). Uncoupling of transfer of the presequence and unfolding of the mature domain in precursor translocation across the mitochondrial outer membrane. *Proc Natl Acad Sci U S A* 96, 3634–3639. doi: 10.1073/pnas.96.7.3634

Kang, Y., Fielden, L. F., and Stojanovski, D. (2018). Mitochondrial protein transport in health and disease. *Semin Cell Dev Biol* 76, 142–153. doi: 10.1016/j.semcdb.2017.07.028

Kiebler, M., Pfaller, R., Söllner, T., Griffiths, G., Horstmann, H., Pfanner, N., et al. (1990). Identification of a mitochondrial receptor complex required for recognition and membrane insertion of precursor proteins. *Nature* 348, 610–616. doi: 10.1038/348610a0

Koehler, C. M., Jarosch, E., Tokatlidis, K., Schmid, K., Schweyen, R. J., and Schatz, G. (1998). Import of mitochondrial carriers mediated by essential proteins of the intermembrane space. *Science* 279, 369–373. doi: 10.1126/science.279.5349.369

Kovermann, P., Truscott, K. N., Guiard, B., Rehling, P., Sepuri, N. B., Müller, H., et al. (2002). Tim22, the essential core of the mitochondrial protein insertion complex, forms a voltage-activated and signal-gated channel. *Mol Cell* 9, 363–373. doi: 10.1016/s1097-2765(02)00446-x

Kümmel, D., Krishnakumar, S. S., Radoff, D. T., Li, F., Giraudo, C. G., Pincet, F., et al. (2011). Complexin cross-links prefusion SNAREs into a zigzag array. *Nat Struct Mol Biol* 18, 927–933. doi: 10.1038/nsmb.2101

Künkele, K. P., Heins, S., Dembowski, M., Nargang, F. E., Benz, R., Thieffry, M., et al. (1998). The preprotein translocation channel of the outer membrane of mitochondria. *Cell* 93, 1009–1019. doi: 10.1016/S0092-8674(00)81206-4

La Cruz, L. de, Bajaj, R., Becker, S., and Zweckstetter, M. (2010). The intermembrane space domain of Tim23 is intrinsically disordered with a distinct binding region for presequences. *Protein Sci* 19, 2045–2054. doi: 10.1002/pro.482

Los Rios, P. de, Ben-Zvi, A., Slutsky, O., Azem, A., and Goloubinoff, P. (2006). Hsp70 chaperones accelerate protein translocation and the unfolding of stable protein aggregates by entropic pulling. *Proc Natl Acad Sci U S A* 103, 6166–6171. doi: 10.1073/pnas.0510496103

Lytovchenko, O., Melin, J., Schulz, C., Kilisch, M., Hutu, D. P., and Rehling, P. (2013). Signal recognition initiates reorganization of the presequence translocase during protein import. *EMBO J* 32, 886–898. doi: 10.1038/emboj.2013.23

Malhotra, K., Modak, A., Nangia, S., Daman, T. H., Gunsel, U., Robinson, V. L., et al. (2017). Cardiolipin mediates membrane and channel interactions of the mitochondrial TIM23 protein import complex receptor Tim50. *Sci Adv* 3, e1700532. doi: 10.1126/sciadv.1700532

Malhotra, K., Sathappa, M., Landin, J. S., Johnson, A. E., and Alder, N. N. (2013). Structural changes in the mitochondrial Tim23 channel are coupled to the proton-motive force. *Nat Struct Mol Biol* 20, 965–972. doi: 10.1038/nsmb.2613

Mapa, K., Sikor, M., Kudryavtsev, V., Waegemann, K., Kalinin, S., Seidel, C. A. M., et al. (2010). The conformational dynamics of the mitochondrial Hsp70 chaperone. *Mol Cell* 38, 89–100. doi: 10.1016/j.molcel.2010.03.010

Marom, M., Dayan, D., Demishtein-Zohary, K., Mokranjac, D., Neupert, W., and Azem, A. (2011). Direct interaction of mitochondrial targeting presequences with purified components of the TIM23 protein complex. *J Biol Chem* 286, 43809–43815. doi: 10.1074/jbc.M111.261040

Martin, J., Mahlke, K., and Pfanner, N. (1991). Role of an energized inner membrane in mitochondrial protein import. Delta psi drives the movement of presequences. *Journal of Biological Chemistry* 266, 18051–18057.

Martinez-Caballero, S., Grigoriev, S. M., Herrmann, J. M., Campo, M. L., and Kinnally, K. W. (2007). Tim17p regulates the twin pore structure and voltage gating of the mitochondrial protein import complex TIM23. *J Biol Chem* 282, 3584–3593. doi: 10.1074/jbc.M607551200

Mayer, A., Neupert, W., and Lill, R. (1995). Mitochondrial protein import: reversible binding of the presequence at the trans side of the outer membrane drives partial translocation and unfolding. *Cell* 80, 127–137. doi: 10.1016/0092-8674(95)90457-3

Mesecke, N., Terziyska, N., Kozany, C., Baumann, F., Neupert, W., Hell, K., et al. (2005). A disulfide relay system in the intermembrane space of mitochondria that mediates protein import. *Cell* 121, 1059–1069. doi: 10.1016/j.cell.2005.04.011

Miao, B., Davis, J. E., and Craig, E. A. (1997). Mge1 functions as a nucleotide release factor for Ssc1, a mitochondrial Hsp70 of Saccharomyces cerevisiae. *J Mol Biol* 265, 541–552. doi: 10.1006/jmbi.1996.0762

Milenkovic, D., Ramming, T., Müller, J. M., Wenz, L.-S., Gebert, N., Schulze-Specking, A., et al. (2009). Identification of the signal directing Tim9 and Tim10 into the intermembrane space of mitochondria. *Mol Biol Cell* 20, 2530–2539. doi: 10.1091/mbc.e08-11-1108

Moczko, M., Bömer, U., Kübrich, M., Zufall, N., Hönlinger, A., and Pfanner, N. (1997). The intermembrane space domain of mitochondrial Tom22 functions as a trans binding site for preproteins with N-terminal targeting sequences. *Mol Cell Biol* 17, 6574–6584. doi: 10.1128/MCB.17.11.6574

Model, K., Prinz, T., Ruiz, T., Radermacher, M., Krimmer, T., Kühlbrandt, W., et al. (2002). Protein translocase of the outer mitochondrial membrane: role of import receptors in the structural organization of the TOM complex. *J Mol Biol* 316, 657–666. doi: 10.1006/jmbi.2001.5365

Mokranjac, D. (2020). How to get to the other side of the mitochondrial inner membrane - the protein import motor. *Biol Chem* 401, 723–736. doi: 10.1515/hsz-2020-0106

Mokranjac, D., Berg, A., Adam, A., Neupert, W., and Hell, K. (2007). Association of the Tim14.Tim16 subcomplex with the TIM23 translocase is crucial for function of the mitochondrial protein import motor. *J Biol Chem* 282, 18037–18045. doi: 10.1074/jbc.M701895200

Mokranjac, D., Bourenkov, G., Hell, K., Neupert, W., and Groll, M. (2006). Structure and function of Tim14 and Tim16, the J and J-like components of the mitochondrial protein import motor. *EMBO J* 25, 4675–4685. doi: 10.1038/sj.emboj.7601334

Mokranjac, D., Paschen, S. A., Kozany, C., Prokisch, H., Hoppins, S. C., Nargang, F. E., et al. (2003a). Tim50, a novel component of the TIM23 preprotein translocase of mitochondria. *EMBO J* 22, 816–825. doi: 10.1093/emboj/cdg090

Mokranjac, D., Popov-Celeketić, D., Hell, K., and Neupert, W. (2005). Role of Tim21 in mitochondrial translocation contact sites. *J Biol Chem* 280, 23437–23440. doi: 10.1074/jbc.C500135200

Mokranjac, D., Sichting, M., Neupert, W., and Hell, K. (2003b). Tim14, a novel key component of the import motor of the TIM23 protein translocase of mitochondria. *EMBO J* 22, 4945–4956. doi: 10.1093/emboj/cdg485

Mokranjac, D., Sichting, M., Popov-Celeketić, D., Mapa, K., Gevorkyan-Airapetov, L., Zohary, K., et al. (2009). Role of Tim50 in the transfer of precursor proteins from the outer to the inner membrane of mitochondria. *Mol Biol Cell* 20, 1400–1407. doi: 10.1091/mbc.E08-09-0934

Mossmann, D., Meisinger, C., and Vögtle, F.-N. (2012). Processing of mitochondrial presequences. *Biochim Biophys Acta* 1819, 1098–1106. doi: 10.1016/j.bbagrm.2011.11.007

Muñoz-Gómez, S. A. (2023). Energetics and evolution of anaerobic microbial eukaryotes. *Nat Microbiol* 8, 197–203. doi: 10.1038/s41564-022-01299-2

Neupert, W. (2015). A perspective on transport of proteins into mitochondria: a myriad of open questions. *J Mol Biol* 427, 1135–1158. doi: 10.1016/j.jmb.2015.02.001

Neupert, W., and Brunner, M. (2002). The protein import motor of mitochondria. *Nat Rev Mol Cell Biol* 3, 555–565. doi: 10.1038/nrm878

Nunnari, J., Fox, T. D., and Walter, P. (1993). A mitochondrial protease with two catalytic subunits of nonoverlapping specificities. *Science* 262, 1997–2004. doi: 10.1126/science.8266095

Nunnari, J., and Suomalainen, A. (2012). Mitochondria: in sickness and in health. *Cell* 148, 1145–1159. doi: 10.1016/j.cell.2012.02.035

Paschen, S. A., Waizenegger, T., Stan, T., Preuss, M., Cyrklaff, M., Hell, K., et al. (2003). Evolutionary conservation of biogenesis of beta-barrel membrane proteins. *Nature* 426, 862–866. doi: 10.1038/nature02208

Patel, D. K., Menon, D. V., Patel, D. H., and Dave, G. (2022). Linkers: A synergistic way for the synthesis of chimeric proteins. *Protein Expr Purif* 191, 106012. doi: 10.1016/j.pep.2021.106012

Pfanner, N., Warscheid, B., and Wiedemann, N. (2019). Mitochondrial proteins: from biogenesis to functional networks. *Nat Rev Mol Cell Biol* 20, 267–284. doi: 10.1038/s41580-018-0092-0

D. Popov-Celeketić, K. Mapa, W. Neupert, and D. Mokranjac (2008). Active remodelling of the TIM23 complex during translocation of preproteins into mitochondria. *EMBO J* 27, 1469–1480. doi: 10.1038/emboj.2008.79

J. Popov-Celeketić, T. Waizenegger, and D. Rapaport (2008). Mim1 functions in an oligomeric form to facilitate the integration of Tom20 into the mitochondrial outer membrane. *J Mol Biol* 376, 671–680. doi: 10.1016/j.jmb.2007.12.006

Popov-Čeleketić, D., Waegemann, K., Mapa, K., Neupert, W., and Mokranjac, D. (2011). Role of the import motor in insertion of transmembrane segments by the mitochondrial TIM23 complex. *EMBO Rep* 12, 542–548. doi: 10.1038/embor.2011.72

Qian, X., Gebert, M., Höpker, J., Yan, M., Li, J., Wiedemann, N., et al. (2011). Structural basis for the function of Tim50 in the mitochondrial presequence translocase. *J Mol Biol* 411, 513–519. doi: 10.1016/j.jmb.2011.06.020

Qiu, J., Wenz, L.-S., Zerbes, R. M., Oeljeklaus, S., Bohnert, M., Stroud, D. A., et al. (2013). Coupling of mitochondrial import and export translocases by receptor-mediated supercomplex formation. *Cell* 154, 596–608. doi: 10.1016/j.cell.2013.06.033

Rahman, B., Kawano, S., Yunoki-Esaki, K., Anzai, T., and Endo, T. (2014). NMR analyses on the interactions of the yeast Tim50 C-terminal region with the presequence and Tim50 core domain. *FEBS Lett* 588, 678–684. doi: 10.1016/j.febslet.2013.12.037

Ramesh, A., Peleh, V., Martinez-Caballero, S., Wollweber, F., Sommer, F., van der Laan, M., et al. (2016). A disulfide bond in the TIM23 complex is crucial for voltage gating and mitochondrial protein import. *Journal of Cell Biology* 214, 417–431. doi: 10.1083/jcb.201602074

Reyes, A., Melchionda, L., Burlina, A., Robinson, A. J., Ghezzi, D., and Zeviani, M. (2018). Mutations in TIMM50 compromise cell survival in OxPhos-dependent metabolic conditions. *EMBO Mol Med* 10. doi: 10.15252/emmm.201708698

Rosenzweig, R., Nillegoda, N. B., Mayer, M. P., and Bukau, B. (2019). The Hsp70 chaperone network. *Nat Rev Mol Cell Biol* 20, 665–680. doi: 10.1038/s41580-019-0133-3

Saitoh, T., Igura, M., Obita, T., Ose, T., Kojima, R., Maenaka, K., et al. (2007). Tom20 recognizes mitochondrial presequences through dynamic equilibrium among multiple bound states. *EMBO J* 26, 4777–4787. doi: 10.1038/sj.emboj.7601888

Schatz, G., and Dobberstein, B. (1996). Common principles of protein translocation across membranes. *Science* 271, 1519–1526. doi: 10.1126/science.271.5255.1519

Schendzielorz, A. B., Bragoszewski, P., Naumenko, N., Gomkale, R., Schulz, C., Guiard, B., et al. (2018). Motor recruitment to the TIM23 channel's lateral gate restricts polypeptide release into the inner membrane. *Nat Commun* 9, 4028. doi: 10.1038/s41467-018-06492-8

Schendzielorz, A. B., Schulz, C., Lytovchenko, O., Clancy, A., Guiard, B., Ieva, R., et al. (2017). Two distinct membrane potential-dependent steps drive mitochondrial matrix protein translocation. *J Cell Biol* 216, 83–92. doi: 10.1083/jcb.201607066

Schulz, C., Lytovchenko, O., Melin, J., Chacinska, A., Guiard, B., Neumann, P., et al. (2011). Tim50's presequence receptor domain is essential for signal driven transport across the TIM23 complex. *J Cell Biol* 195, 643–656. doi: 10.1083/jcb.201105098

Schulz, C., Schendzielorz, A., and Rehling, P. (2015). Unlocking the presequence import pathway. *Trends Cell Biol* 25, 265–275. doi: 10.1016/j.tcb.2014.12.001

Shahrour, M. A., Staretz-Chacham, O., Dayan, D., Stephen, J., Weech, A., Damseh, N., et al. (2017). Mitochondrial epileptic encephalopathy, 3-methylglutaconic aciduria and variable complex V deficiency associated with TIMM50 mutations. *Clin Genet* 91, 690–696. doi: 10.1111/cge.12855

Shiota, T., Imai, K., Qiu, J., Hewitt, V. L., Tan, K., Shen, H.-H., et al. (2015). Molecular architecture of the active mitochondrial protein gate. *Science* 349, 1544–1548. doi: 10.1126/science.aac6428

Shiota, T., Mabuchi, H., Tanaka-Yamano, S., Yamano, K., and Endo, T. (2011). In vivo protein-interaction mapping of a mitochondrial translocator protein Tom22 at work. *Proc Natl Acad Sci U S A* 108, 15179–15183. doi: 10.1073/pnas.1105921108

Sideris, D. P., Petrakis, N., Katrakili, N., Mikropoulou, D., Gallo, A., Ciofi-Baffoni, S., et al. (2009). A novel intermembrane space-targeting signal docks cysteines onto Mia40 during mitochondrial oxidative folding. *J Cell Biol* 187, 1007–1022. doi: 10.1083/jcb.200905134

Sikor, M., Mapa, K., Voithenberg, L. V. von, Mokranjac, D., and Lamb, D. C. (2013). Real-time observation of the conformational dynamics of mitochondrial Hsp70 by spFRET. *EMBO J* 32, 1639–1649. doi: 10.1038/emboj.2013.89

Sikorski, R. S., and Hieter, P. (1989). A system of shuttle vectors and yeast host strains designed for efficient manipulation of DNA in Saccharomyces cerevisiae. *Genetics* 122, 19–27. doi: 10.1093/genetics/122.1.19

Sinzel, M., Tan, T., Wendling, P., Kalbacher, H., Özbalci, C., Chelius, X., et al. (2016). Mcp3 is a novel mitochondrial outer membrane protein that follows a unique IMP-dependent biogenesis pathway. *EMBO Rep* 17, 965–981. doi: 10.15252/embr.201541273

Sirrenberg, C., Bauer, M. F., Guiard, B., Neupert, W., and Brunner, M. (1996). Import of carrier proteins into the mitochondrial inner membrane mediated by Tim22. *Nature* 384, 582–585. doi: 10.1038/384582a0

Spinelli, J. B., and Haigis, M. C. (2018). The multifaceted contributions of mitochondria to cellular metabolism. *Nat Cell Biol* 20, 745–754. doi: 10.1038/s41556-018-0124-1

Suomalainen, A., and Battersby, B. J. (2018). Mitochondrial diseases: the contribution of organelle stress responses to pathology. *Nat Rev Mol Cell Biol* 19, 77–92. doi: 10.1038/nrm.2017.66

Tamura, Y., Harada, Y., Shiota, T., Yamano, K., Watanabe, K., Yokota, M., et al. (2009). Tim23-Tim50 pair coordinates functions of translocators and motor proteins in mitochondrial protein import. *J Cell Biol* 184, 129–141. doi: 10.1083/jcb.200808068

Tang, K., Zhao, Y., Li, H., Zhu, M., Li, W., Liu, W., et al. (2017). Translocase of Inner Membrane 50 Functions as a Novel Protective Regulator of Pathological Cardiac Hypertrophy. *J Am Heart Assoc* 6. doi: 10.1161/JAHA.116.004346

Ting, S.-Y., Yan, N. L., Schilke, B. A., and Craig, E. A. (2017). Dual interaction of scaffold protein Tim44 of mitochondrial import motor with channel-forming translocase subunit Tim23. *Elife* 6. doi: 10.7554/eLife.23609

Truscott, K. N., Kovermann, P., Geissler, A., Merlin, A., Meijer, M., Driessen, A. J., et al. (2001). A presequence- and voltage-sensitive channel of the mitochondrial preprotein translocase formed by Tim23. *Nat Struct Biol* 8, 1074–1082. doi: 10.1038/nsb726

Tucker, K., and Park, E. (2019). Cryo-EM structure of the mitochondrial protein-import channel TOM complex at near-atomic resolution. *Nat Struct Mol Biol* 26, 1158–1166. doi: 10.1038/s41594-019-0339-2

van der Laan, M., Meinecke, M., Dudek, J., Hutu, D. P., Lind, M., Perschil, I., et al. (2007). Motor-free mitochondrial presequence translocase drives membrane integration of preproteins. *Nat Cell Biol* 9, 1152–1159. doi: 10.1038/ncb1635

van der Laan, M., Wiedemann, N., Mick, D. U., Guiard, B., Rehling, P., and Pfanner, N. (2006). A role for Tim21 in membrane-potential-dependent preprotein sorting in mitochondria. *Current Biology* 16, 2271–2276. doi: 10.1016/j.cub.2006.10.025

van Wilpe, S., Ryan, M. T., Hill, K., Maarse, A. C., Meisinger, C., Brix, J., et al. (1999). Tom22 is a multifunctional organizer of the mitochondrial preprotein translocase. *Nature* 401, 485–489. doi: 10.1038/46802

Vitali, D. G., Käser, S., Kolb, A., Dimmer, K. S., Schneider, A., and Rapaport, D. (2018). Independent evolution of functionally exchangeable mitochondrial outer membrane import complexes. *Elife* 7. doi: 10.7554/eLife.34488

Vögtle, F.-N., Prinz, C., Kellermann, J., Lottspeich, F., Pfanner, N., and Meisinger, C. (2011). Mitochondrial protein turnover: role of the precursor intermediate peptidase Oct1 in protein stabilization. *Mol Biol Cell* 22, 2135–2143. doi: 10.1091/mbc.E11-02-0169

Vögtle, F.-N., Wortelkamp, S., Zahedi, R. P., Becker, D., Leidhold, C., Gevaert, K., et al. (2009). Global analysis of the mitochondrial N-proteome identifies a processing peptidase critical for protein stability. *Cell* 139, 428–439. doi: 10.1016/j.cell.2009.07.045

Voisine, C., Craig, E. A., Zufall, N., Ahsen, O. von, Pfanner, N., and Voos, W. (1999). The protein import motor of mitochondria: unfolding and trapping of preproteins are distinct and separable functions of matrix Hsp70. *Cell* 97, 565–574. doi: 10.1016/s0092-8674(00)80768-0

Waegemann, K., Popov-Čeleketić, D., Neupert, W., Azem, A., and Mokranjac, D. (2015). Cooperation of TOM and TIM23 complexes during translocation of proteins into mitochondria. *J Mol Biol* 427, 1075–1084. doi: 10.1016/j.jmb.2014.07.015

Wang, W., Chen, X., Zhang, L., Yi, J., Ma, Q., Yin, J., et al. (2020). Atomic structure of human TOM core complex. *Cell Discovery* 6, 67. doi: 10.1038/s41421-020-00198-2

Wenz, L.-S., Opaliński, L., Schuler, M.-H., Ellenrieder, L., Ieva, R., Böttinger, L., et al. (2014). The presequence pathway is involved in protein sorting to the mitochondrial outer membrane. *EMBO Rep* 15, 678–685. doi: 10.1002/embr.201338144

Wiedemann, N., Kozjak, V., Chacinska, A., Schönfisch, B., Rospert, S., Ryan, M. T., et al. (2003). Machinery for protein sorting and assembly in the mitochondrial outer membrane. *Nature* 424, 565–571. doi: 10.1038/nature01753

Wiedemann, N., and Pfanner, N. (2017). Mitochondrial Machineries for Protein Import and Assembly. *Annu Rev Biochem* 86, 685–714. doi: 10.1146/annurev-biochem-060815-014352

Yamamoto, H., Esaki, M., Kanamori, T., Tamura, Y., Nishikawa, S. i., and Endo, T. (2002). Tim50 is a subunit of the TIM23 complex that links protein translocation across the outer and inner mitochondrial membranes. *Cell* 111, 519–528. doi: 10.1016/s0092-8674(02)01053-x

Yamamoto, H., Itoh, N., Kawano, S., Yatsukawa, Y., Momose, T., Makio, T., et al. (2011). Dual role of the receptor Tom20 in specificity and efficiency of protein import into mitochondria. *Proceedings of the National Academy of Sciences* 108, 91–96. doi: 10.1073/pnas.1014918108

Yamano, K., Yatsukawa, Y., Esaki, M., Hobbs, A. E. A., Jensen, R. E., and Endo, T. (2008). Tom20 and Tom22 share the common signal recognition pathway in mitochondrial protein import. *Journal of Biological Chemistry* 283, 3799–3807. doi: 10.1074/jbc.M708339200

Zhang, X., Han, S., Zhou, H., Cai, L., Li, J., Liu, N., et al. (2019). TIMM50 promotes tumor progression via ERK signaling and predicts poor prognosis of non-small cell lung cancer patients. *Mol Carcinog* 58, 767–776. doi: 10.1002/mc.22969

Zhang, Y., Ou, X., Wang, X., Sun, D., Zhou, X., Wu, X., et al. (2021). Structure of the mitochondrial TIM22 complex from yeast. *Cell Res* 31, 366–368. doi: 10.1038/s41422-020-00399-0

Abbreviations

°C	Degree Celsius
4-DPS	4,4’-dipyridyl disulfide
5-FOA	5-fluoroorotic acid
ADP	Adenosine diphosphate
Amp	Ampicillin
APS	Ammonium persulfate
ATP	Adenosine triphosphate
BMH	Bismaleimidohexane
BMOE	Bismaleimidoethane
BSA	Bovine serum albumin
CuP	Copper phenanthroline
$CuSO_4$	Copper sulfate
DFDNB	1,5-difluoro-2,4-dinitrobenzene
dH_2O	Deionized water
DHFR	Dihydrofolate reductase
DMSO	Dimethyl sulfoxide
DNA	Deoxyribonucleic acid
dNTP(s)	Deoxyribonucleoside triphosphate
DSP	3,3’-dithiobis-succinimidylpropionate
DTT	Dithiotreitol
EDTA	Ethylendiaminetetraacetate
fw	Forward (primer)
GPD	Glyceraldehyde-3-phosphate dehydrogenase
h	Hour(s)
HEPES	4-(2-hydroxyethyl)-1-piperazineethanesulfonic acid
His	Histidine
IgG	Immunoglobuline G
IM	Inner membrane
IMS	Intermembrane space
Kb	Kilobases
kDa	Kilodalton
L	Liter
M	Molar
mA	Milliampere
mL	Milliliter
mM	Millimolar
NADH	Nicotinamide adenine dinucleotide
Ni-NTA	Nickel-nitrilotriacetic acid
NMR	Nuclear magnetic resonance

OM	Outer membrane
ON	Overnight
PAS	Protein A sepharose
PCR	Polymerase chain reaction
PI	Pre-immune serum
PK	Proteinase K
PMSF	Phenylmethylsulfonyl fluoride
PVDF	Polyvinylidene difluoride
REC	Restriction enzyme cloning
RNA	Ribonucleic acid
RNase	Ribonuclease
rpm	Revolutions per minute
RT	Room temperature
rv	Reverse (primer)
SDM	Site-directed mutagensis
sec	Second(s)
TAE	Tris base, acetic acid, EDTA
TBS	Tris-buffered saline
TCA	Trichloroacetic acid
TEMED	N,N,N',N'-tetramethylene-1,2-diamine
TEV	Tobacco Etch Virus
TM	Transmembrane
Tris	Tris(hydroxymethyl)aminomethane
V	Volt
v/v	Volume per volume
w/v	Weight per volume
ΔΨ	Membrane potential
µL	Microliter
µM	Micromolar

Publications from this thesis

A part of this thesis has already been published by the author in the publications listed below.

Genge, M. G., Roy Chowdhury, S., Dohnálek, V., Yunoki, K., Hirashima, T., Endo, T., et al. (2023). Two domains of Tim50 coordinate translocation of proteins across the two mitochondrial membranes. Life Sci Alliance 6. doi: 10.26508/lsa.202302122

Genge, M. G., and Mokranjac, D. (2021). Coordinated Translocation of Presequence-Containing Precursor Proteins Across Two Mitochondrial Membranes: Knowns and Unknowns of How TOM and TIM23 Complexes Cooperate With Each Other. Front Physiol 12, 806426. doi: 10.3389/fphys.2021.806426

Acknowledgments

"And now, the end is near, and so I face that final curtain…" – My Way, Frank Sinatra

First, I would like to express my deepest gratitude to **PD Dr. Dejana Mokranjac**, for giving me the opportunity to work in her lab and allowing me to pursue my doctorate through exploring the world of protein import into mitochondria. **Dejana**, thank you so much for your supervision and valuable guidance on my projects throughout my PhD. Whenever colleagues or friends were again complaining about their boss, I was always able to say that I am so grateful to have such a passionate and dedicated scientist, but at the same time also an absolutely kind, understanding and, one definitely must not forget, funny person as my supervisor. You have a unique ability to pass on to your students your love for science, and I am forever thankful for all the knowledge that you have taught me on protein biochemistry and all the scientific experiences that you gave me the opportunity to go through. It has been a wonderful chapter and an honor doing science together! And in case I come up with the idea to make a few more truncation mutants in the future again, I will always remember: "Science is fun, don't lose faith" ;).

I would also like to thank the members of my thesis committee for their time and effort they put into reviewing my thesis: **Prof. Dr. Laura Busse, Prof. Dr. Heinrich Jung, Prof. Dr. Thomas Nägele, Prof. Dr. Christof Osman and PD Dr. Serena Schwenkert**.

All the (past and present) **members of the Mitoclub**, in particular **Angie, Christof and Kai**, I would like to thank for allowing me to improve my presentation skills in our Mito-family meetings and for their stimulating discussions, inspiring scientific ideas and very valuable feedback on my data and projects.

I will forever be thankful for the (past and present) members of the Mokranjac lab. **Nils, Petra, Shalini, Soraya and Umut**, thank you for being the greatest lab mates I could've imagined and becoming good friends along the way. I owe a very big chunk to you guys that I came to work with a smile everyday throughout the years. The atmosphere in the lab, especially since moving to Biocenter with all our students (Laura, Rachel, Sara, Zeynep,…) was extremely fun and very often felt like a second family (yes Soraya, you can call me big brother now :)). **Petra**, tausend Dank für Deine ganze experimentelle Unterstützung mit dem "old50split" (Du weißt schon wie ich's meine ;)). Mit Deiner warmherzigen und lustigen Art, und der „politisch korrekten" Rumalberei zusammen mit Moritz und mir, hast Du mir die Zeit, als das Labor zwischenzeitlich etwas kleiner war, definitiv versüßt. To my students, **Annalena, Moritz K. and Ruhita**, thanks for all the effort and work you put into my projects.

A very special THANK YOU goes to all the (past and present) lab neighbors in the BMC and Biocenter. To name a few, **Abu, Andreia, Basti, Christiane, Felix, Flavia, Heiko, Julia P., Moritz R., Nupur, Ria, Sandra, Shao, Simon S., Simon U., Thomas P., Ulrike**, some of you that I have developed into really close friendships

with; I thank you so much for all the activities next to pipetting: lunch at 11, non-scientific conversations & coffee in the kitchen, after-journal-club Pizza&Beer sessions, Mcfit mornings, Biergarten, late bar and club nights, Starkbierfeste and Wiesn (of course with After-Wiesn until 5), Theater-Schnaps or any other Schnaps in the labs and several memorable bridge- and kitchen-parties!! Even though it happened several times that the next day I had an important meeting or experiment early in the morning, I would have done it all over and the same way, again!

I additionally would like to thank **Nils and Nupur** for reading and correcting my thesis draft.

Ich möchte mich auch bei **Christine** für die Unterstützung bei vielen organisatorischen bzw. Vertragsangelegenheiten bedanken. **Marianne, Sylvia, Tatjana und Zdenka** danke ich für den gesamten Reinigungs- und Autoklavierservice. Auch nochmal einen speziellen Dank an **Zdenka** für die vielen Mito-preps, Induktionen und das Vorbereiten verschiedener Medien im BMC.

Nun kommen wir zu den Personen, die mich in den letzten Jahren außerhalb der Promotion auf andere Gedanken gebracht haben; die meine Freizeit, Abende und Wochenenden mit Leben gefüllt haben! Ihr wisst, wer Ihr seid und wie Ihr dazu beigetragen habt, und besonders **Berny, Caro, David, Felix, Jakob, Jan, Janna, Juli, Kathi, Loui, Louis, Markus, Matze, Mira, Mo, Nathalie, Oli, Pamina, Ruben, Tin**, ich danke EUCH ALLEN wirklich von HERZEN!

Manchmal entstehen aus Freunden auch Familie, und diese Personen haben einen wirklich ganz besonderen Dank verdient, da sie mich in meinen Hoch- sowie Tiefphasen begleitet haben. **Anja, Carina, Fabi und Mokka**, ohne Euch, Euer bewusstes Zuhören, Euren wertvollen Ratschlägen, tiefgründigen Gespräche und etlichen Freizeitablenkungen sowie Urlaube mit Euch, hätte ich das Ganze hier niemals schaffen können. DANKE, dass Ihr mich kontinuierlich dran erinnert habt, was wirklich wichtig im Leben ist. Auf noch ganz viele Abenteuer zusammen in den nächsten Jahrzehnten!

Alles kann zerbrechen, aber Familie bleibt für immer Familie! **Mein Bruder Mark**, danke für Deine stetige Unterstützung, Deine Lehren, die Du mir von klein auf mitgegeben hast und dass ich mich im Notfall immer auf Dich verlassen kann! Als kleiner Bruder, sehe ich Dich in so vielen Aspekten des Lebens, als mein Vorbild! **Joni, Johanna und Kathi**, auch wenn ich nicht immer da sein kann, bei den wichtigen Momenten geht mir das Herz auf, Zeit bei Euch sowie mit Euch zu verbringen. An meine Eltern, **Mami und Papi**, ich bin Euch so unglaublich dankbar für Alles was Ihr für mich getan habt. Für Eure immerwährende Unterstützung und Liebe, dir Ihr mir jeden Tag schenkt und dass Ihr es mir ermöglicht habt, diesen Weg zu gehen. Hab Euch ganz doll lieb!

Ohne meine Familie und engsten Freunde, wäre ich jetzt nicht an dem Punkt, wo ich mich gerade befinde, und auch nicht die Person, die ich bin. Deshalb noch einmal… Danke!